IXPE
Imaging
X-Ray
Polarimetry
Explorer

The Imaging X-ray Polarimetry Explorer (IXPE) and new directions for the future

Paolo Soffitta

IXPE Italian PI

(INAF-IAPS)

Advances in Space AstroParticle Physics

19-23 June 2023 Perugia (IT)

WHY X-RAY POLARIMETRY

POLARIZATION FROM CELESTIAL SOURCES MAY DERIVE FROM:

- **Emission processes themselves: cyclotron, synchrotron, non-thermal bremsstrahlung**

(Westfold, 1959; Gnedin & Sunyaev, 1974; Rees, 1975)

- **Scattering on aspherical accreting plasmas: disks, blobs, columns.**

(1975; Sunyaev & Titarchuk, 1985; Mészáros, P. et al. 1988)

- **Vacuum polarization and birefringence through extreme magnetic fields**

(Gnedin et al., 1978; Ventura, 1979; Mészáros & Ventura, 1979)

IXPE Imaging X-Ray Polarimetry Explorer

THE FORMALISM

Fit function: $\mathcal{M}(\phi) = A + B\cos^2(\phi - \phi_0)$

Modulation: $\frac{\mathcal{M}_{max} - \mathcal{M}_{min}}{\mathcal{M}_{max} + \mathcal{M}_{min}} = \frac{B}{B + 2A}$

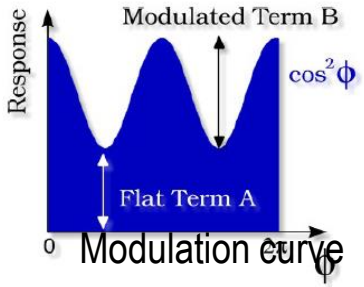

Modulation curve

Polarization: $\frac{1}{\mu}\frac{B}{B + 2A}$ μ is the modulation factor, i.e. the modulation for 100% polarized radiation

Or by using Stokes Parameters

$$S(\varphi) = I + Qsin(2\varphi) + Ucos(2\varphi)$$

$$I = (A + \frac{B}{2}) \qquad U = \left(\frac{B}{2}\right) * \sin(2\varphi_0) \qquad Q = \left(\frac{B}{2}\right) * \cos(2\varphi_0)$$

$$P = \frac{\sqrt{Q2+U2}}{I} \qquad \varphi = \frac{1}{2} atan \frac{U}{Q}$$

Kislat et al. (2015) introduced the Stokes parameters from the direction of the single carrier of polarimetric observation

No V → no circular polarization with present techniques

THE FIRST LIMIT: IN POLARIMETRY THE SENSITIVITY IS A MATTER OF PHOTONS

$$MDP = \frac{4.29}{\mu R_S}\sqrt{\frac{R_S + R_B}{T}}$$

Minimum Detectable Polarization (MDP)

R_S is the Source rate, R_B is the Background rate, T is the observing time
μ is the modulation factor: the response of the polarimeter to a 100% polarized beam (spanning from 0 or no sensitivity, to 1 or maximum sensitivity)

If background is negligible: $$\mathrm{MDP} = \frac{4.29}{\mu\sqrt{N_{ph}}}$$

To reach MDP=1% with μ=0.5: $$N_{ph} = \left(\frac{4.29}{\mu\ \mathrm{MDP}}\right)^2 = 736\ 10^3\ \mathrm{ph}$$

Source detection > 10 counts
Source spectral slope > 100 counts
Source polarization > 100.000 counts

Caution: the MDP describes the capability of rejecting the null hypothesis (no polarization) at 99% confidence. For a 3-sigma meaurement an observing time 2.2 times longer is needed while the 1-sigma error scales like : 28°.5/S/N

IXPE
Imaging
X-Ray
Polarimetry
Explorer

IXPE INSTITUTIONS AND INDUSTRIES

PI Steve O'Dell NASA-MSFC (PI emeriti Martin Weisskopf and Brian Ramsey)

THE IXPE OBSERVATORY

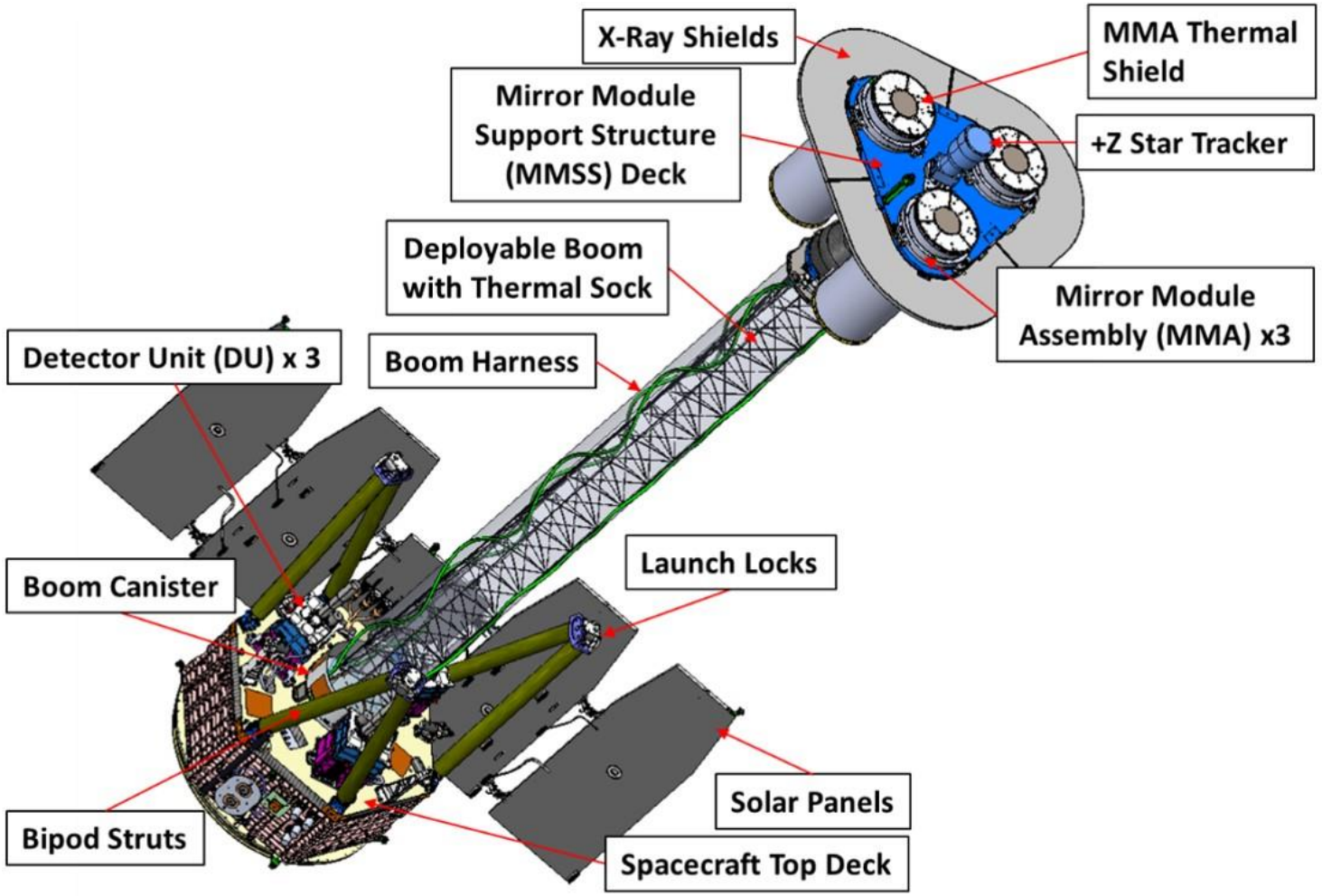

FALCON 9 LAUNCHER VS PEGASUS XL LAUNCHER

Stowed Views

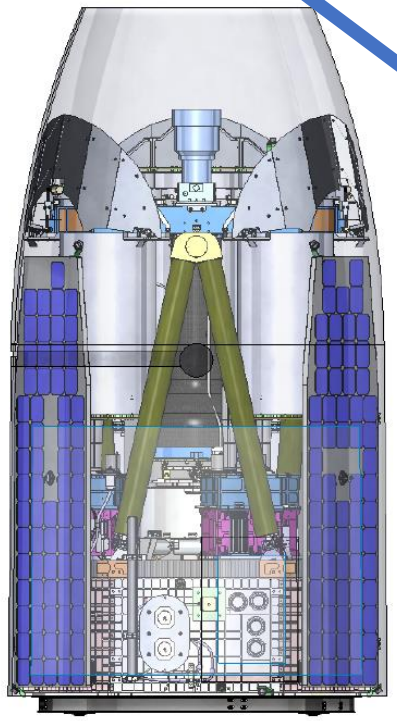

IXPE in the Pegasus XL fairing.

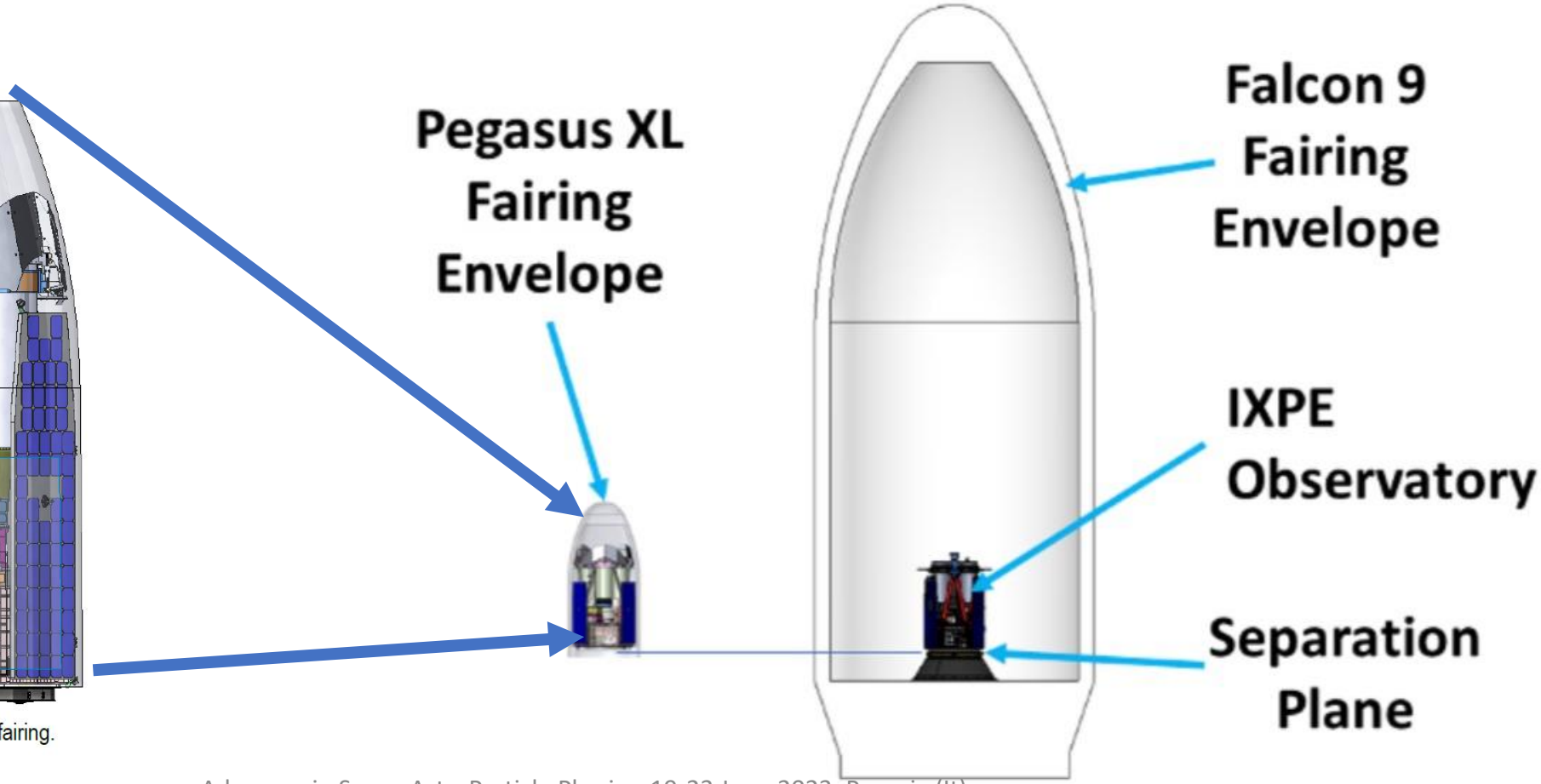

IXPE
Imaging
X-Ray
Polarimetry
Explorer

THE OBSERVATORY

Credit: Ball Aerospace

IXPE
Imaging
X-Ray
Polarimetry
Explorer

LAUNCH (DECEMBER 9, 2021)

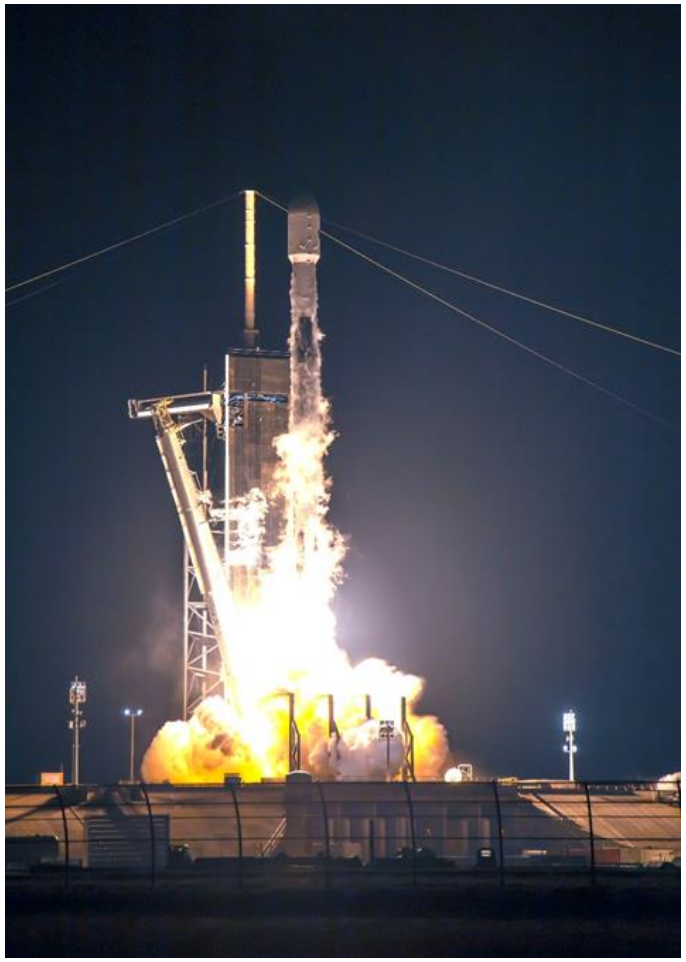

Equatorial Orbit
600 km altitude

IXPE
Imaging
X-Ray
Polarimetry
Explorer

RELEASE FROM THE FALCON 9

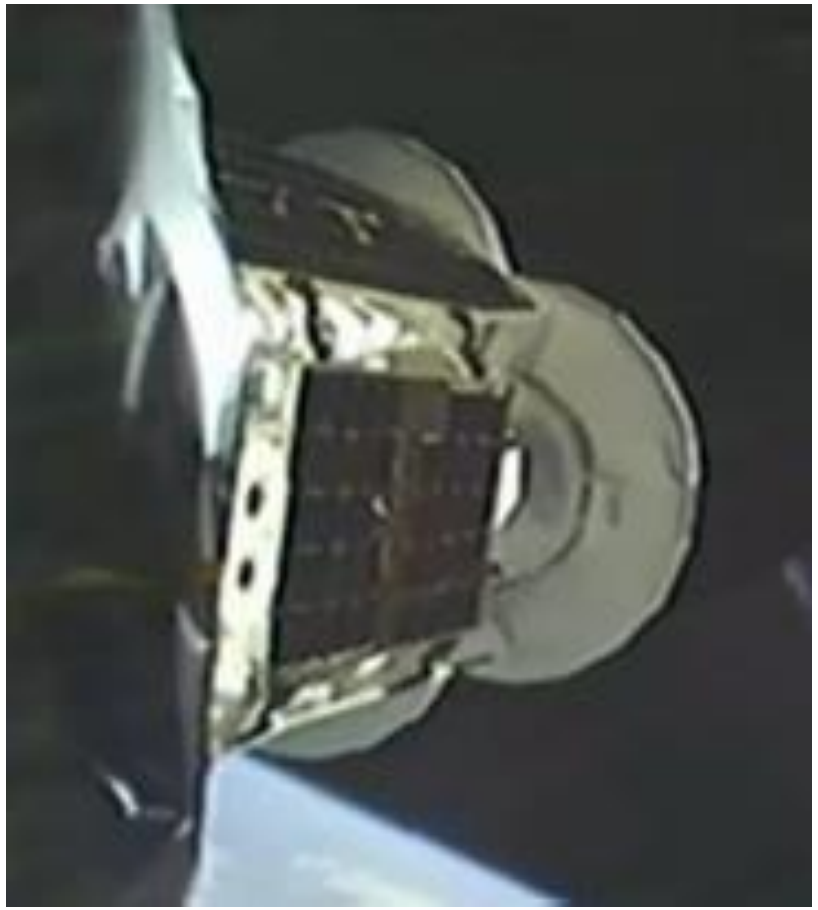

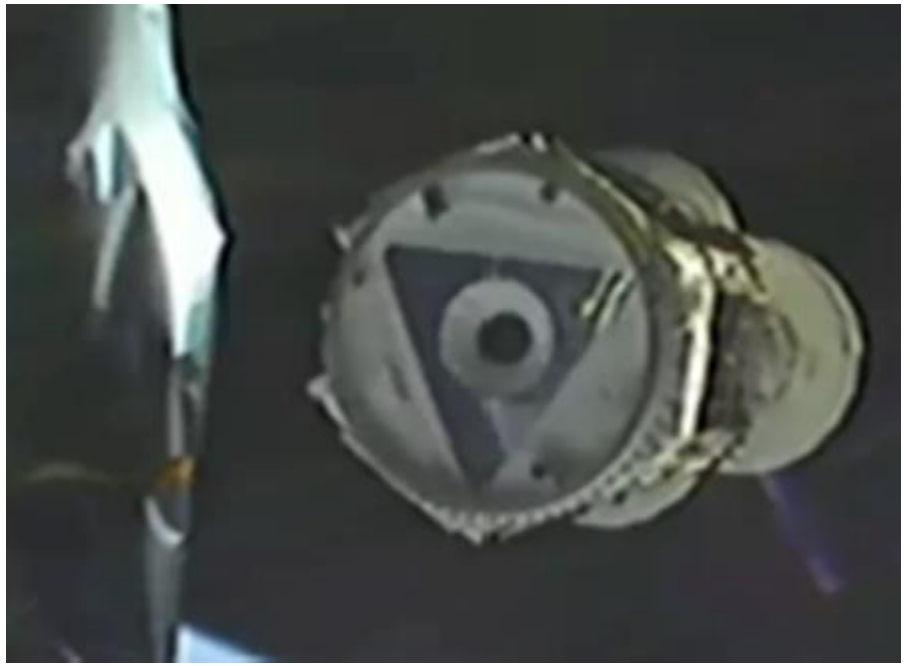

IXPE
Imaging
X-Ray
Polarimetry
Explorer

Optics Production Process

Mandrel fabrication

1. Machine mandrel from aluminum bar

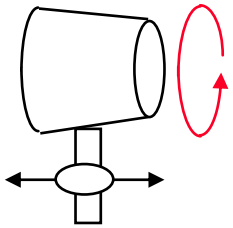

2. Coat mandrel with electroless nickel (Ni-P)

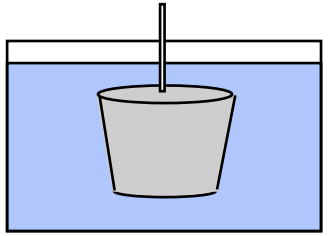

3. Diamond turn mandrel to sub-micron figure accuracy

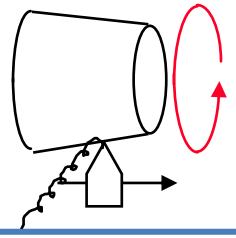

4. Polish mandrel to 0.3-0.4 nm RMS

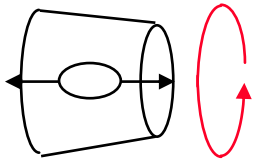

5. Conduct metrology on the mandrel

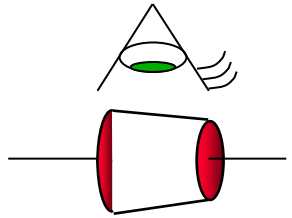

Mirror-shell forming

6. Passivate mandrel surface to reduce shell adhesion

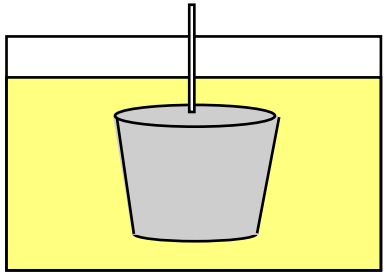

7. Electroform Nickel/Cobalt shell onto mandrel

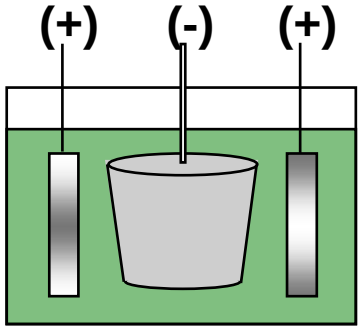

8. Separate shell from mandrel in chilled water

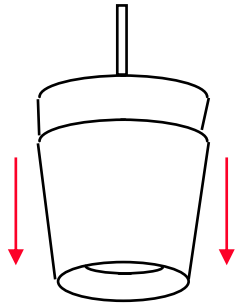

Ni/Co electroformed IXPE mirror shell

MIRROR MODULE ASSEMBLY PROPERTIES

Property	Value
Number of modules	3
Mirror shells per module	24
Inner, outer shell diameter	162, 272 mm
Total shell length	600 mm
Inner, outer shell thickness	180, 250 um
Shell material	Nickel cobalt alloy
Effective area per module	163 cm^2 (2.3 keV) ~ 192 cm^2 (3-6 keV)
Angular resolution	< 30 arcsec HPD
Detector limited FOV	12.9 arcmin
Focal length	4 m
Mass (3 assemblies)	93.12 kg

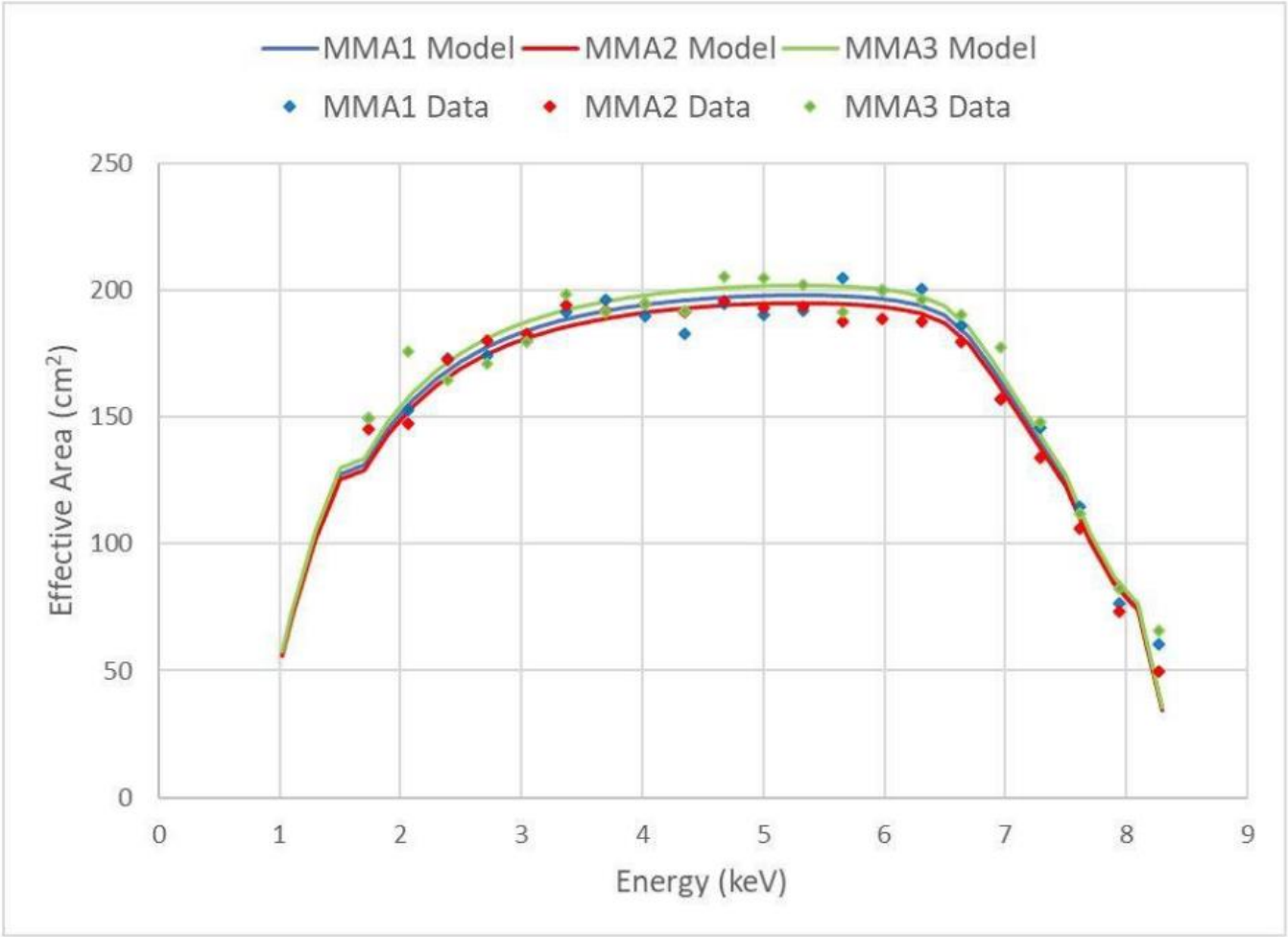

ANGULAR RESOLUTION

MMA	#1	#2	#3
6.4 keV	18.9"	24.8"	24.2"
4.5 keV	18.9"	25.0"	26.9"
2.3 keV	18.7"	24.5"	26.7"

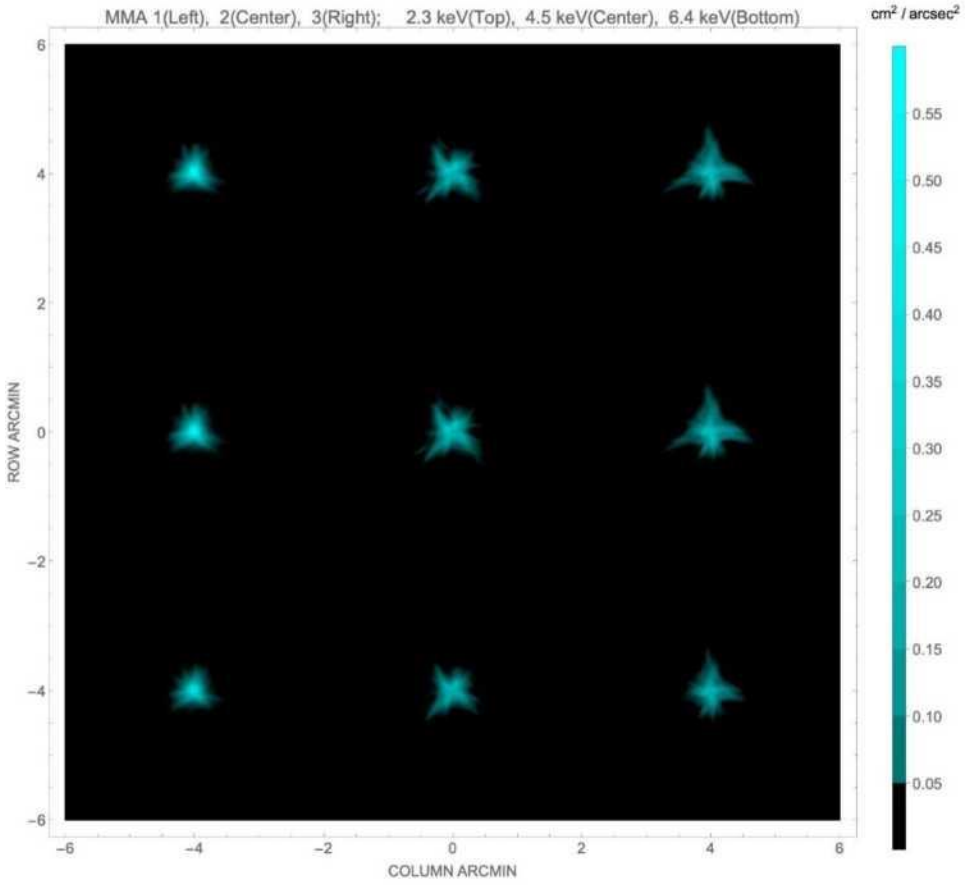

Values in the table are half-power diameters (HPDs) for the individual MMAs alone. These need to be adjusted for alignment errors, detector resolution, focus etc. to determine the on-orbit system-level resolution.

Based upon X-ray calibration, analysis, and on-orbit performance the system-level performance is ≈ 30" HPD

HPD MEASURED IN-FLIGHT

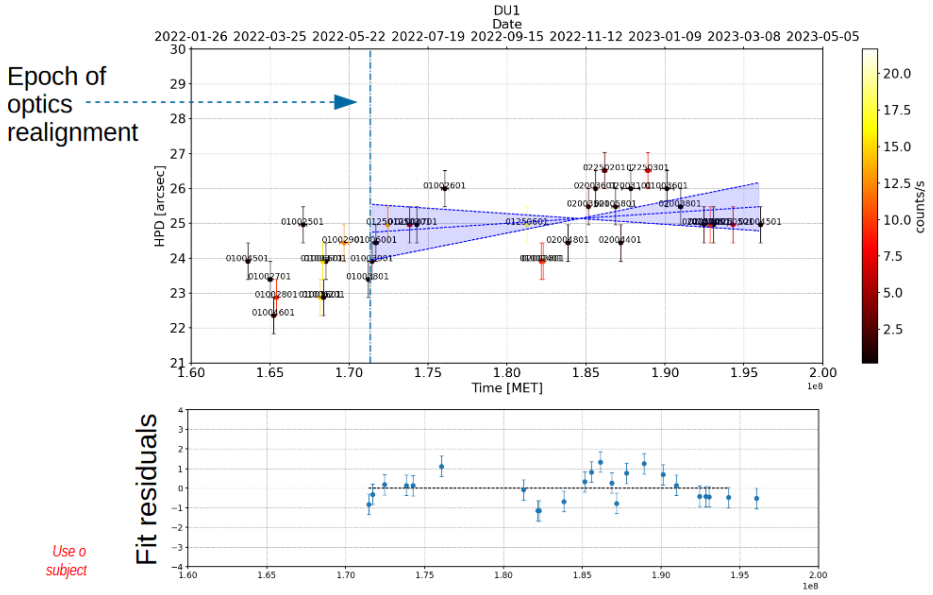

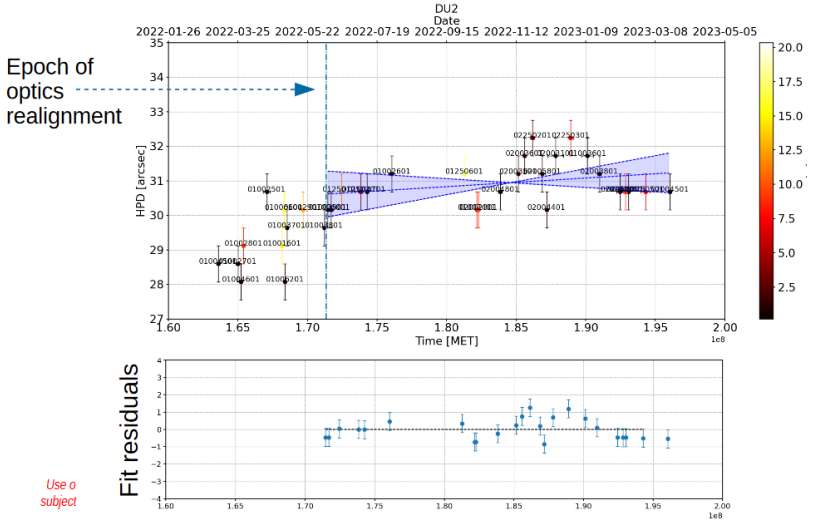

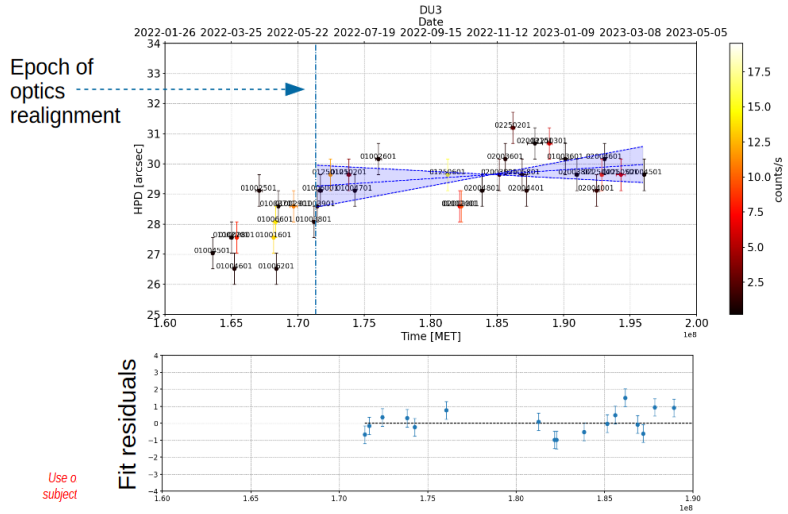

The inflight performcance of the detector + mirror systems are in line with the expectation. The HEW is indeed dominated by the quality of the optics, then to the inclined penetration effects finally much less by the position resolution of the detector

IXPE
Imaging
X-Ray
Polarimetry
Explorer

PHOTOELECTRIC EFFECT TO MEASURE POLARIZATION OF X-RAYS

Proposed missions to date

Mission	Date	PI
XMM	Late 80’	G.W. Fraser (UK)
SXRP /SRG	Late 80’ Early 00’	R.Novick (USA)
XEUS/IXO	2007-2012	R. Bellazzini (IT)
POLARIX	2007-2008	E. Costa (IT)
IXPE (OLD)	2007	M. Weisskopf (USA)
HXMT	2007-2009	E. Costa (IT)
NHXM	2011	G. Tagliaferri (IT)
LAMP	2013	H. Feng (China)
XIPE (Small)	2014	E. Costa (IT)
ADAELI+	2014	F. Berrilli (IT)
SEEPE (ESA-CAS)	2014	S.Liu-P. Soffitta
XIPE M4	2014-2017	P. Soffitta (IT)
IXPE	**2017+**	**M. Weisskopf (USA)**

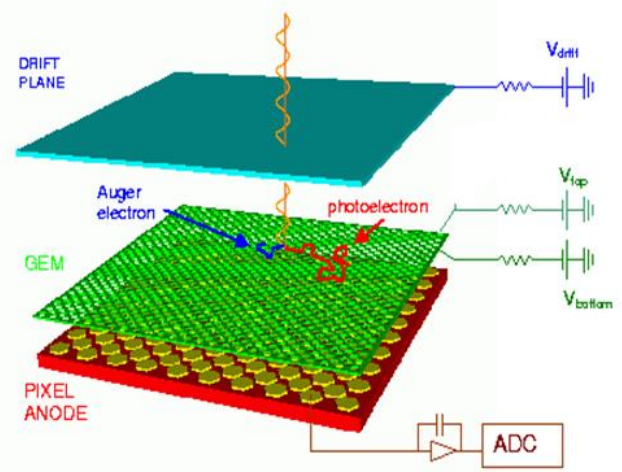

Costa et al., 2001, Bellazzini et al, 2005,2006, Baldini et al., 2021, Soffitta et al. 2022

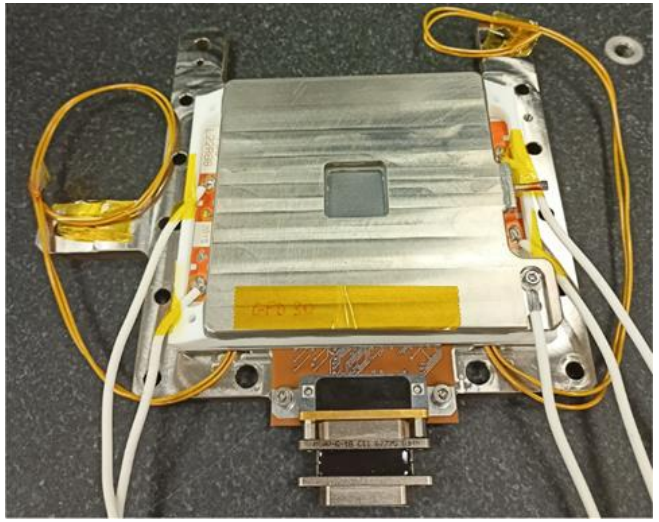

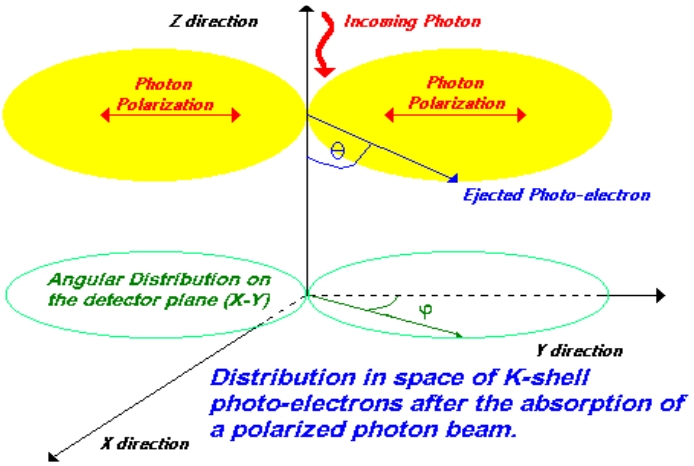

Linear Polarization, Image, Energy, Time

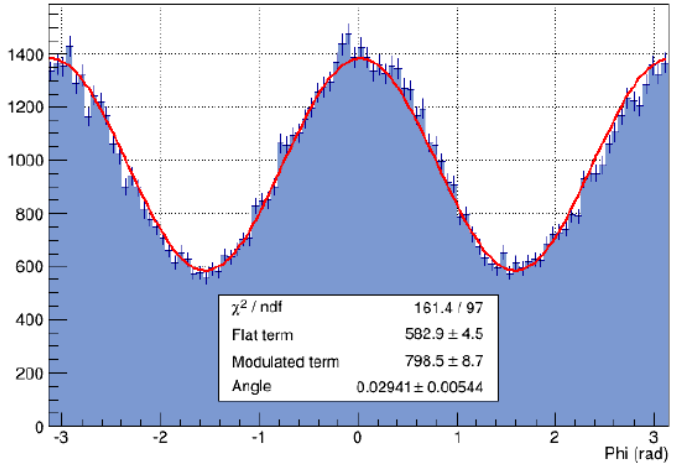

Real modulation curve derived from the measurement of the emission direction of the photoelectron.

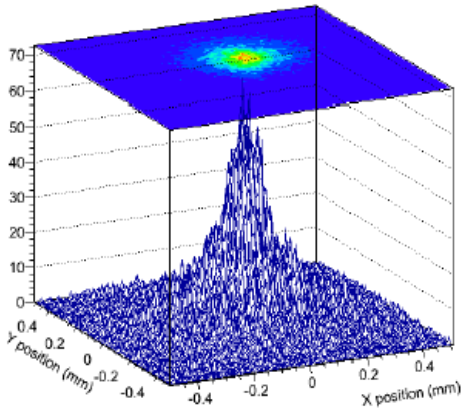

Position resolution < 120 µm (HEW)

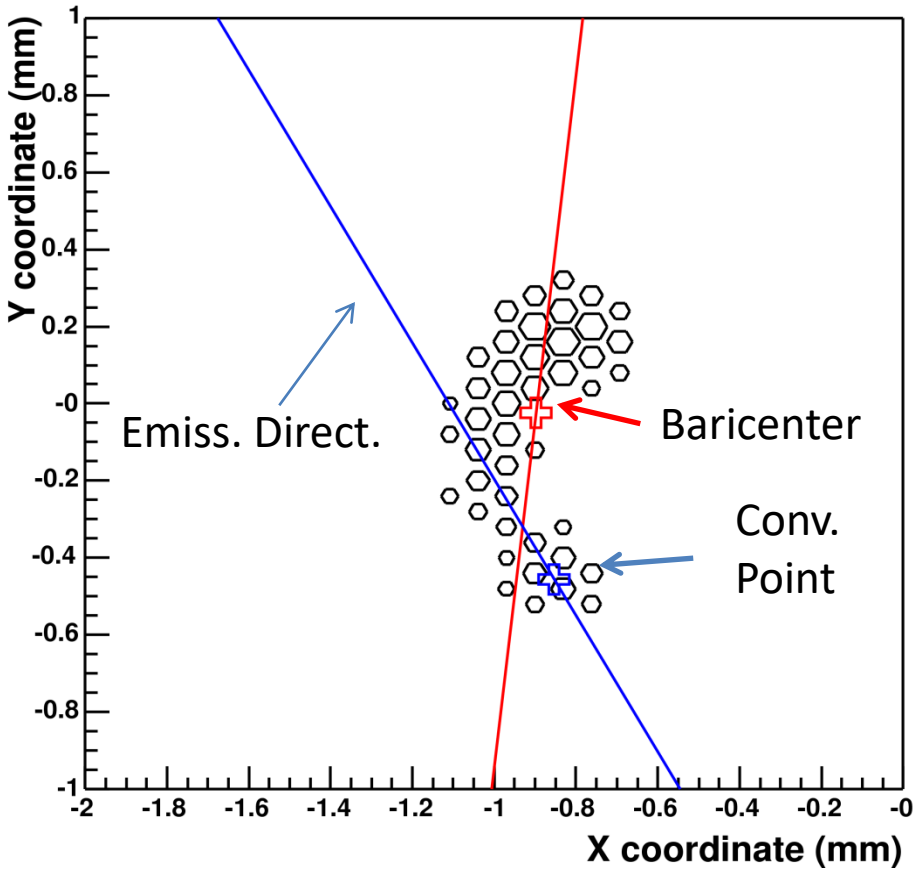

Energy, space and time resolved X-ray polarimetry

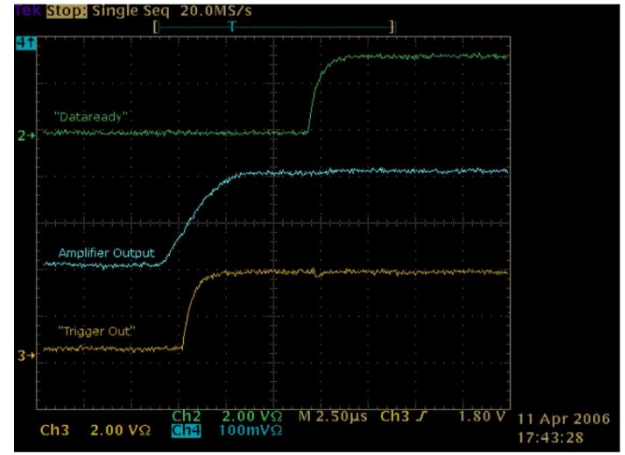

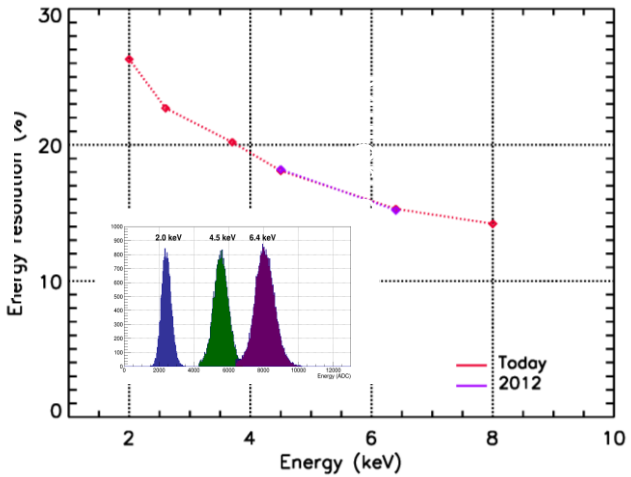

Energy resolution as function of energy

IXPE
Imaging
X-Ray
Polarimetry
Explorer

INFN-TEAM ASSEMBLY OF THE DUS

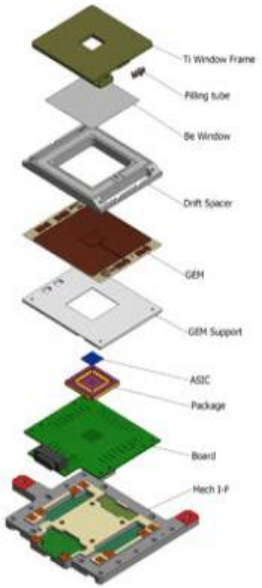

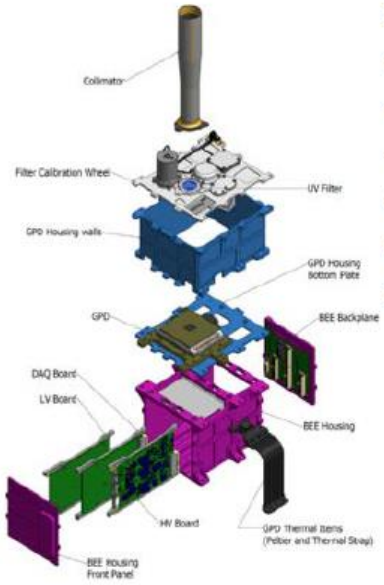

- DU mechanical housing design and procurement.
- DU thermal design and parts procurement
- Stray-light collimator design & procurement
- DU alignment system (collab. with MSFC & Ball &INAF)
- BEE electronics design and procurement
- BEE DAQ firmware, BEE software
- BEE Test

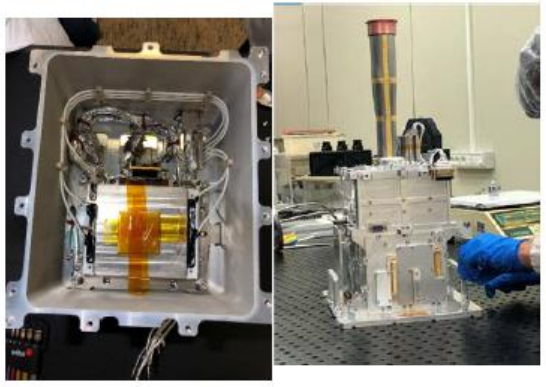

INAF Calibration of 3 flight DUs + 1 Spare, AIV&T

- **Calibration of DU have been carried out in Italy at INAF-IAPS, before Instrument integration and delivery to USA**
- **40 days for each DU (3 flight + 1 spare units)**
  - Up to 24/7 data acquisition
- **First unit started calibration on 26th July, DU-FM2 started on 6th Sep 2019, DU3 on 23 Oct. 2019, DU 4 on 16 Dec. 2019**
- **60% of time dedicated to characterization of the response to unpolarized radiation at 6 energies**
- **17.5% of time dedicated to measurements of modulation factor at 7 energies**
- **Remaining time to calibrate other parameters of interest**
- **Energy calibration and dead-time are by-product of previous measurements**

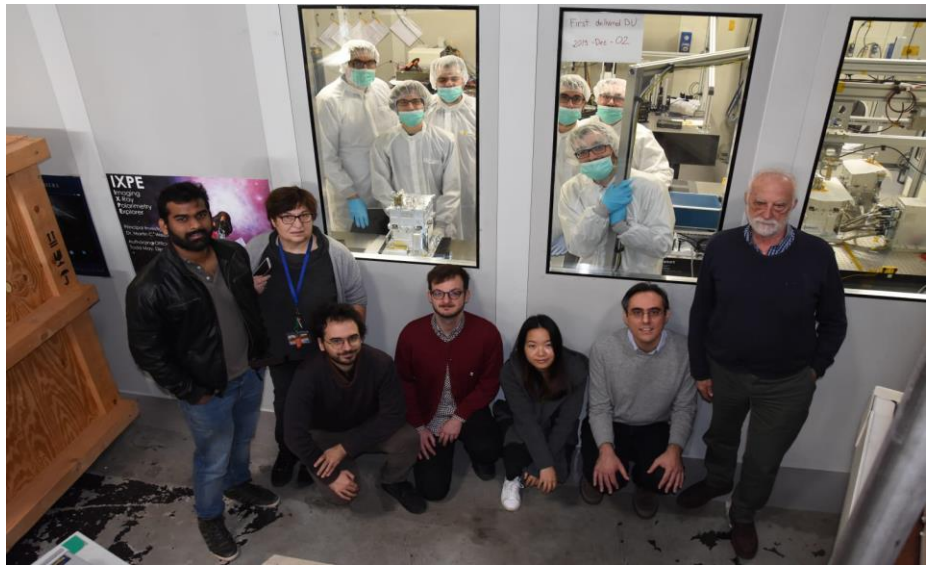

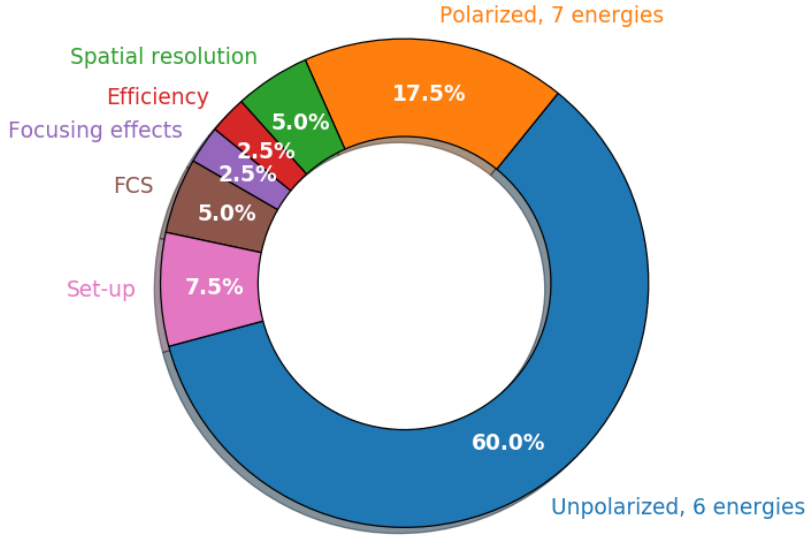

Muleri et al., 2021

IXPE
Imaging
X-Ray
Polarimetry
Explorer

FILTER Calibration Wheel Assembly (In-flight calibration)

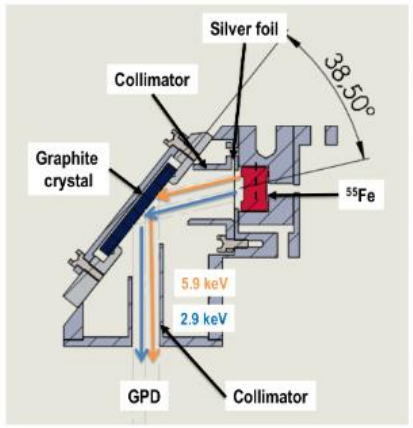

Flight Polarized X-ray sources

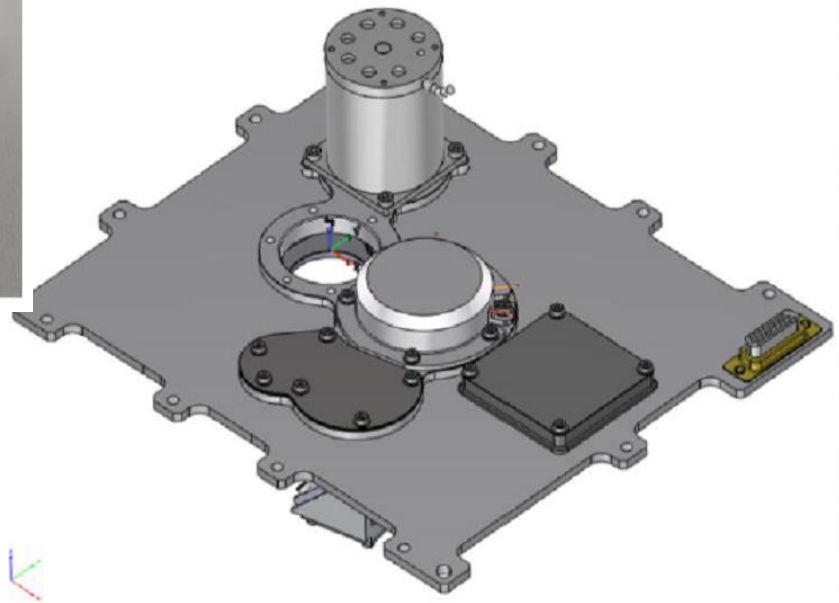

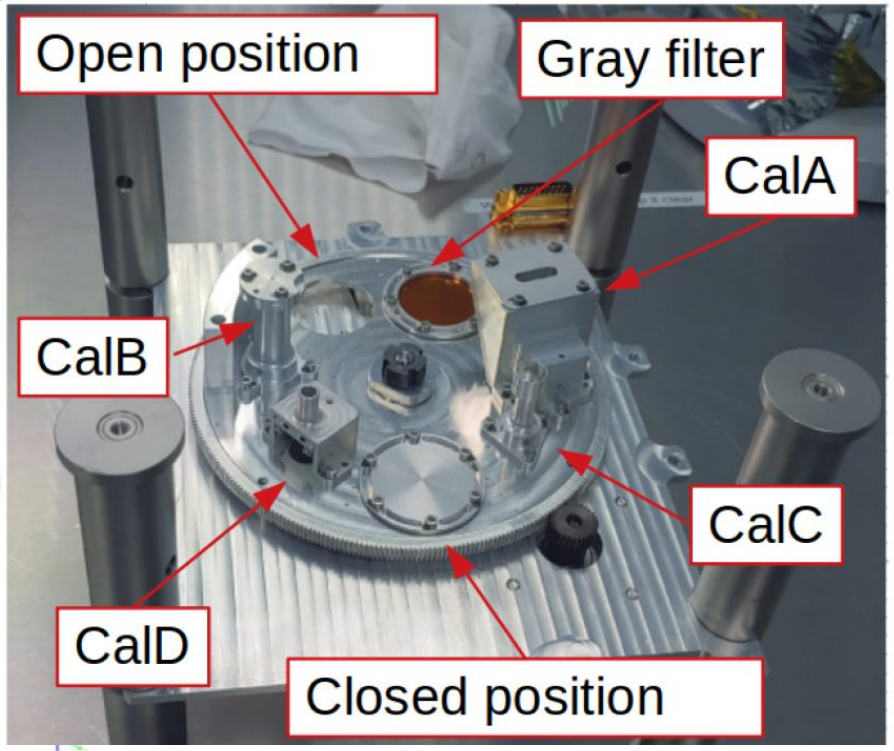

Ferrazzoli et al., 2020

^{55}Fe-powered calibration sources:

Cal A – Bragg-reflected polarized 2.98-keV (Ag-Lα fluorescence) and 5.89-keV (Mn-Kα)

Cal B – unpolarized 5.89-keV spot

Cal C – unpolarized 5.89-keV flood

Cal D – unpolarized 1.74-keV (Si-Kα fluorescence) flood

IXPE
Imaging X-Ray Polarimetry Explorer

Marshall Space Flight Center

agenzia spaziale italiana

IMAGES AND MODULATION FACTORS OF THE CALIBRATION SOURCES

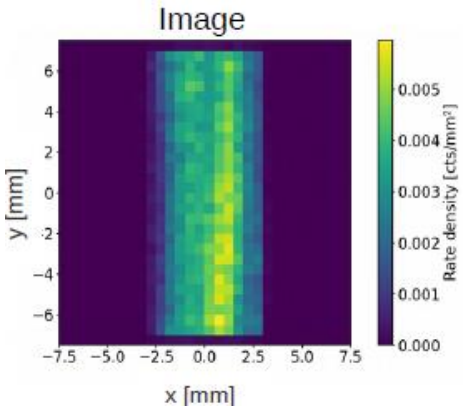

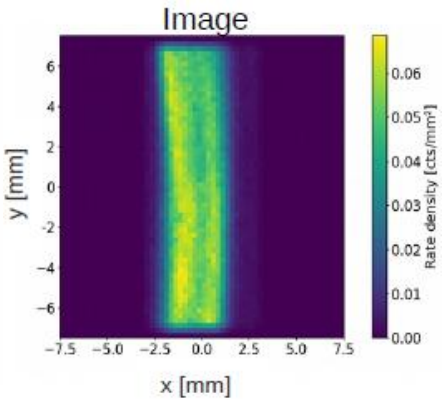

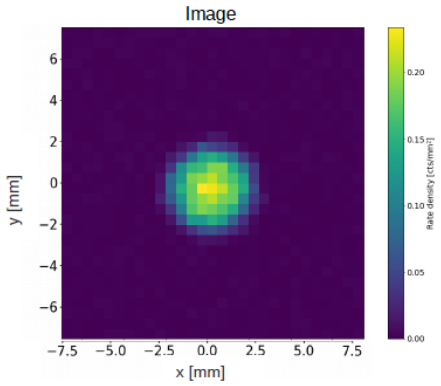

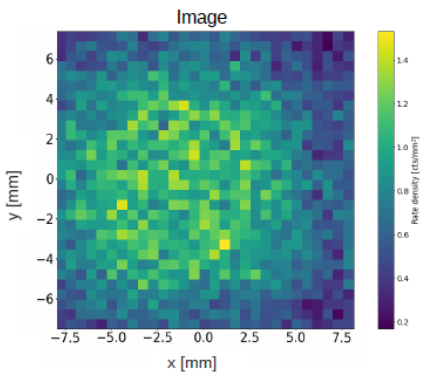

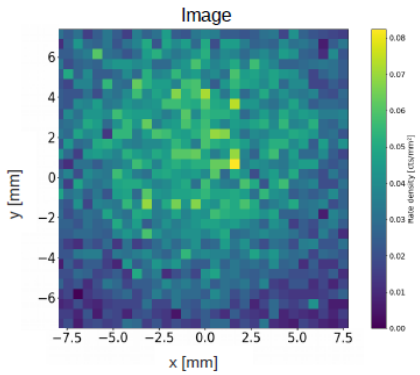

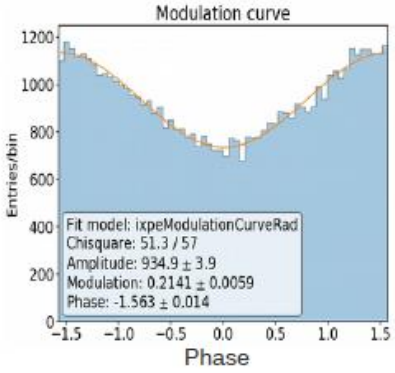

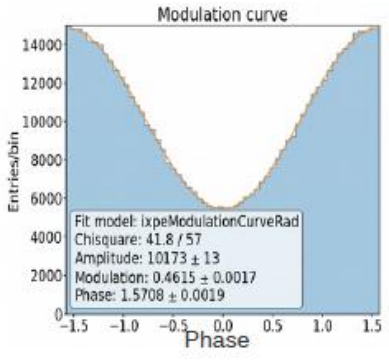

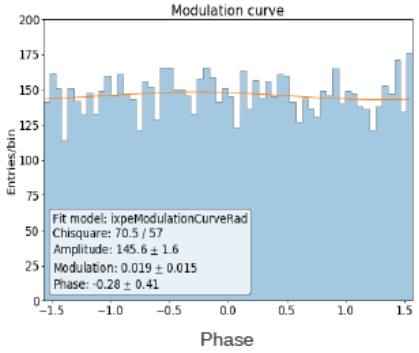

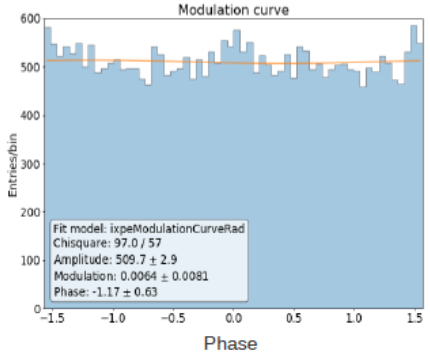

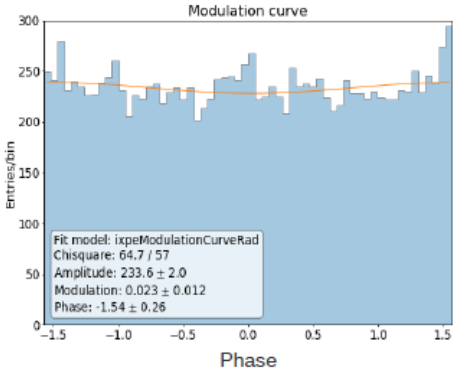

3.0 keV Cal A Pols

5.9 keV Cal A Pol

5.9 keV Cal B

5.9 keV Cal C

1.7 keV Cal D

IXPE Imaging X-Ray Polarimetry Explorer

DETECTOR PROPERTIES

Parameter	Value
Sensitive area	15 mm x 15 mm (13 x 13 arcmin)
Fill gas and composition	DME @ 0.8 atmosphere
Detector window	50-µm thick beryllium
Absorption and drift region depth	10 mm
GEM (gas electron multiplier)	copper-plated 50-µm liquid-crystal polymer
GEM hole pitch	50 µm triangular lattice
Number ASIC readout pixels	300 x 352
ASIC pixelated anode	Hexagonal @ 50-µm pitch
Spatial resolution (FWHM)	< 123 µm (6.3 arcsec) @ 2 keV
Energy resolution (FWHM)	1.0 keV @ 6.4 keV (scaling as sqrt(E))
Useful energy range	2 - 8 keV

IXPE
Imaging
X-Ray
Polarimetry
Explorer

MODULATION FACTOR (FROM CALIBRATION)

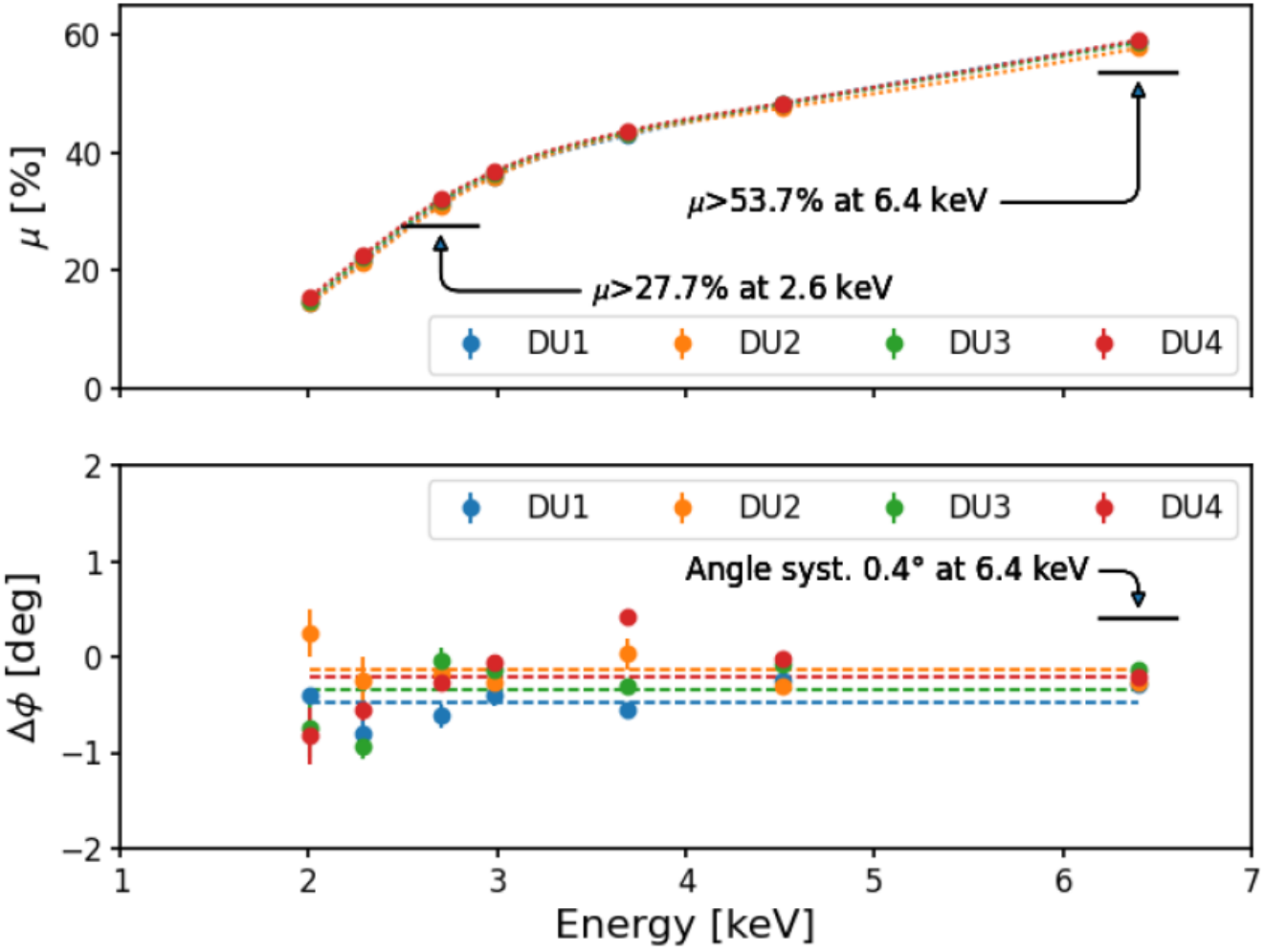

Di Marco et al., 2022, AJ under review

IXPE
Imaging
X-Ray
Polarimetry
Explorer

RESPONSE (3 POLARIMETERS)

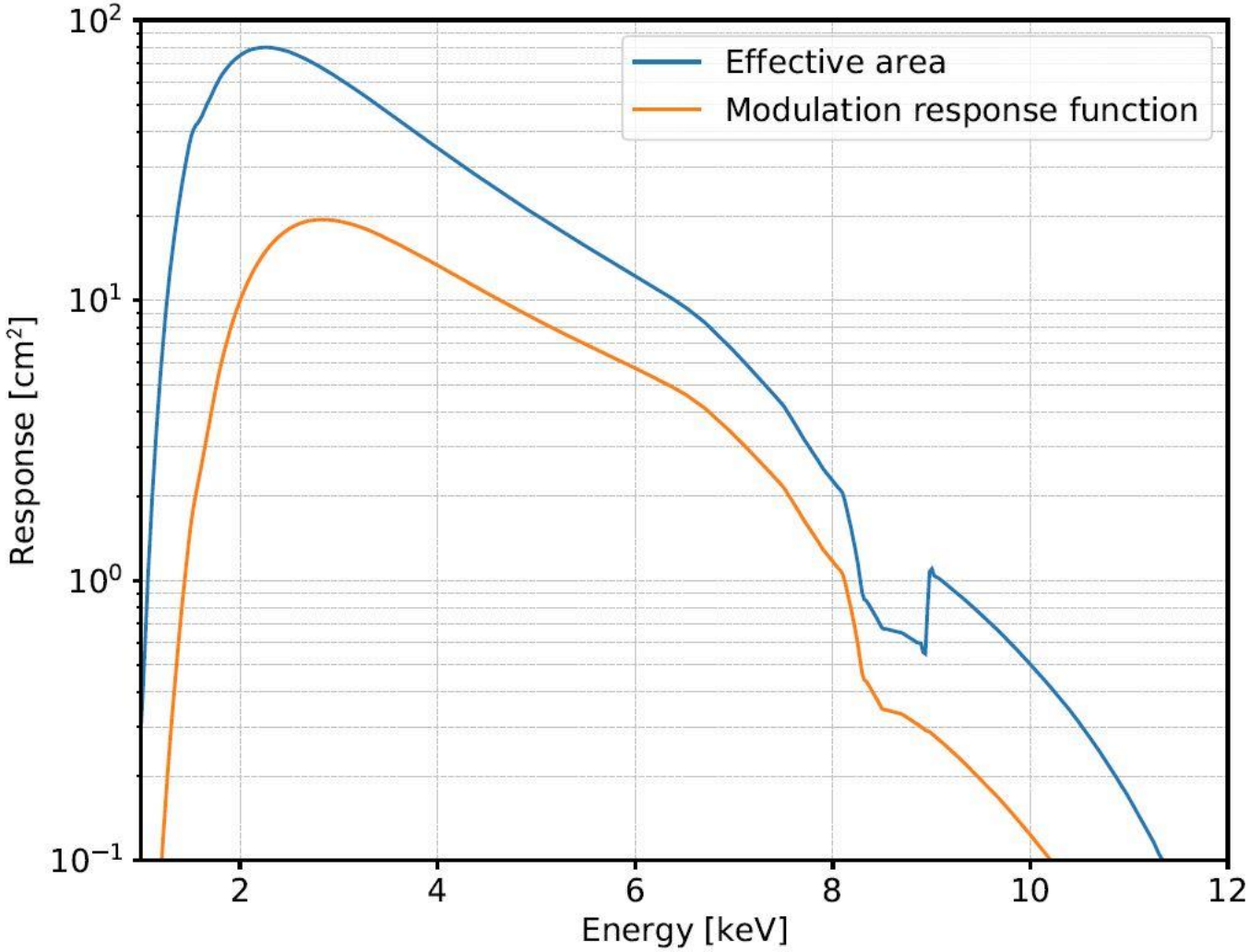

DITHERING

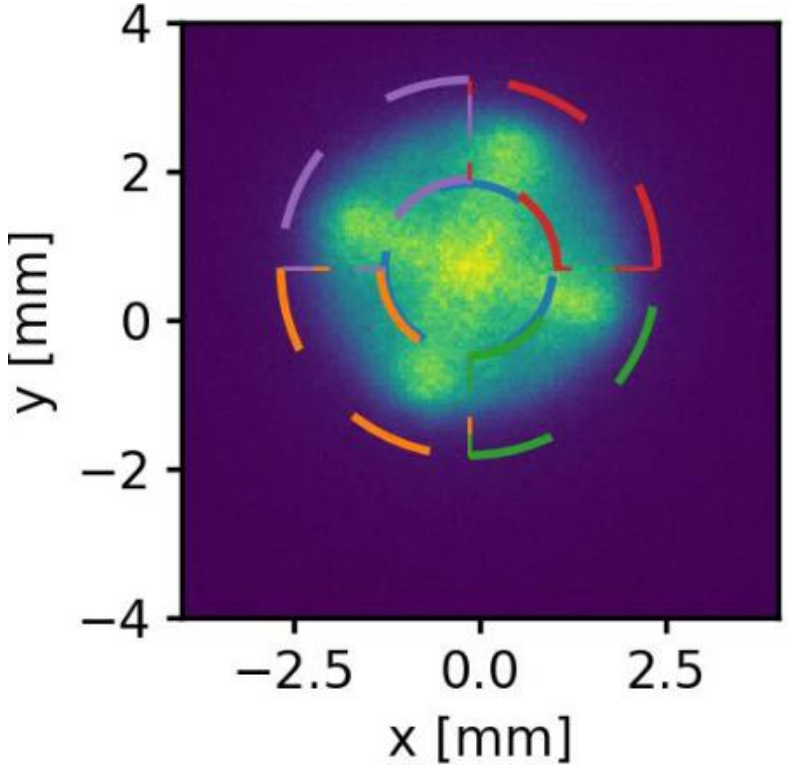

Dithering has three selectable radius

- (small) 0.8 arcmin
- (medium) 1.6 arcmin periods in few hundreds s range
- (large) 2.6 arcmin

x = A*cos(wa*t + phiA)*cos(wx*t + phiX)
y = B*sin(wa*t + phiB)*sin(wy*t + phiY)

Given the lack of useful rotation a dithering is required to average out the systematic effects (Spurious Modulation) and to facilitate the ground calibration

TOPICAL WORKING GROUPS

Science Advisory Team (chaired by Giorgio Matt and Roger Romani)

Coordinates science activities required for planning, analyzing, interpreting, and reporting IXPE observations

Organized into seven Topical Working Groups

- *TWG1 Pulsar Wind Nebulae, led by Niccolò Bucciantini (INAF-Arcetri)*

  Obtain polarimetric imaging to constrain the magnetic-field geometry of the nebula and the phase-dependent polarization of the pulsar

- *TWG2 Supernova Remnants, led by Pat Slane (CfA)*

  Obtain spectral polarimetric imaging of Supernova Remnants (SNR) to constrain the magnetic-field structure of the X-ray emitting regions

- *TWG3 Accreting Black Holes, led by Michal Dovčiak (CAS-ASU)*

  Obtain spectral polarimetry of microquasars to constrain the value of the black-hole spin parameter (if in soft state), or constrain the geometry of the corona (if in hard state)

- *TWG4 Accreting Neutron Stars, led by Juri Poutanen (Turku)*

  Obtain phase-dependent polarimetry of accreting X-ray pulsars (high-magnetic-field binaries) to constrain models and geometries for the pulsing emission. Obtain polarimetry of non pulsating accreting NS to constrain the geometry of the system

- *TWG5 Mag*netars, led *by Roberto Turolla (Uni Padua)*

  Obtain phase-dependent polarimetry of magnetars to constrain the effects of vacuum polarization (birefringence in a strong magnetic field)

- *TWG6 Radio-Quiet AGN & Sgr A, led by Frédéric Marin (Strasbourg)*

  Obtain polarimetry of RQ AGN to constrain the geometry of the emitting regions

- *TWG7 Blazars & Radio Galaxies, led by Alan Marscher (Boston U)*

  Obtain polarimetry of Blazars and RG to study jet emission

YEAR-1 TARGETS

Galactic Coordinates

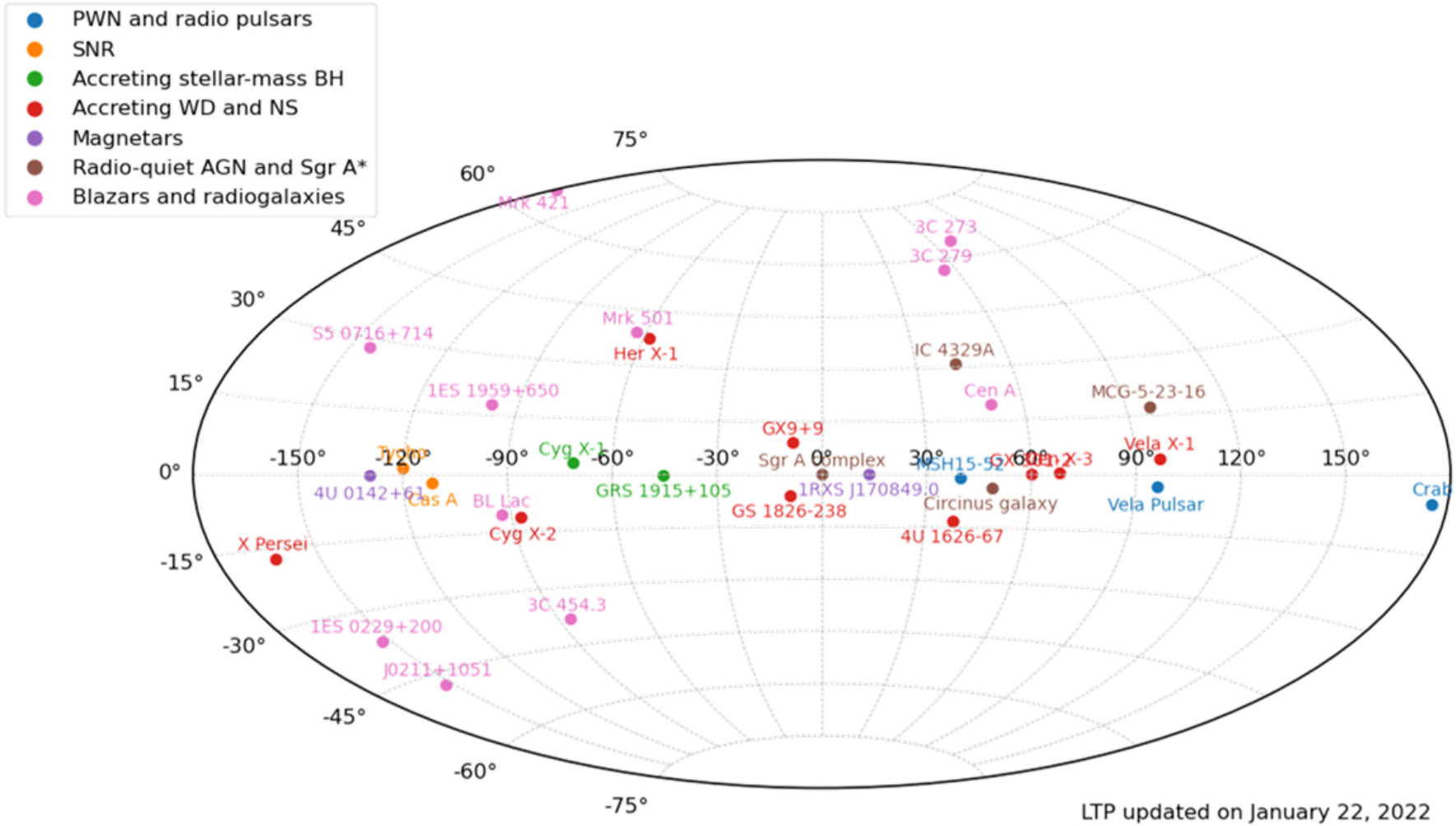

IXPE
Imaging
X-Ray
Polarimetry
Explorer

48 SOURCES OBSERVED

		Number of objects
TWG -1	3 PWNe and isolated pulsars	Crab PWN, Vela PWN, MSH 15-52, PSR B0540-69
TWG-2	3 SNR	Cas A, Tycho's, NE SN 1006
TWG-3	4 Accreting stellar-BH	Cyg X-1, 4U 1630-472, Cyg X-3, LMC X-1, SS433, 4U 1957-115
TWG-4	13 Accreting NS & WD	Cen X-3, Her X-1, GS1826-67, Vela X-1, Cyg X-2, GX 301-2, Xpersei, GX 9-9, 4U 1820, GRO J1008-57, XTE 1701-46, EXO 2030+375, LS V+44 17, GX 5-1
TWG-5	2 Magnetars	4U 0142+61, 1RXS J170849, SGR 1806
TWG-6	4 Radio-quiet AGN & Sgr A*	MCG 5-23-16, Circinus Galaxy, NGC 4151, IC 4329 A Sgr A* Complex
TWG-7	13 Blazars & radio galaxies	Cen A, S5-0716-714, 1ES 19-59-650, Mrk 421, BL Lac, 3C 454, 3C 273, 3C 279, Mrk 501,1ES 1959-650, BL-Lac, 1ES 0229-200, PG 1553 -113

- Some sources have been revisited

Mrk 421, Mrk 501, BL Lac, Vela X1, Her X-1, MCG 5-23-16, Crab, MSH 15-52, 4U1820, Cyg X-1

IXPE
Imaging X-Ray Polarimetry Explorer

From Quick-look analysis (phase, Time and angle averaged)
19 Detections at more than 6-sigma on 48 Sources

Source	Type
Crab	PWN
Vela PWN	PWN
MSH 15-52	PWN
Cyg X-1	Accreting stellar black-hole
4U-1630-47	Accreting stellar black-hole
Cyg X-3	Accreting stellar black-hole
Her X-1	Accreting Neutron Star
Cen X-3	Accreting Neutron Star
XTE 1701-46	Accreting Neutron Star
GRO J1008-57	Accreting Neutron Star
4U 0142+61	Magnetar
1RXS j170849	Magnetar
Mrk 501	Blazar
Mrk 421	Blazar
1ES1959+650	Blazar
Cyg X-3	Accreting Stellar Black-Hole
GRO J1008-57	Accreting Neutron Star
LSV 44-17	Accreting Neutron Star
GX 5-1	Accreting Neutron Star

SOME RESULTS FROM IXPE CHANGED THE GAME

(Xie et al., 2022)

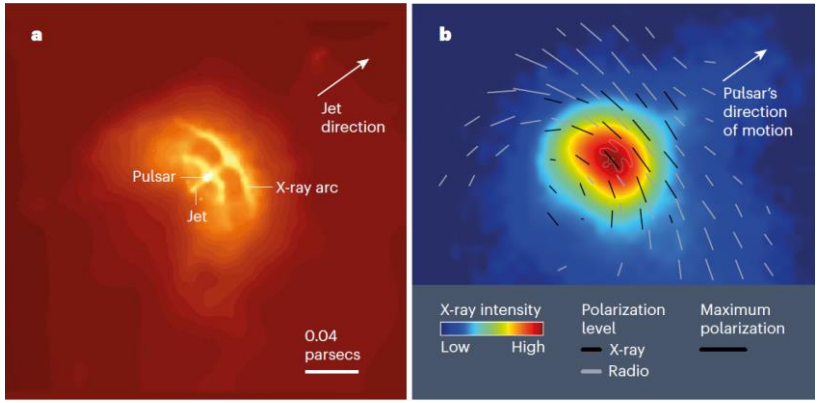

Vela PWN showed a polarization close to the synchrotron limit

(Doroshenko et al., 2022)

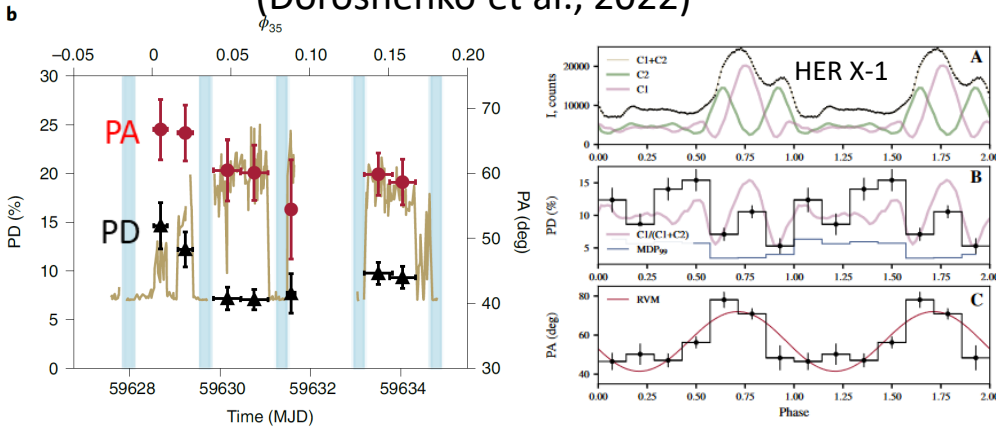

X-ray binary pulsars much less polarized than expected.

Taverna et al. 2022

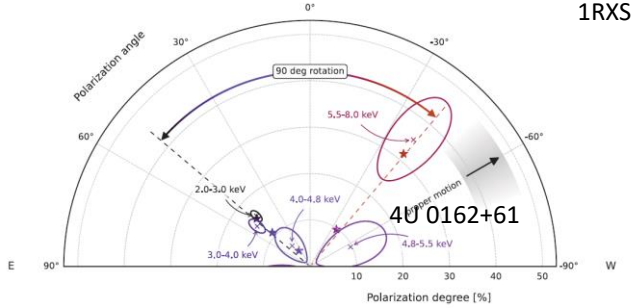

Zane et al. 2023

1RXS J170849.0-400910

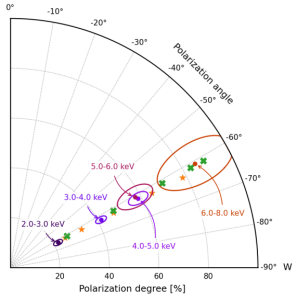

Two magnetars: two different behaviors of energy-resolved polarimetry challenge models

Krawczynski et al., 2022

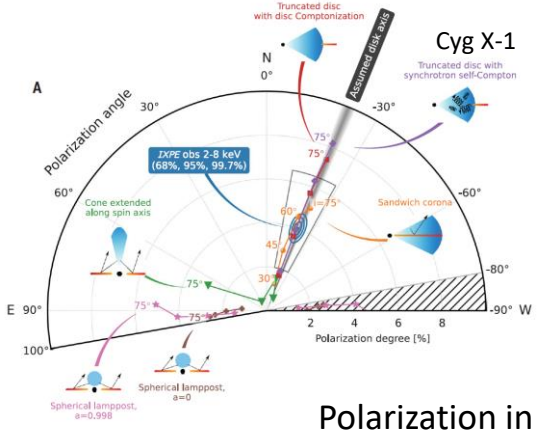

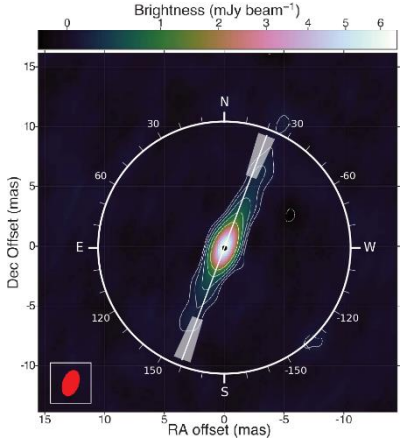

Polarization in Cyg X-1 larger then expected. Sandwich corona for both Cyg X-1 and NGC 4151

Gianolli et al., 2023

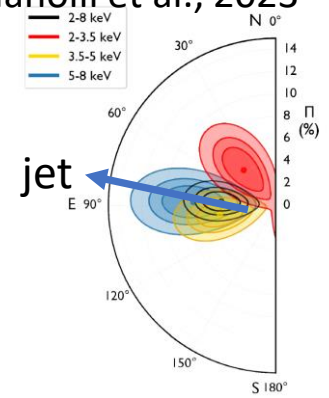

NGC 4151

CEN X-3 AND HER X-1 DISENTANGLING THE GEOMETRY

Cen X-3

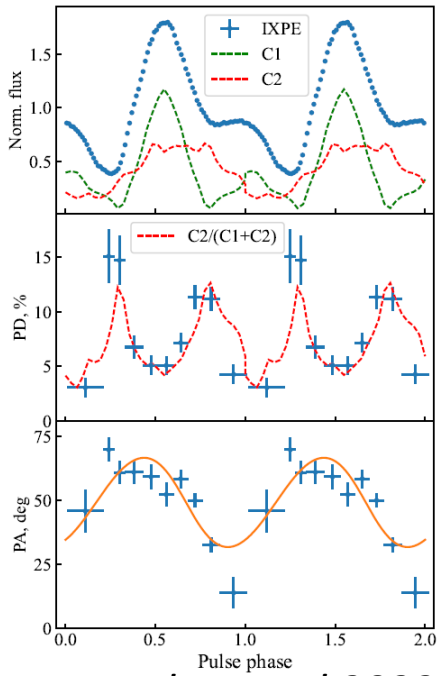

Tsygankov et al 2022

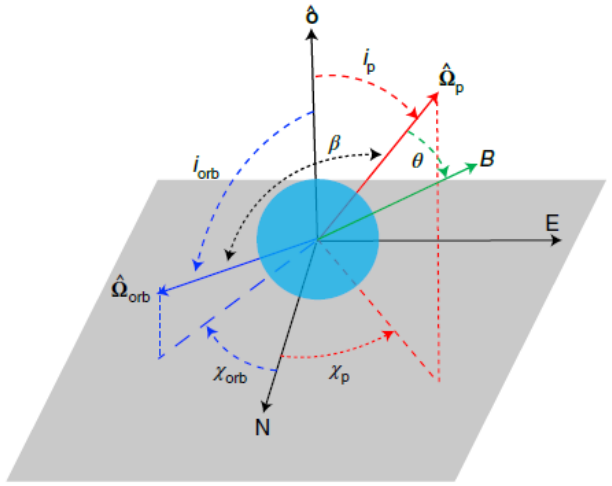

Fig. 4 | Geometry of the system from the observer's perspective. The grey plane is the plane of the sky, labelled with north and east axes, perpendicular to the line of sight towards the observer $\hat{o}$. The angles between the line of sight and the vectors of the pulsar spin $\hat{\Omega}_p$ and the orbital angular momentum $\hat{\Omega}_{orb}$ are the inclinations i_{orb} and i_p. The corresponding position angles χ_p and χ_{orb} are the azimuthal angles of the spin vectors projected onto the sky, measured from north to east. The misalignment angle β is defined as the angle between $\hat{\Omega}_p$ and $\hat{\Omega}_{orb}$. The magnetic obliquity θ is the angle between magnetic dipole and the rotational axis.

Her X-1

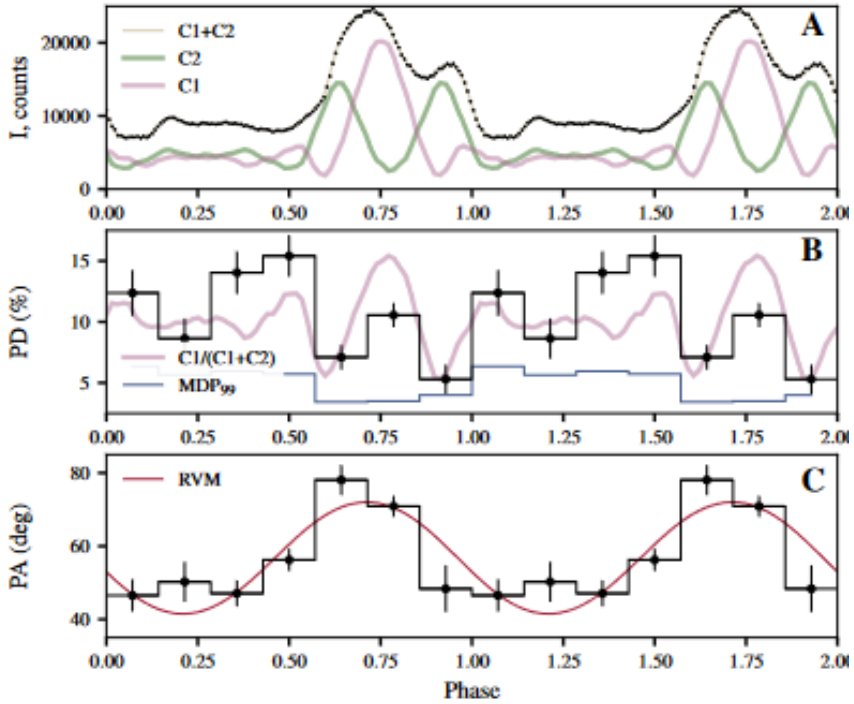

Doroshenko et al., 2022

Rotating Vector Model	
Magnetic obliquity	Θ = 16.4(±1.3)°
Inclination	I_p = 70°.2
Position angle	X_p = (49.2 ± 1.1)°

Table 1 | Orbital and pulsar geometrical parameters of Her X-1

$\chi_{p,*}$	θ	i_p	$\chi_{orb,*}$	i_{orb}
deg	deg	deg	deg	deg
56.9±1.6	12.1±3.7	Eq. (2)	28.9±5.9	100.4±4.9

SuperNova Remnants

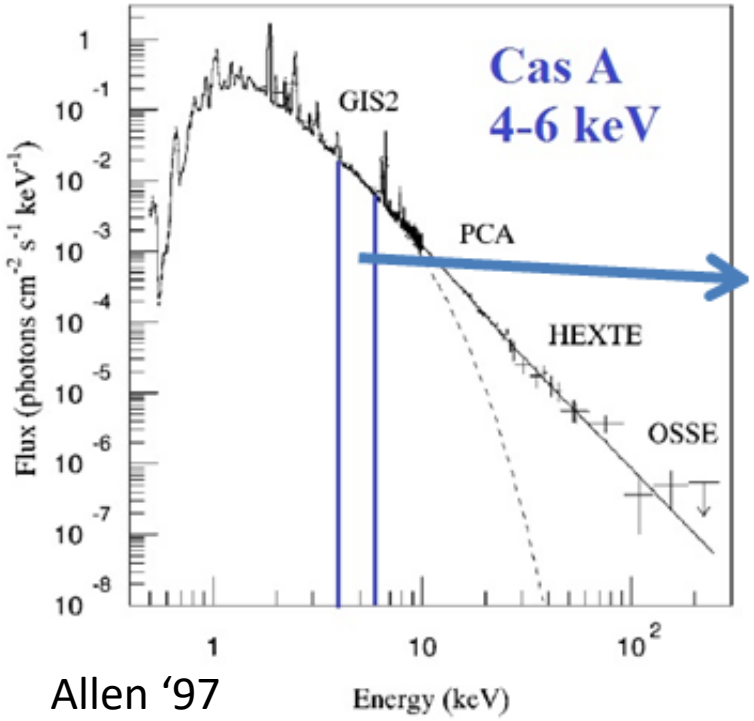

Allen '97

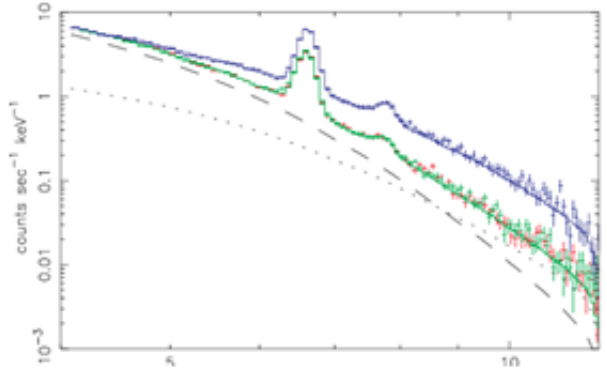

Bleeker 2001

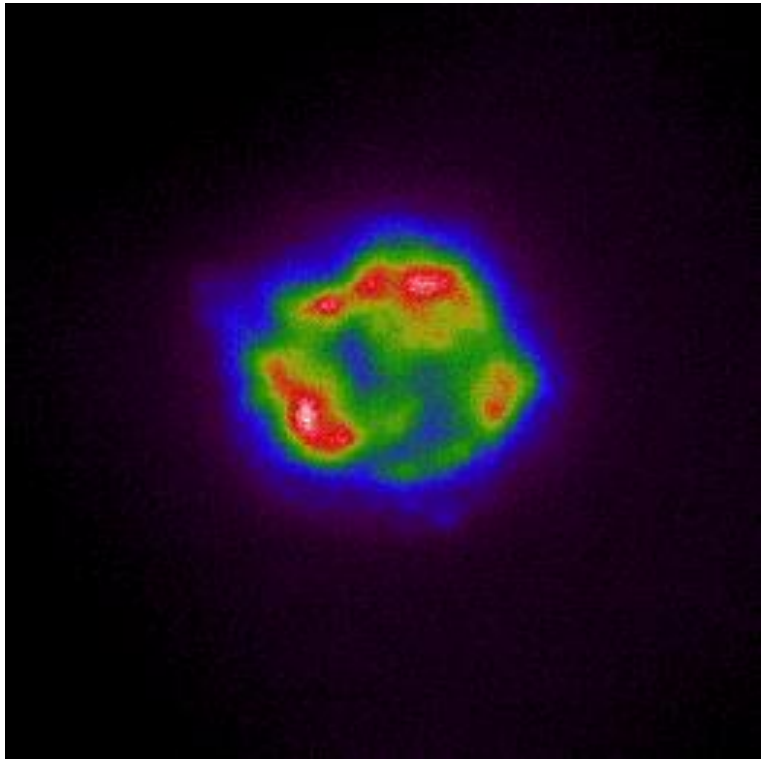

Rotating each photon with respect to the center and selecting the energy range between the calcium line and the Iron line we demonstrated that, as in radio, the polarization angle is perpendicular to the radius of the SNR as in radio band *(Vink et al. 2022)*

SNR: Cas A

Polarization of the non-thermal emission is low (2-5 %) similar to radio.
Both radio and X-rays point to radial magnetic field → Turbulent magnetic field realignment close to the shock.

Vink et al., 2022

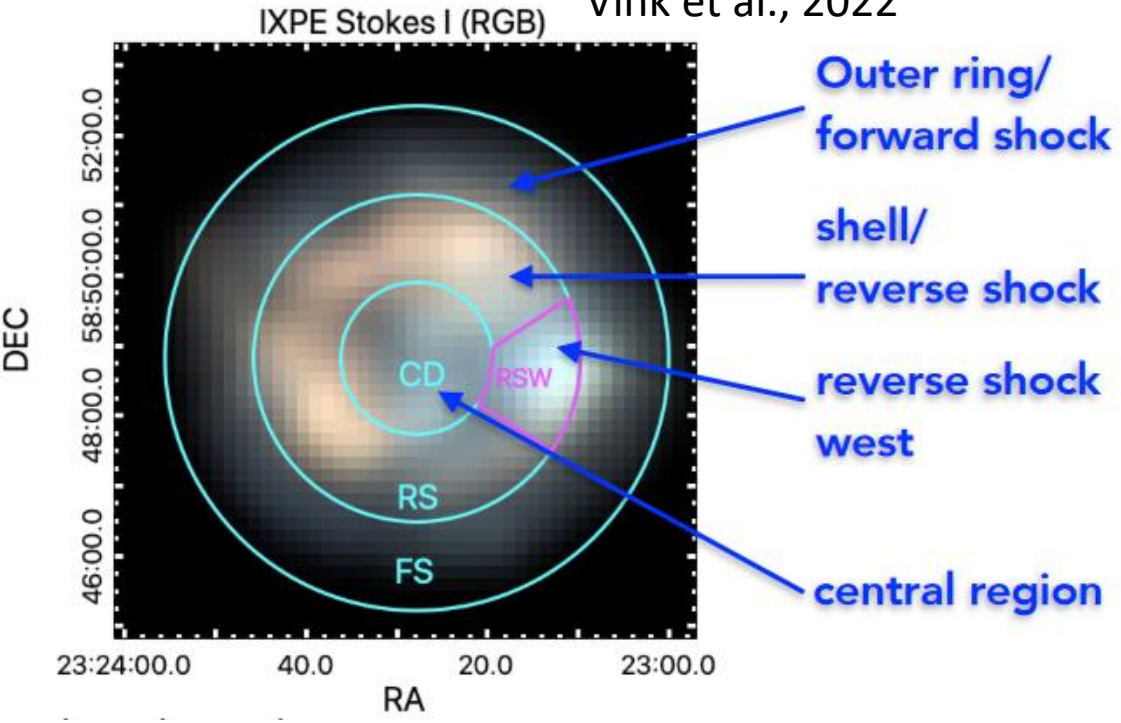

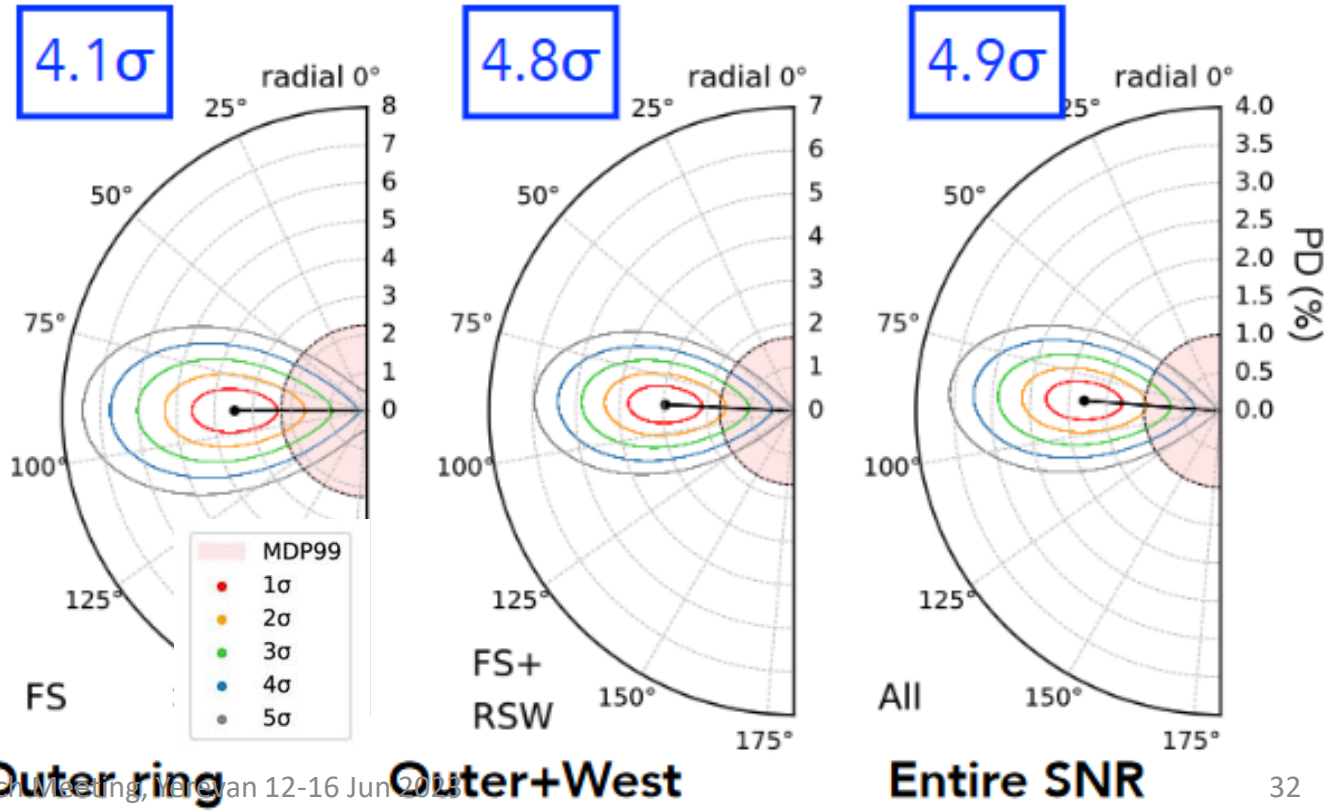

Core collapse, AD 1667?

SNR: Tycho

Qualitatively similar results for Tycho (i.e. radial magnetic field), but with larger polarization degrees, up to 23±4 % in the west region *(Ferrazzoli et al. 2023)*

→ Less turbulent magnetic field (or a larger maximum turbulence scale)

Type Ia, AD 1572

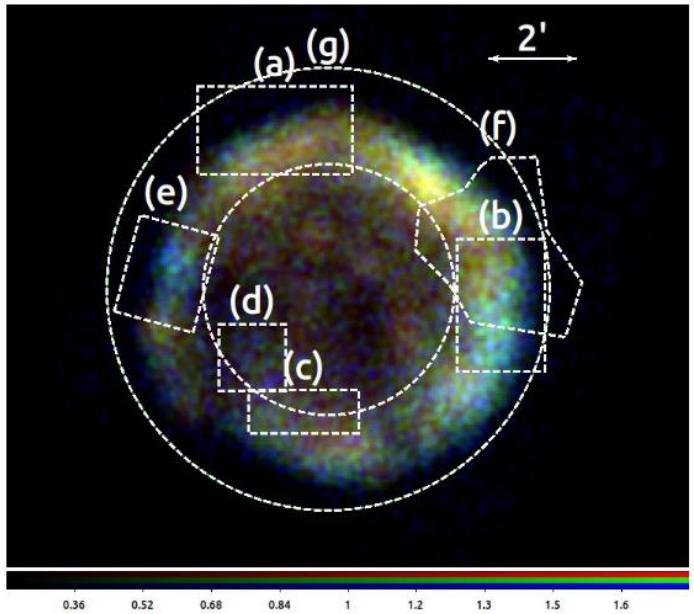

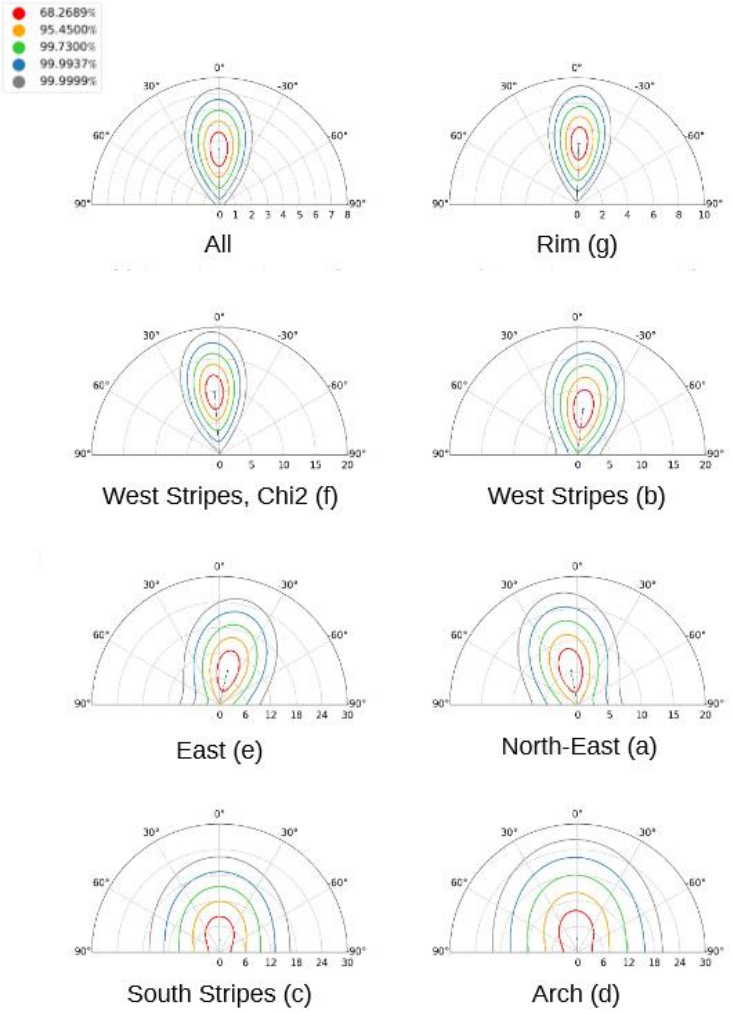

Figure 2. IXPE three color image of Tycho combined from the three detectors based on the 2–3 keV (red), 3–4 keV (green), and 4–6 keV (blue) bands. Superimposed are the regions considered in this work: the northeast (a), the west stripes (b), the south stripes (c), and the Arch (d) are the ones identified by Eriksen et al. (2011). The regions (e) and (f) are, respectively, the east knot and the west region where strong X-ray polarization is detected. Finally the region (g) identifies the rim and the entire SNR.

FROM POLARIMETRY OF MOLECULAR CLOUDS IN THE GALACTIC CENTER REGION TO ROTATING POLARIZATION IN BLAZARS

IXPE Imaging X-Ray Polarimetry Explorer

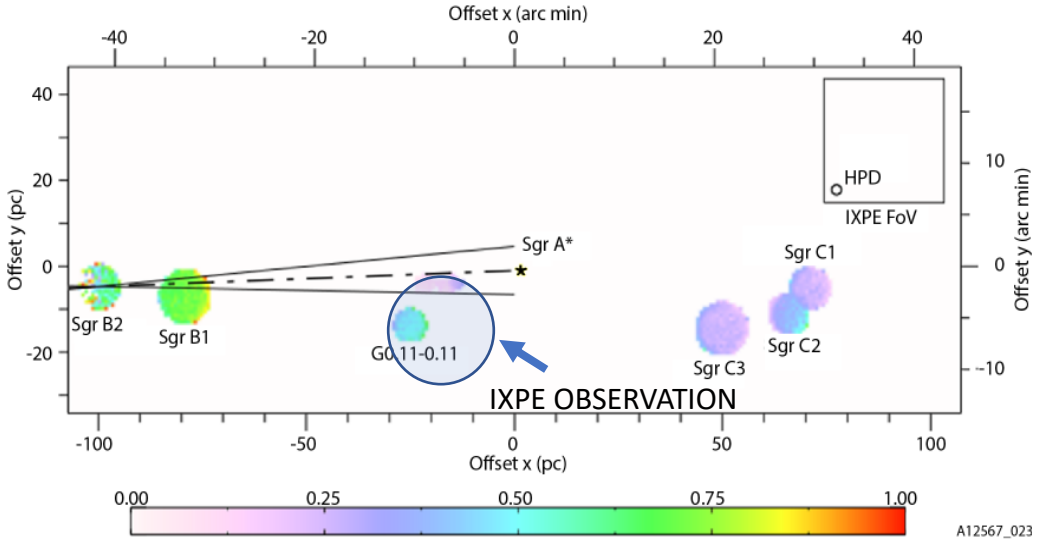

Molecular clouds are cold clouds emitting X-rays.

Possibly they are reflecting emission from the past from Sgr A*

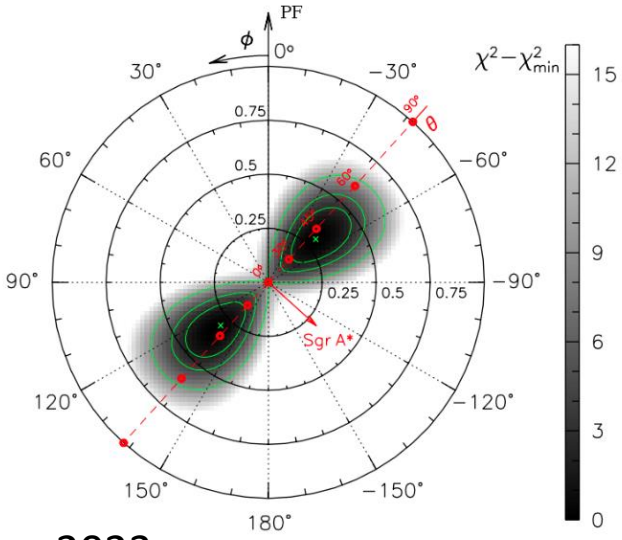

Marin et al., Nature 2023

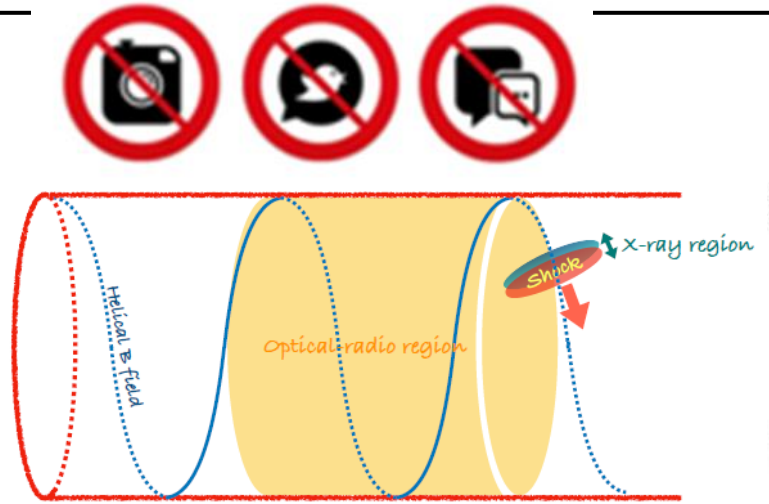

Radio Galaxies with relativistivc jets directed toward us are called Blazars

IXPE detected for the first time a rotation of the polarization angle with time. An helical magnetic field.

No rotation at longer wavelength

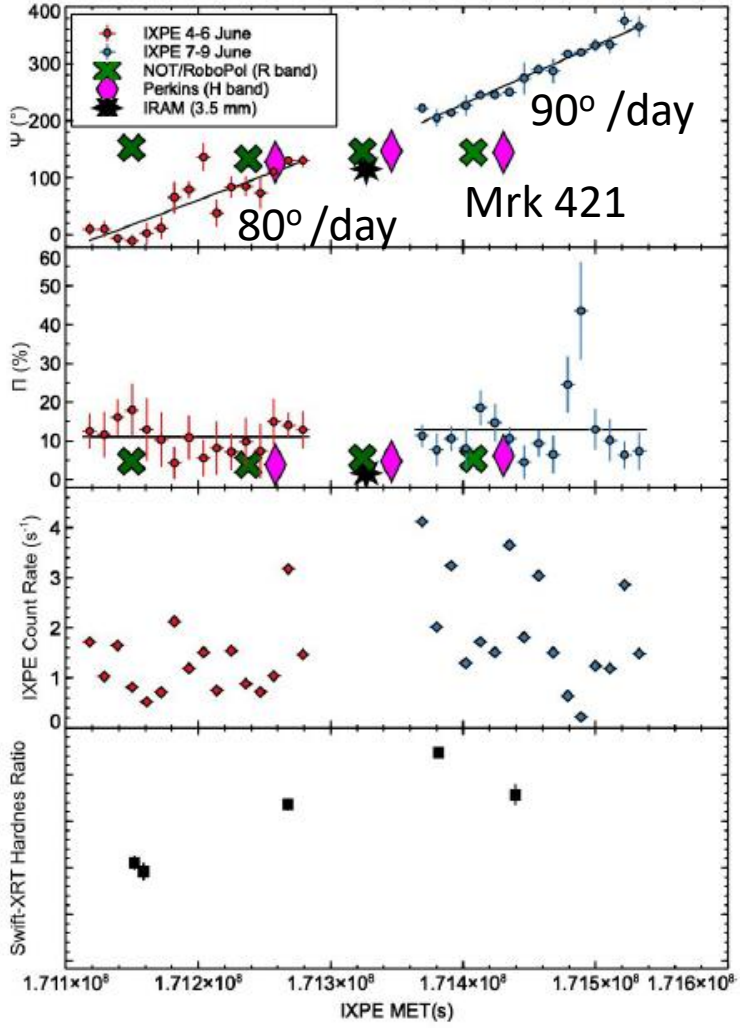

Di Gesu et al., Nature Astronomy

2-D round track image: emission direction or scattering ?

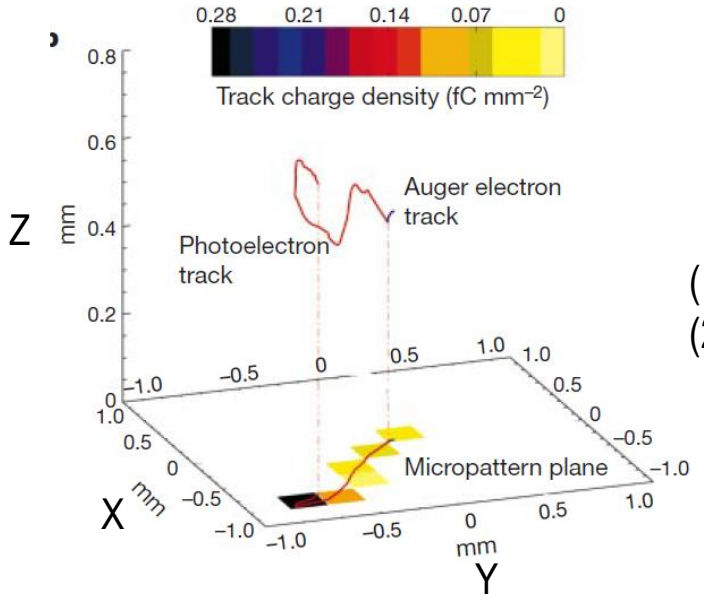

Costa et al., 2001

Ambiguity: is the 2-D image of a track round

(1) Because of the scattering Rutherford ?
(2) Because it is ejected perpendicularly to the readout plane ?

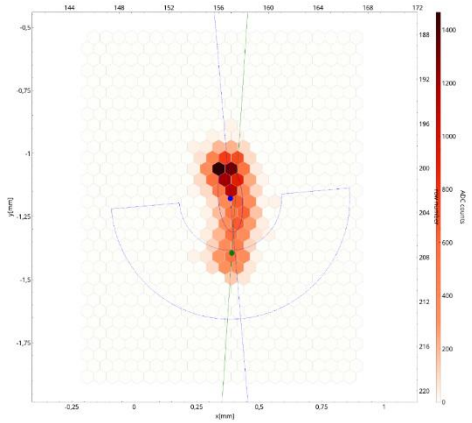

Photoelectron track ejected parallel to the X-Y plane

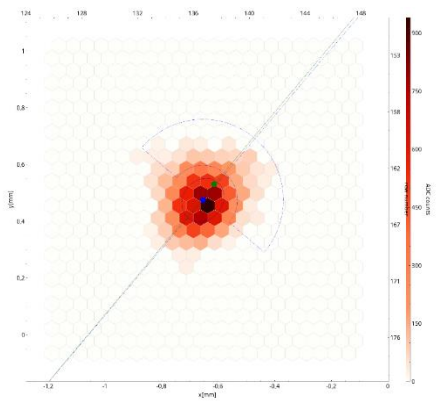

Track either randomized or ejected along Z

TimePIX3: from MEDIPIX CERN collaboration

Timepix3: a 65K channel hybrid pixel readout chip with simultaneous ToA/ToT and sparse readout

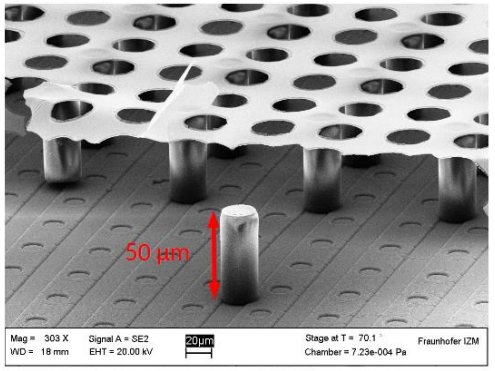

Kaminski, 2017, Lupberger 2015

Parameter	Value
Pixel matrix	256 x 256 = 65536 pixels (2x4 superpixels)
Pixel size	55 x 55 µm^2
Technology	CMOS 120 nm
Measurement type	1. Simultaneous 10 bit TOT, 14 + 4 bit ToA 2. 14 + 4 bit ToA only 3. 14 bit integral ToT
Readout type	1. Data Driven (zero-suppression) 2. Frame based (zero-suppression)
Dead time per pixel	ToT + 457 ns (pulse processing + data transfer)
Output bandwidth	Up to 5.12 Gbs (parallel 8 channels x 640 Mbps)
Maximum Counting rate	Data Driven up to 40Mhits/cm^2/s with duty cycle of 100 %
TOA precision (resolution)	1.56ns
Front End noise, minimum threshold	60 e_{rms} , 500 e^-

Ongoing collaboration with University of Bonn

Wider energy band & imaging for Supernova Remnants

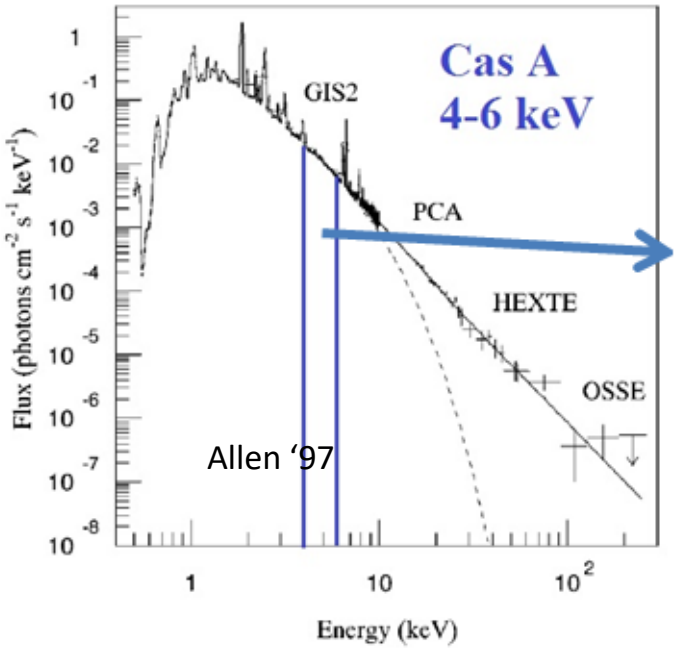

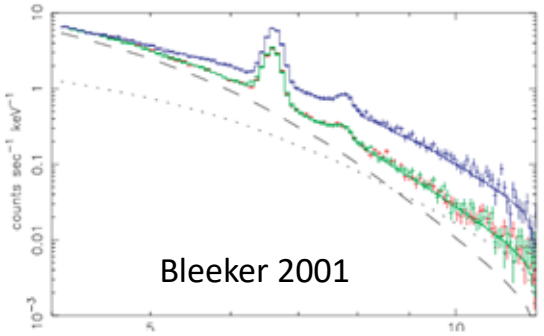

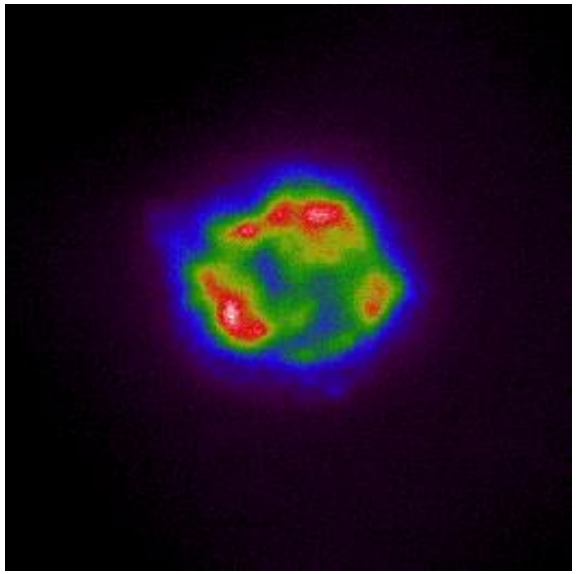

Rotating each photon with respect to the center and selecting the energy range between the calcium line and the Iron line we demonstrated that, as in radio, the polarization angle is perpendicular to the radius of the SNR *(Vink et al. 2022)*

Imaging polarimetry beyond 6.4 keV will measure polarization directly of the non-thermal emission due to synchrotron
10 m focal length will impose multiple observations for Tycho Supernova a single observation for Cas A

A wide field/collimated experiment of X-ray polarimetry requires a large area

Li, 2021

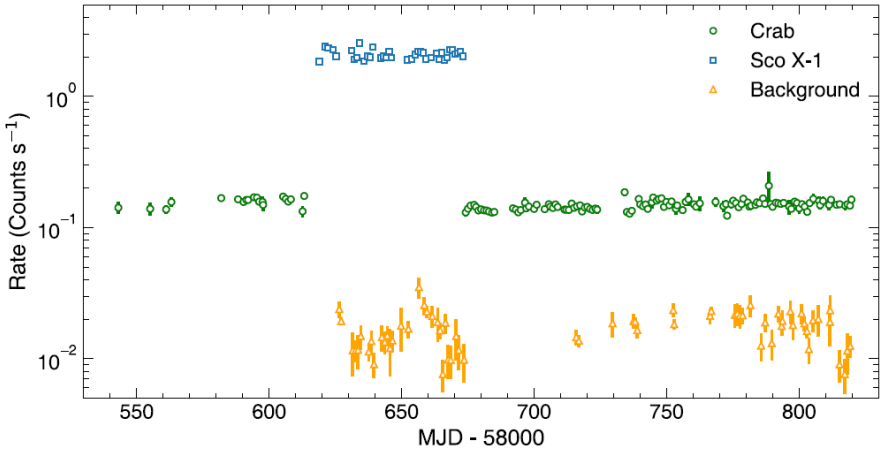

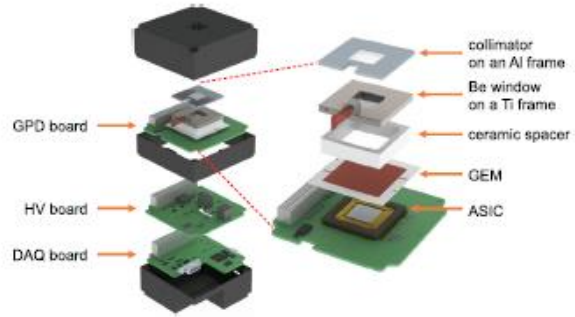

Feng et al.,, 2019

An alternative approach

- Background Polar Light : about 80 mCrab after discrimination, (Jiahuan Zhu 2021)
- Collimator open fraction 71 %
- Area 1000 cm^2
- Crab rate = 65 c/s (2-8 keV)
- Background = 5 c/s
- MDP (1 Crab 100 000 s) = 0.5 %

512x448 pixels (55x55 µm^2)
Area 1 ASIC 7 cm^2
Tiling on 4 Sides
200 ps time resolution
140 ASICs to cover 1000 cm^2

Large power required

Llopart et al., 2022

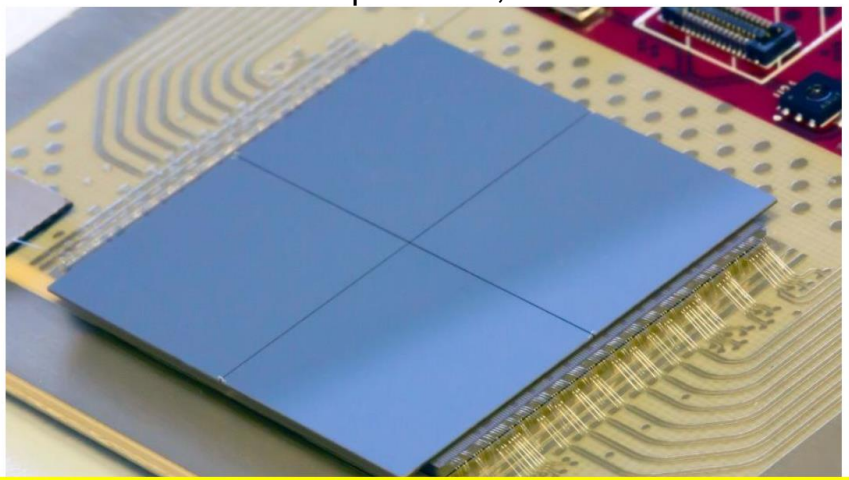

Timepix4v0 with 4x300 µm (256x256) edgeless Si sensor (August 2020)

Optical photoelectron track imaging
(see the talk by Elisabetta Baracchini)

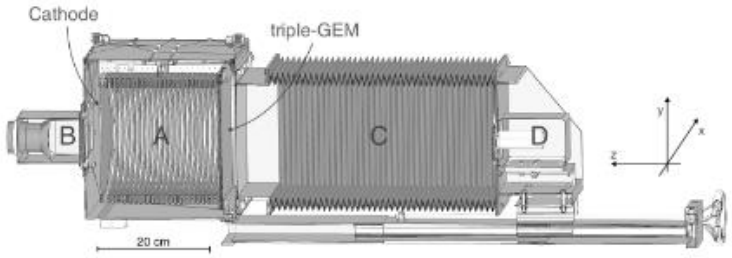

Baracchini et al., 2020, Amaro et al., 2022

Possible future photoelectric X-ray polarimetry experiments

Imaging wide energy range (ESA or NASA)

- **2-10 keV band: focal plane with large troughput conventional X-ray optics (3.5-4 meters Focal Length)**
  - DME or low diffusion mixtures
  - Scientfic objectives: all the IXPE ones but with a much larger sentitivity.Possibly add GRB afterglow and tidal disruption events if rapid repointing is available
  - Possible missions: eXTP (ESA-CAS), NGXM (ESA), XPP (NASA)
- **6-35 keV band: focal plane (photoelectric) and 20-80 segmented Compton polarimetry: multilayer optics: (10 m focal length)**
  - Pressurized Ar-DME or Ar-CO_2
  - Additional Scientific objectives:
    - Cyclotron lines
    - Hard tails of Magnetars
    - Reflections in Binaries and AGNs
    - Reflection Nebulae

    Possible missions NGXM (ESA), XPP (NASA)

Non imaging

- **Collimated narrow field experiment: Photelectric effect (2-10 keV) or (6-35 keV)**
  - Bright Galactic sources > 100 mCrab
  - Already observed by IXPE but interesting for monitoring
- **Wide field experiment (Photoelectric: charge or optical readout (see talk E. Baracchini)**
  - Broad collimator
  - Area >> 1000 cm^2
  - Prompt GRB and X-ray transients studies (Magnetars, BH binaries)

END

Improving and expanding the capabilities of X-ray Polarimetry beyond IXPE

Wide energy band and no imaging for binary X-ray pulsars

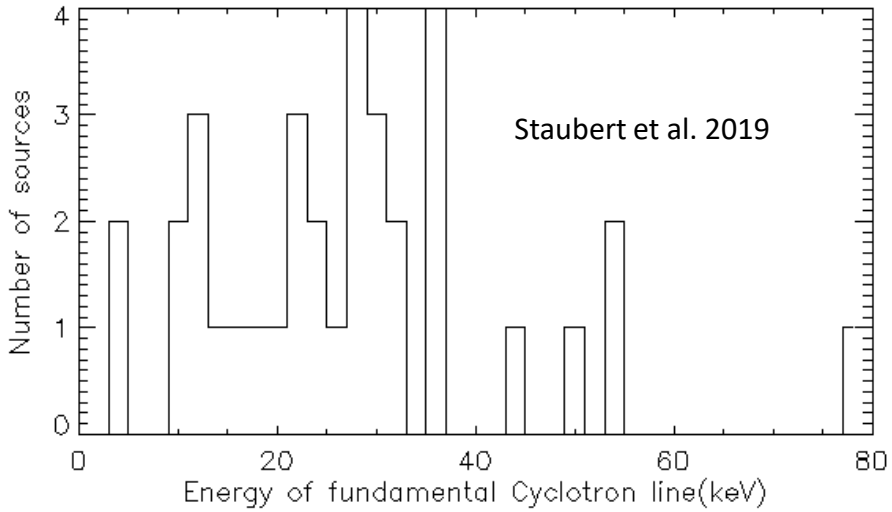

In outburst now!
But not visible by IXPE ☹

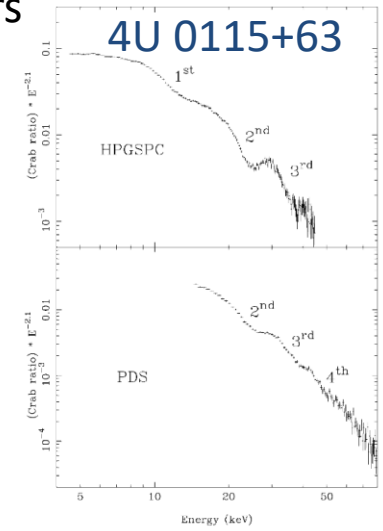

MAXI/GSC observation of brightest outburst of the Be/X-ray binary pulsar 4U 0115+63 in 27 years

ATel #15975; *M. Nakajima, H. Negoro (Nihon U.), W. Iwakiri (Chiba U.), K. Kobayashi, M. Tanaka, Y. Soejima (Nihon U.), T. Mihara, T. Kawamuro, S. Yamada, T. Tamagawa, M. Matsuoka (RIKEN), T. Sakamoto, M. Serino, S. Sugita, H. Hiramatsu, H. Nishikawa, A. Yoshida (AGU), Y. Tsuboi, J. Kohara, S. Urabe, S. Nawa, N. Nemoto (Chuo U.), M. Shidatsu, M. Iwasaki (Ehime U.), N. Kawai, M. Niwano, R. Hosokawa, Y. Imai, N. Ito, Y. Takamatsu (Tokyo Tech), S. Nakahira, S. Ueno, H. Tomida, M. Ishikawa, T. Kurihara (JAXA), Y. Ueda, S. Ogawa, K. Setoguchi, T. Yoshitake, K. Inaba, Y. Nakatani (Kyoto U.), M. Yamauchi, T. Sato, R. Hatsuda, R. Fukuoka, Y. Hagiwara, Y. Umeki (Miyazaki U.), K. Yamaoka (Nagoya U.), Y. Kawakubo (LSU), M. Sugizaki (NAOC)*
on 3 Apr 2023; 14:28 UT

High Energy Polarimeter (Scattering)

Medium Energy Polarimeter (Photoelectric)

Most of the cyclotron fundamental lines can be probed by photoelectric imaging Polarimeters (Pressurized Argon, Medium Energy). The higher energy end requires Active Compton scattering polarimeter

X-ray polarimetry in a wide energy band

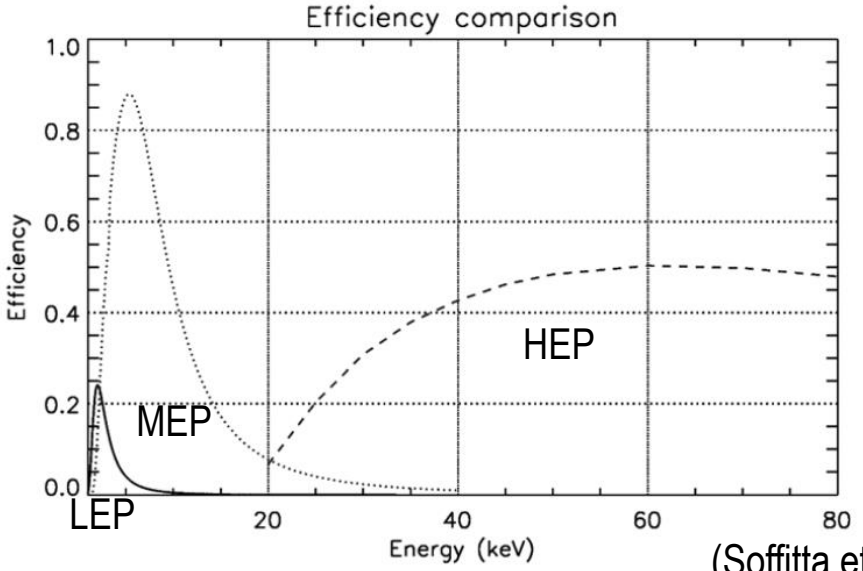

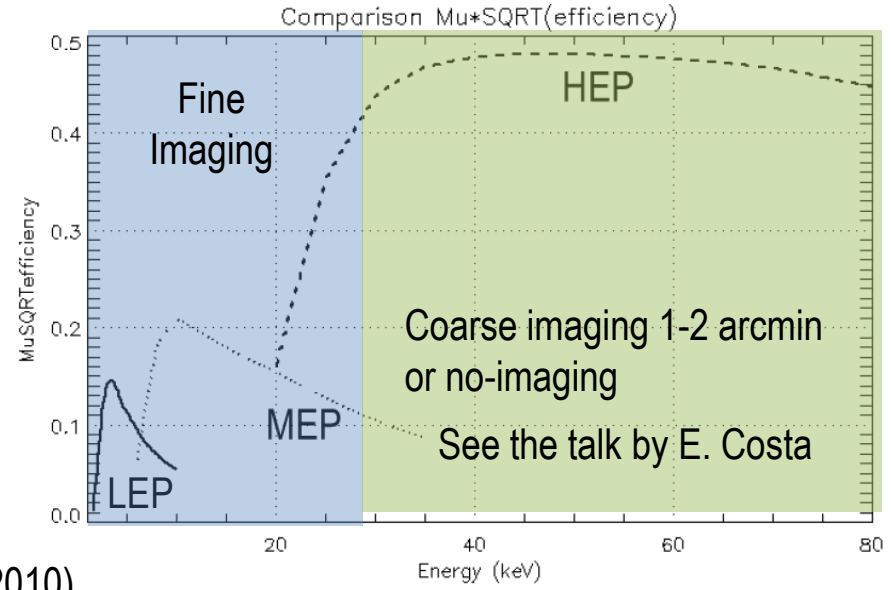

(Soffitta et al., 2010)

Low Energy Polarimeter (photoelectric, LEP, 2-8 keV) configuration IXPE-like
Medium Energy Polarimeter (photoelectric, MEP, 6-30 keV (3 bar Ar-DME 80-20 Mixture)
High Energy Polarimeter (Compton: segmented scatterer or single scatterer HEP, 20-80 keV)

The quality factor of the three polarimeters is well matched providing similar sensitivity at the focus of a multi-layer cptics

Collabortion with University of Bonn for GridPIX detector

X-ray polarimetry in a wide energy band

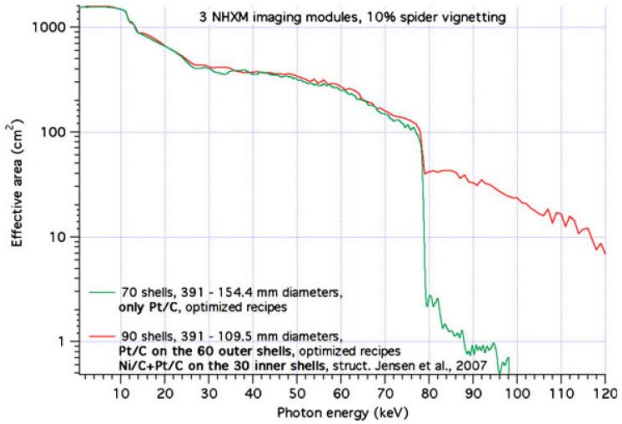

Tagliaferri et al., 2010

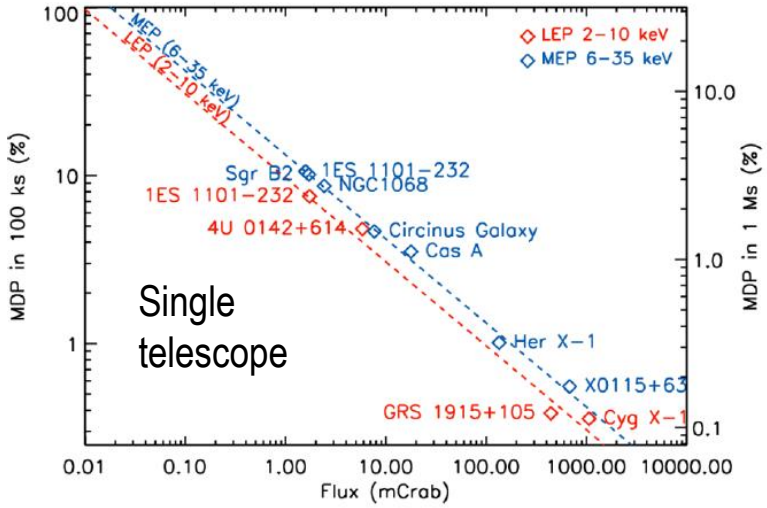

Tagliaferri et al., 2010

One NHXM-type telescope provides the sensitivity of the three IXPE telescopes

NGXM-New generation X-ray Mission
- White paper ESA Voyage 2050 (Experimental Astronomy Soffitta et al., 2020)

XPP X-ray Polarization Probe
- White paper 2020 Decadal Survey (Yahoda et al., 2019)

Fine Imaging telescopes: (2-8 keV) & (6-35 keV)
Hard X-ray imaging polarimeter (20-80 keV)
Non Imaging TPC-like experiment
Wide Field Polarimeter and Imager

- Stacked TPC (non-imaging)+ Passive Compton polarimeter
- Low energy (multilayer) polarimeter
- Imaging polarimeter

Ongoing experiments:

XL-Calibur (high background passive scatterer 10 m FL)

IXPE
Imaging
X-Ray
Polarimetry
Explorer

BACKGROUND REJECTION AND SUBTRACTION

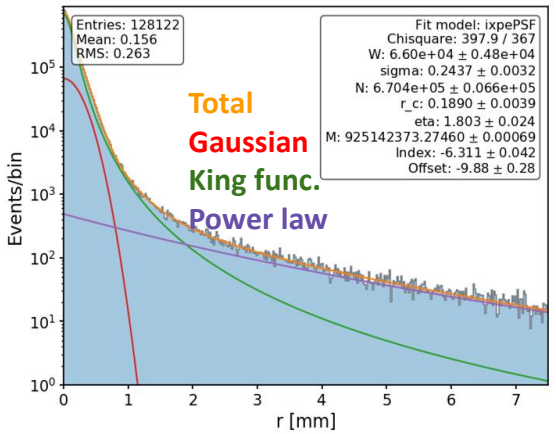

Di Marco et al., 2023 AJ accepted

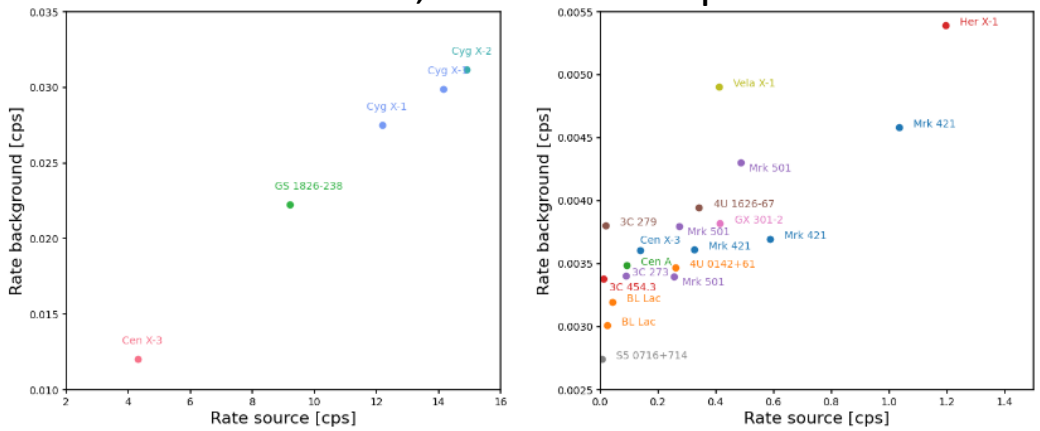

Background counting rate 0.003 c/s /arcmin^2

- *Bright source* counting rate > 2 c/s /arcmin^2 (~15 mCrab)
  No Rejection and No Subtraction to be applied to the data
- *Faint Sources* counting rate < 1 c/s /arcmin^2 (~7.5 mCrab)
  Either Rejection and Subtraction to be applied to the data
- *Intermediate source*
  Rejection to be applied No subtraction unless background template

In the current pipeline *background rejection* is not applied. Needed Level 1 data
Background subtraction can be performed on Level 2 data as for any X-ray imaging satellite

Photoelectric polarimetry for HETE-2 GRB

A wide field polarimeter with 1000 cm^2

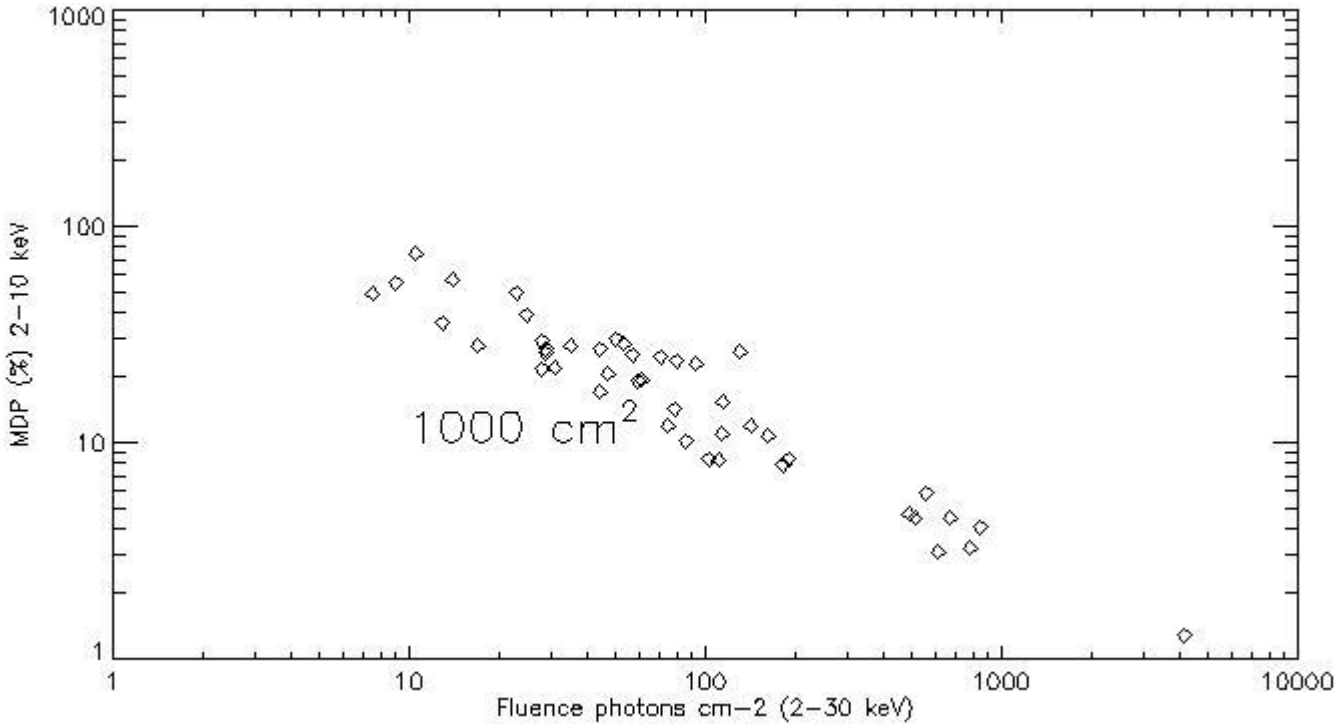

DME 1 Atm 4 cm deph

IXPE Imaging X-Ray Polarimetry Explorer

GRB 221009A

We did not plan to follow-up on GRBs, because of the relatively slow reaction time (2-3 days).

However, GRB 221009A (the 'BOAT' GRB) was so exceptional in terms of brightness, that we decided to observe it.

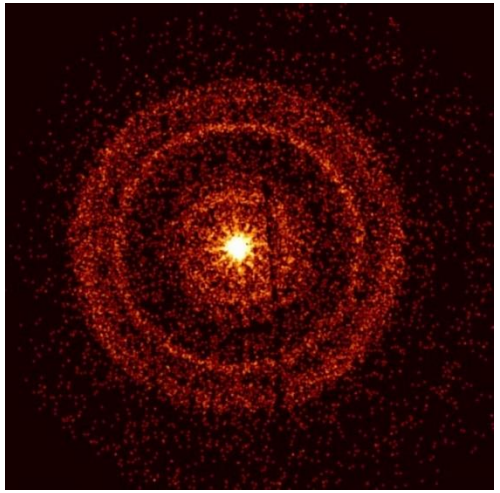

Swift/XRT image

P<13.8% (99% c.l.)

(Negro et al. 2023)

Dust rings also observed →

polarization of the prompt emission (<55%)

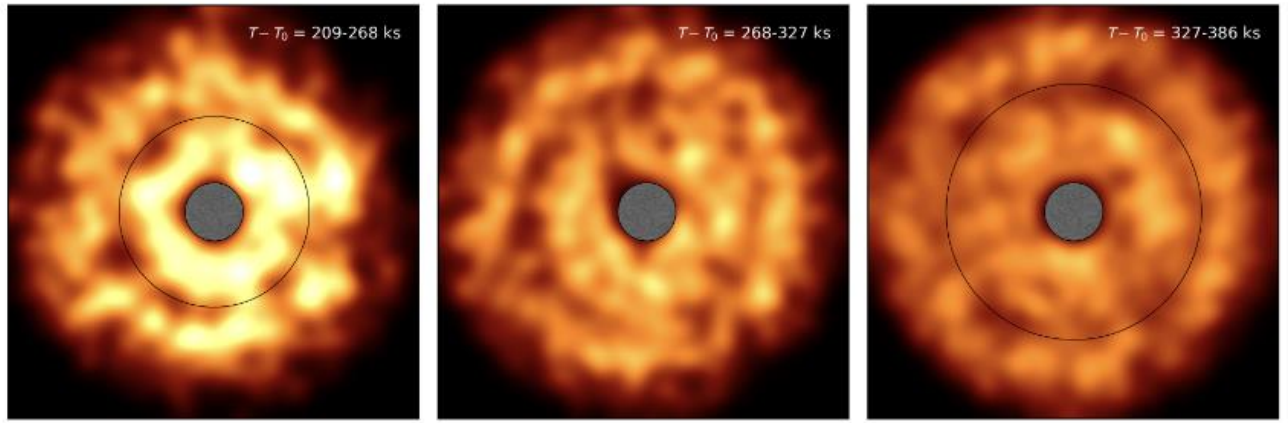

Time evolution of dust rings as seen by IXPE

Improving and expanding the capabilities of X-ray Polarimetry beyond IXPE

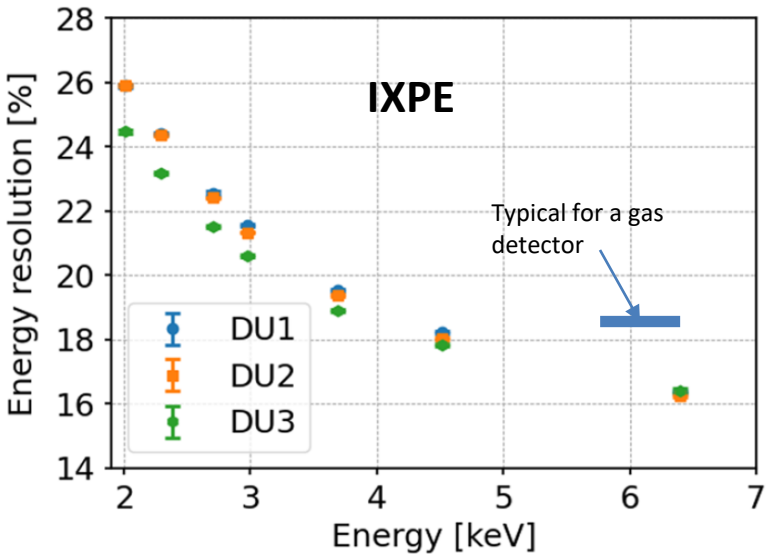

Weisskopf et al., 2022

Energy resolution

The energy resolution is already better than that the typical proportional counter

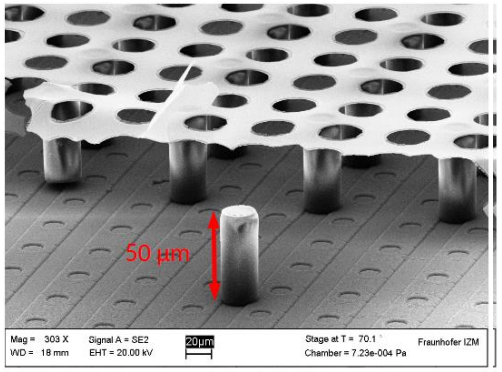

Kaminski 2017

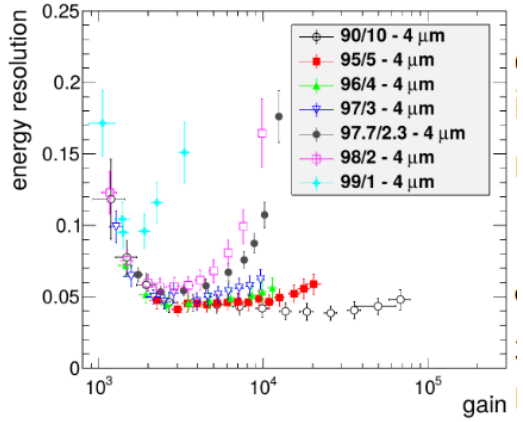

An energy resolution down to 10 % can be reached with GridPIX technologies at 6 keV

Wide energy band and no imaging for Low Magnetized Neutron Stars

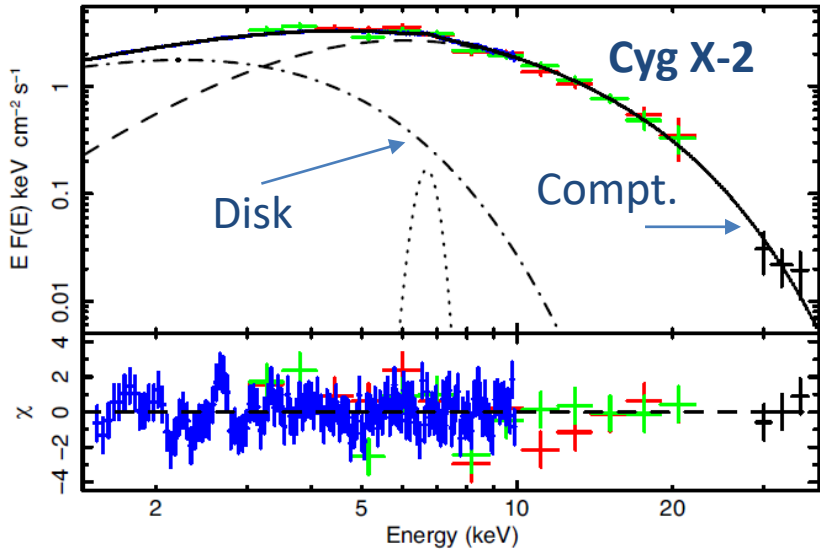

Farinelli et al., 2022

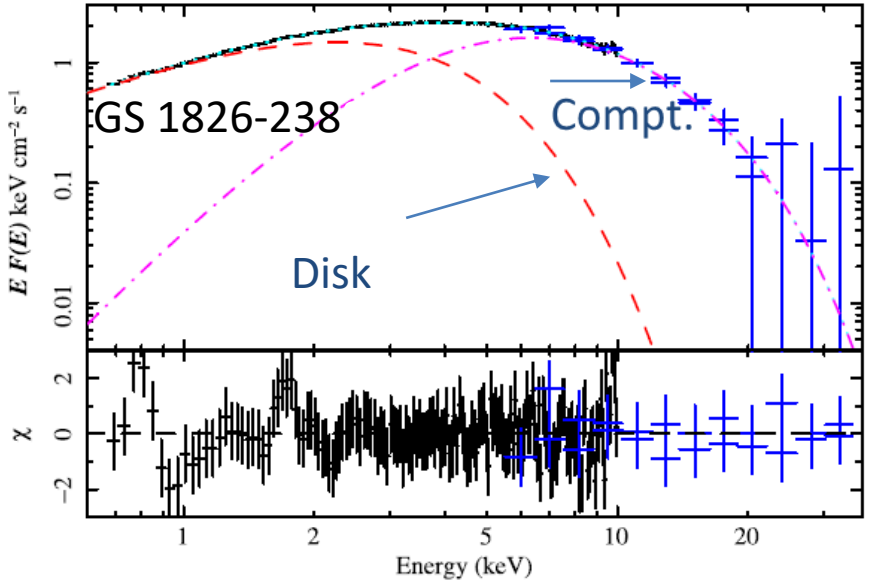

Capitanio et al., 2022

Comptonization extends up to 20-30 keV. It might be interesting to explore polarimetry in this energy band. It might help to constrain the geometry of the reflecting elements

Improving and expanding the capabilities of X-ray Polarimetry beyond IXPE

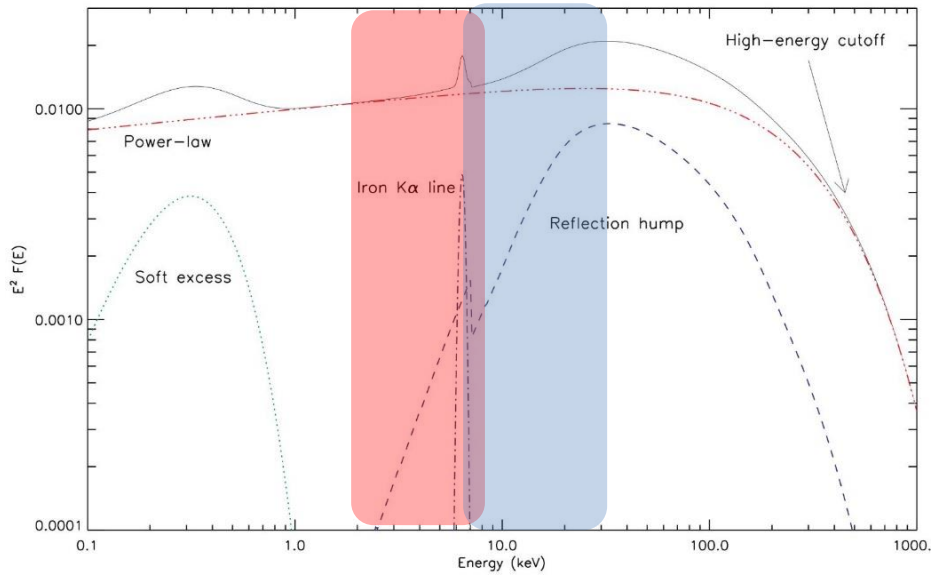

IXPE energy band

Future Hard X-ray imaging polarimetry

Wider energy band & imaging for AGNs

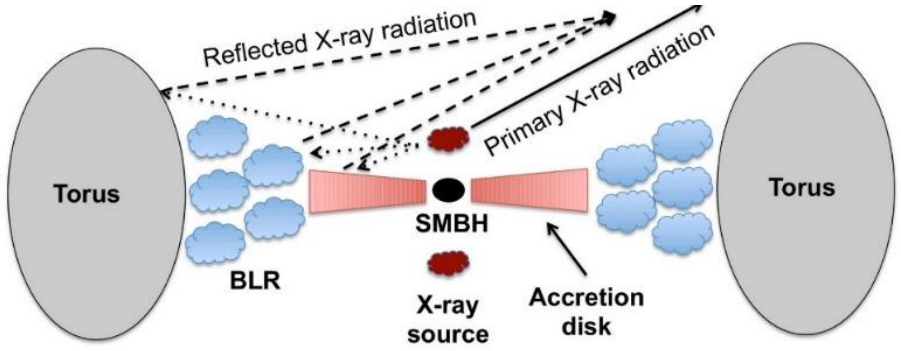

Credit Ricci, C.

Polarimetry above 6 keV to study reflection phenomena suffers of both a small detector quantum efficiency/mirror effective area. Reflection phenomena are poorely constrained

Improving and expanding the capabilities of X-ray Polarimetry beyond IXPE

Larger Effective area & better Point Spread Function

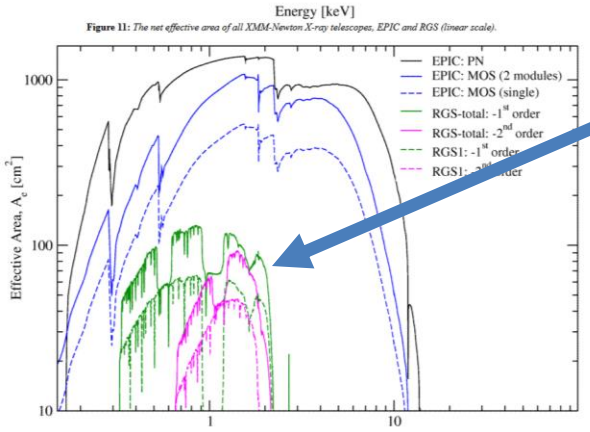

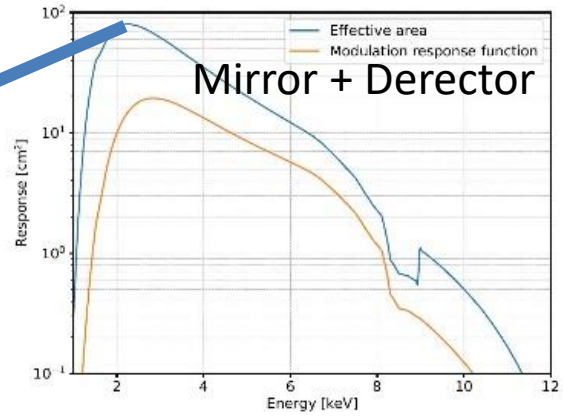

Larger mirror effective area

Larger detector Q.E.-> electro-negative mixtures

Better than 30’ HEW

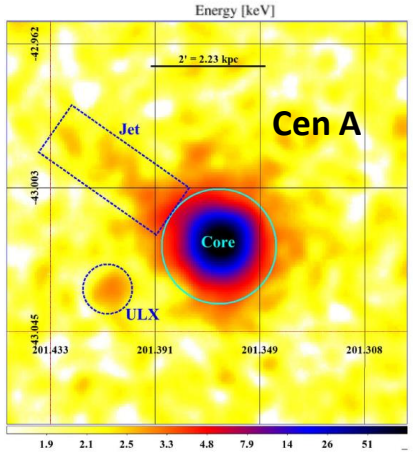

36 % MDP on the jet (100 ks)

Ehlert et al., 2022

Two magnetars showed different behavior with 1 Ms net observing time (20 days each). Needed a large area to improve the sensitivity.

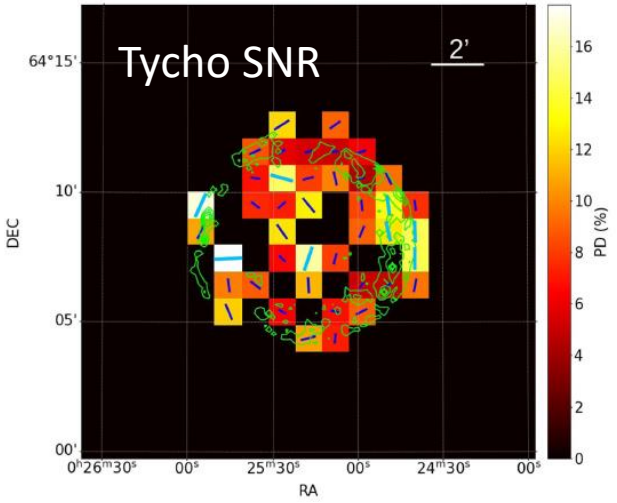

Ferrazzoli et al., 2023

Few pixels showed significant polarimetry

IXPE
Imaging
X-Ray
Polarimetry
Explorer

MRK 501

Mrk 501 HBL Blazar
Peak @2.8 10^{15} Hz

γ-ray > 0.1 TeV

IXPE observed Mrk 501
at an average X-ray flux.

Observed three times for total 300

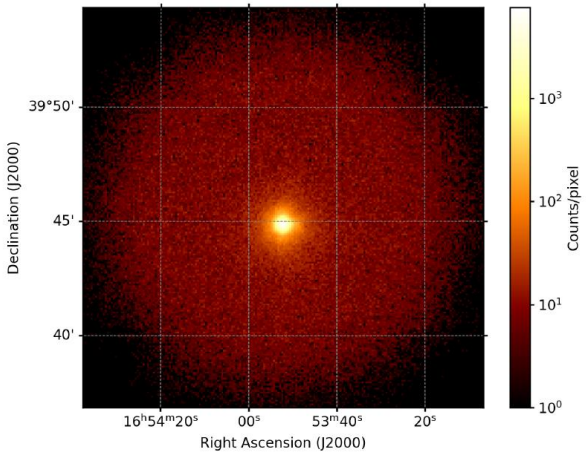

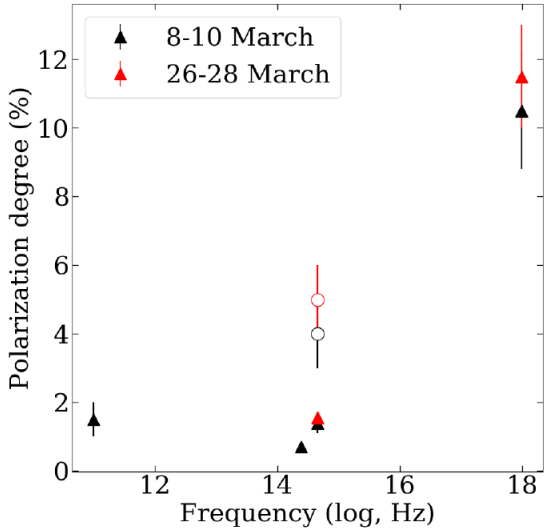

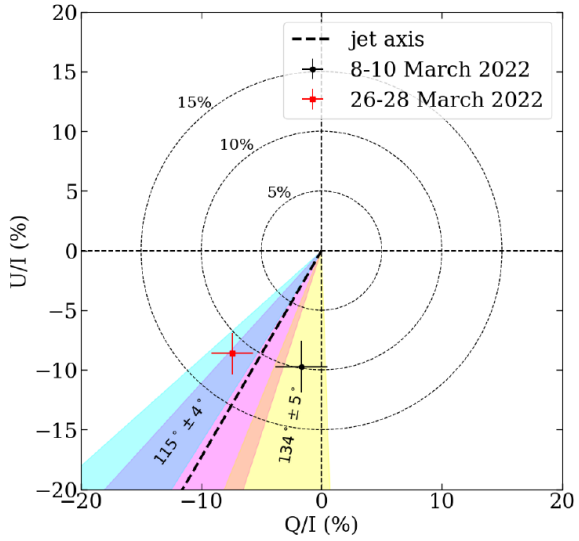

Model	Mltiwavelength polatization	X-ray polarization variability	X-ray polarization angle
Single-zone	Constant	Few-days/week	any
Multi-zone	Mildly chromatic	Less of 1 day	any
Energy stratified (shock)	Strongly chromatic	Few-days/week	Along the jet axis
Magnetic reconnection (kink instability)	Constant	Moderate	Perpendiculat to the jet axis
IXPE Finding	**Stronghly chomatic**	**Few-days/week**	**Along the jet axis**

- Shock acceleration: the higher energy particles probe more magnetically ordered regions closer to the shock
- Downstream of the shock the magnetic field becomes more turbulent were less energetic photons are emitted

Liodakis, Y. et al., Nature 2022

IXPE
Imaging
X-Ray
Polarimetry
Explorer

A ROTATION OF THE POLARIZATION ANGLE IS DETECTED IN X-RAYS

- During X-ray rotation millimiter-wave, infrared and optical polarization angle didn't vary substantially.
- Rotation in optical light is few-few tens of degree/day
- PD_X was roughly constant and higher wrt Optical, Infrared and Radio
- At GeV was in a quiescent state

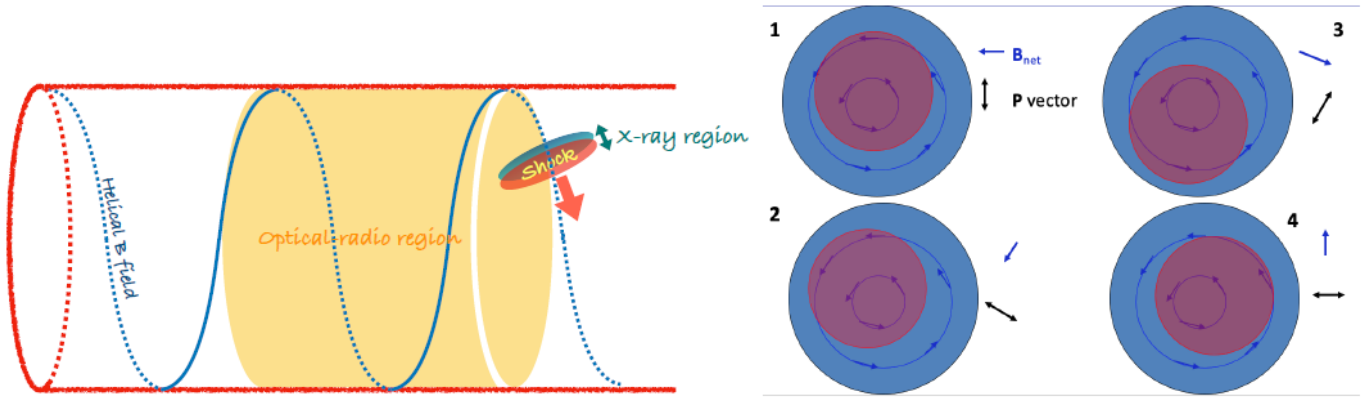

Fig. 2 Sketches of the scenario proposed to explain the X-ray polarization angle rotation in Mrk 421. Left: an off axis emission feature, e.g., a magnetosonic shock, propagates along helical magnetic field lines down the jet. Right: the appearance of the emission feature, magnetic field, and polarization vector at 4 azimuthal positions along its spiral path as viewed by a distant observer aligned with the jet. The red circle represents the emission feature, while the blue-shaded region is the ambient jet.

Di Gesu, Nature Astronomy in press

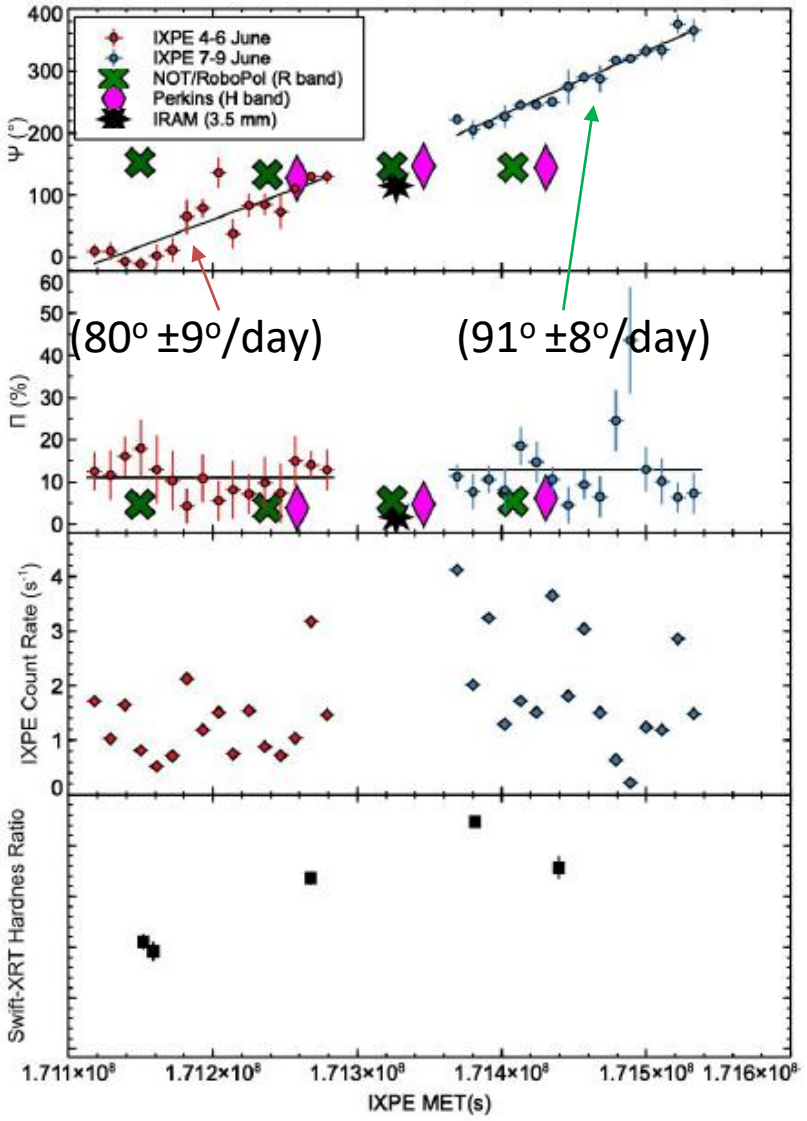

IXPE Imaging X-Ray Polarimetry Explorer

TARGETS

- **OBJECTIVE 1: Active Galactic Nuclei (AGN)**
  - Obtain polarimetry of RQ AGN to constrain the geometry of the emitting regions, and of Blazars and RG to study jet emission
- **OBJECTIVE 2: Microquasars**
  - Obtain spectral polarimetry of microquasars to constrain the value of the black-hole spin parameter (if in soft state), or constrain the geometry of the corona (if in hard state)
- **OBJECTIVE 3: Radio Pulsars and Pulsar-Wind Nebulae**
  - Obtain polarimetric imaging of the Crab to constrain the magnetic-field geometry of the nebula and the phase-dependent polarization of the pulsar
- **OBJECTIVE 4: Supernova Remnants**
  - Obtain spectral polarimetric imaging of Supernova Remnants (SNR) to constrain the magnetic-field structure of the X-ray emitting regions
- **OBJECTIVE 5: Magnetars**
  - Obtain phase-dependent polarimetry of magnetars to constrain the effects of vacuum polarization (birefringence in a strong magnetic field)
- **OBJECTIVE 6: Accreting Neutron Stars**
  - Obtain phase-dependent polarimetry of accreting X-ray pulsars (high-magnetic-field binaries) to constrain models and geometries for the pulsing emission.
    Obtain polarimetry of non pulsating accreting NS to constrain the geometry of the system.

Was the galactic center active 200 years ago ?

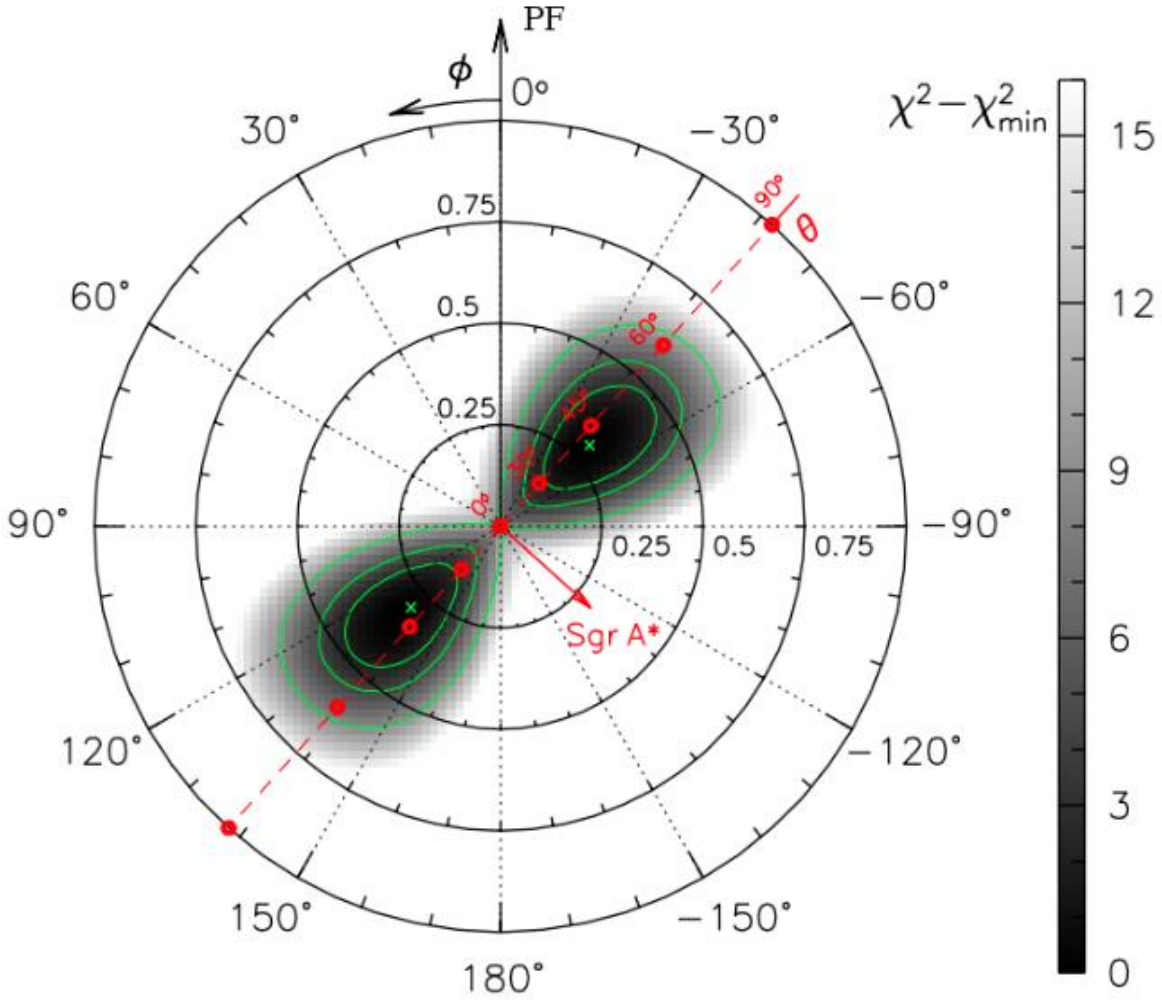

2.8σ result. Polarization angle consistent with Sgr A* as the origin of the illuminating radiation.

From the polarization degree, two solutions for the age of the burst: ~30 or ~200 years ago. Second solution much more probable a flare 30 years old should have been visible.

Marin et al., Nature in press (June 2021)

TO CONCLUDE

Beside a larger effective area and better HEW mirror

Determination of geometrical parameters

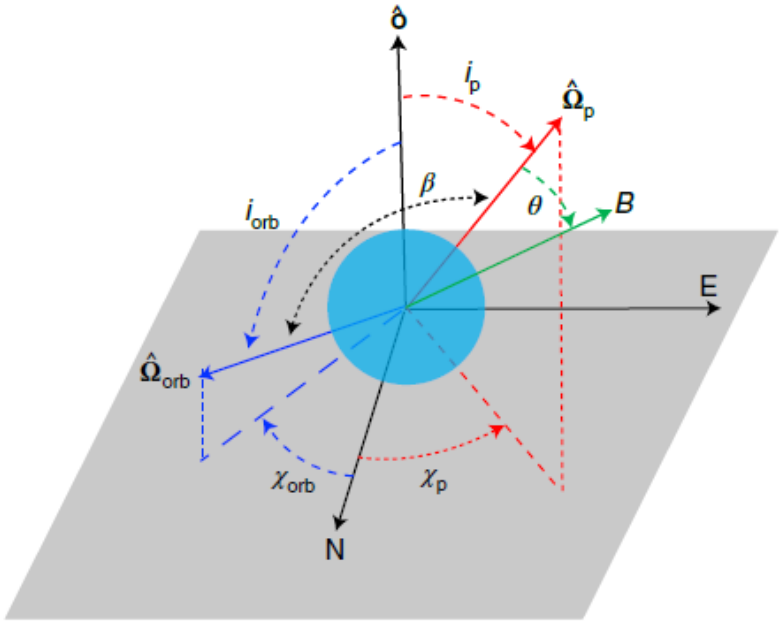

Fig. 4 | Geometry of the system from the observer's perspective. The grey plane is the plane of the sky, labelled with north and east axes, perpendicular to the line of sight towards the observer $\hat{\mathbf{o}}$. The angles between the line of sight and the vectors of the pulsar spin $\hat{\Omega}_p$ and the orbital angular momentum $\hat{\Omega}_{orb}$ are the inclinations i_{orb} and i_p. The corresponding position angles χ_p and χ_{orb} are the azimuthal angles of the spin vectors projected onto the sky, measured from north to east. The misalignment angle β is defined as the angle between $\hat{\Omega}_p$ and $\hat{\Omega}_{orb}$. The magnetic obliquity θ is the angle between magnetic dipole and the rotational axis.

Table 1 | Orbital and pulsar geometrical parameters of Her X-1

$\chi_{p,*}$	θ	i_p	$\chi_{orb,*}$	i_{orb}
deg	deg	deg	deg	deg
56.9±1.6	12.1±3.7	Eq. (2)	28.9±5.9	100.4±4.9

$$\tan(\mathrm{PA} - \chi_p) = \frac{-\sin\theta \sin(\phi - \phi_0)}{\sin i_p \cos\theta - \cos i_p \sin\theta \cos(\phi - \phi_0)}$$

As promised from the swing of the polarization angle is possible to derive geometrical properties: Projection of the spinning vector in the plane of the sky and the angle between the rotationa axix and the dipole axis.
These are usually free parameters in spectral fittings now they are directly measured by X-ray polarimetry

Improving and expanding the capabilities of X-ray Polarimetry beyond IXPE

Algorithms

$$MDP_{99} = 5.5\ \% \sqrt{\frac{1}{\frac{T}{10\ days} * \frac{F}{0.5\ mCrab}}}^{2} \quad (2\text{-}8\ \text{keV})$$ Requirement

- The mirror effective area after construction is about 20 % smaller than expected.
- The detector is about 20 % less efficient than expected (but larger modulation factor)

$$MDP_{99} = 6.2\ \% \sqrt{\frac{1}{\frac{T}{10\ days} * \frac{F}{0.5\ mCrab}}}^{2}$$

Unweighted analysis

$$MDP_{99} = 5.5\ \% \sqrt{\frac{1}{\frac{T}{10\ days} * \frac{F}{0.5\ mCrab}}}^{2}$$

Weighted analysis
Di Marco et al., 2022 AJ

$$MDP_{99} = 5.0\ \% \sqrt{\frac{1}{\frac{T}{10\ days} * \frac{F}{0.5\ mCrab}}}^{2}$$

Convolutional Neural Network
(Peirson& Romani, 2021 ApJ)

?

Visual Transformer & Graph Neural Network

Di Marco et al., 2022

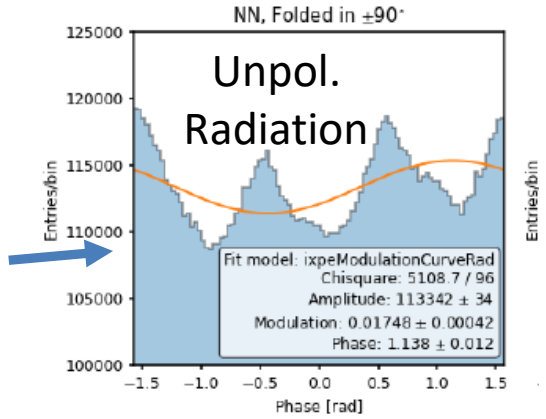

Neural Networks seems promising techniques. They need to be validated with real calibration data because Monte Carlo training can hide a non uniform response to unpolarized radiation. Measuring flat response to unpolarized radiation is very difficult.

Pulsar Wind Nebulae

IXPE observations of PWN (Crab, Vela) confirmed they are highly polarized (very high in certain regions, close to the synchrotron limit) *(Bucciantini et al. 2023, Xie et al. 2022).*

Crab result consistent with OS0-8, when integrated over the entire nebula. However, polarization map shows a complex pattern, not surprisingly given the Chandra image

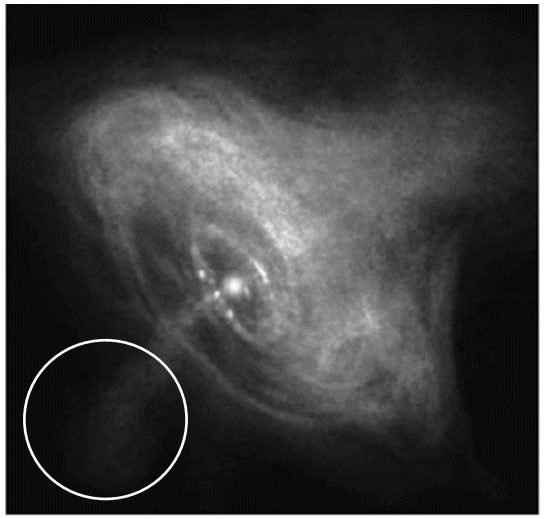

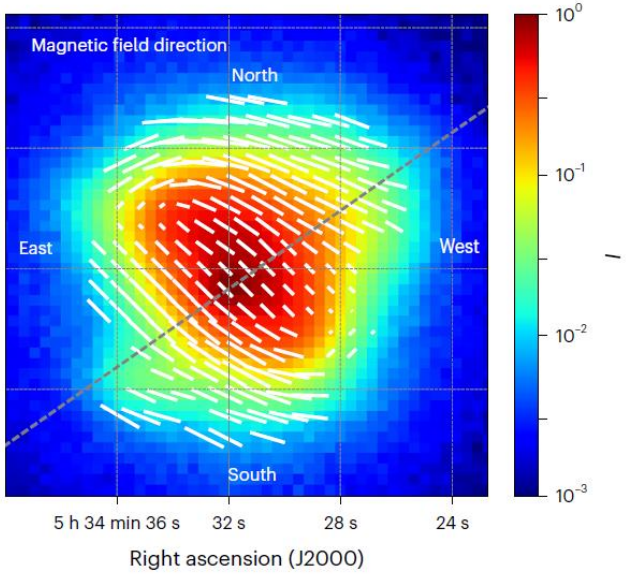

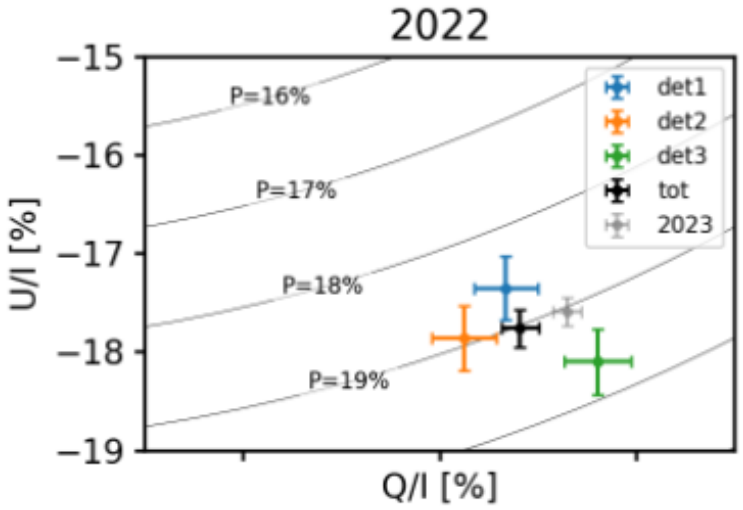

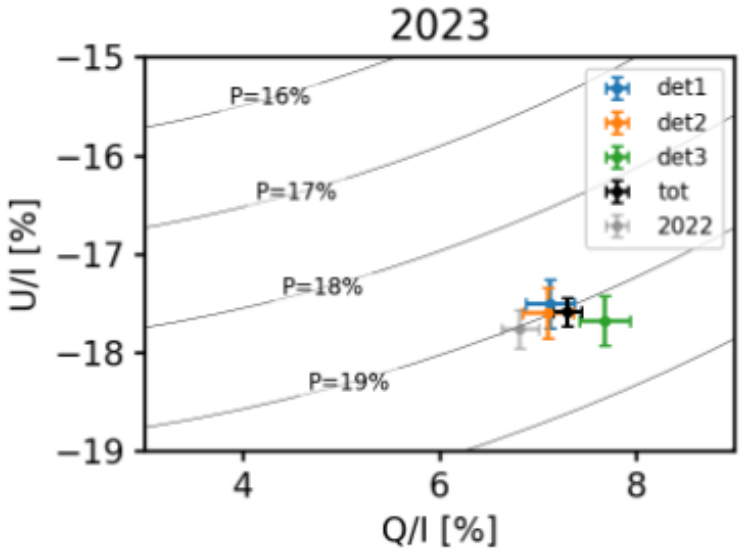

Crab nebula and pulsar

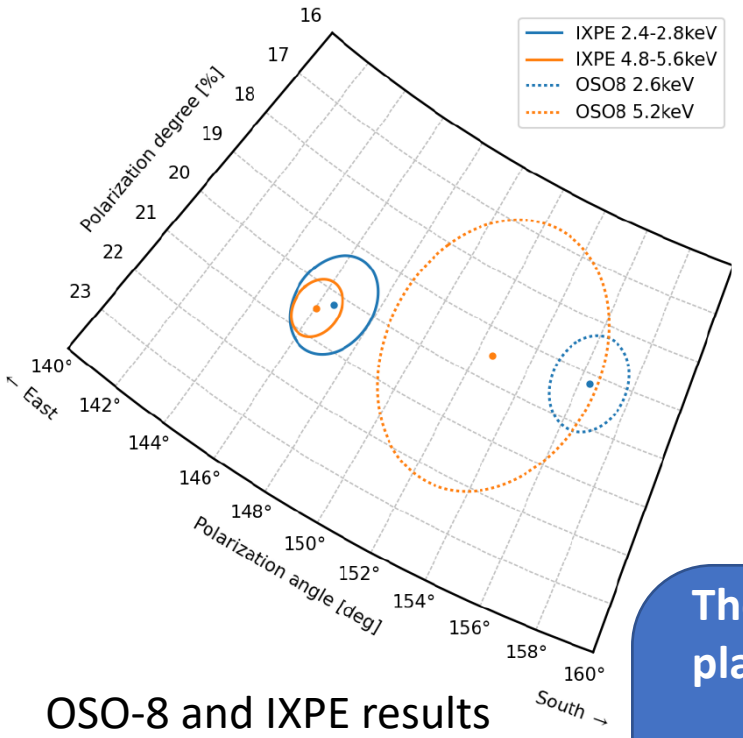

OSO-8 and IXPE results

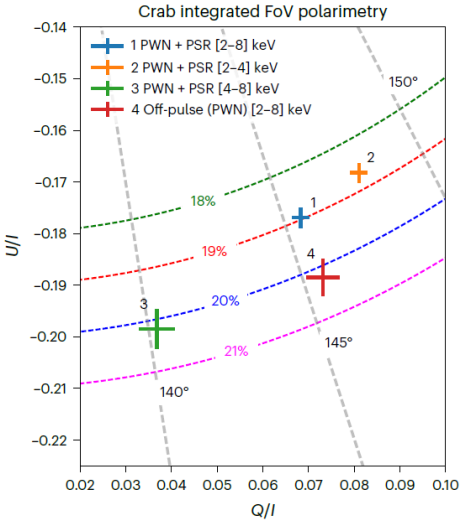

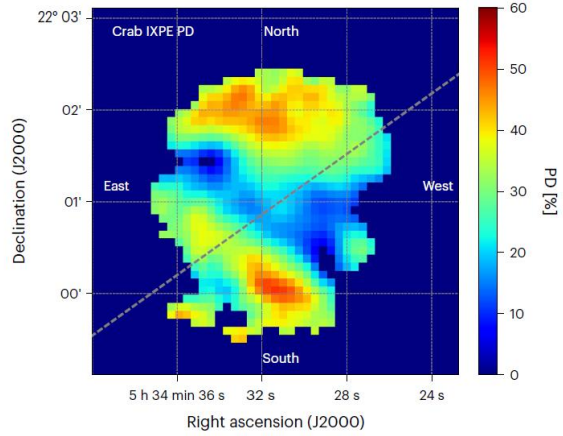

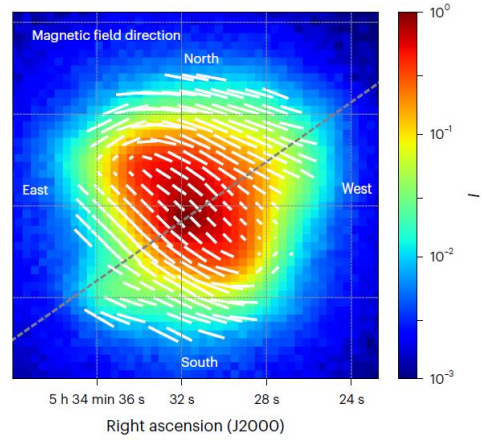

Fig. 4 | Polarized structure of the Crab nebula. The right panel shows the total intensity map of the Crab PWN + PSR complex in the [2–8] keV energy band, overlaid with the reconstructed polarization direction (magnetic field). The left panel shows a map of the PD cut above 5σ confidence level. The grey dashed line is the nebular axis inferred from X-ray intensity maps[31]. Overlaid are the sky directions for ease of reference.

The overall polarization pattern confirms the expectation that synchrotron emission takes place in the (mostly) toroidal magnetic field.

There is a change in PA between the low [2-4] keV and high [4-8] keV energy band. (Same trend of OP)

The level of angular resolved polarization suggest that turbulence is not as strong as predicted

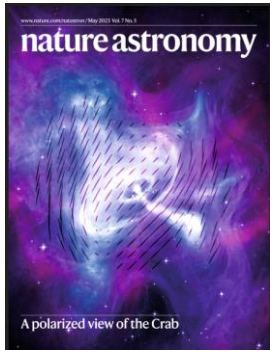

Crab Pulsar polarimetry

Polarization has been positively measured in the central bin (core) of the P1 pulse

PD = 15.4 +/- 2.5% PA = 105 +/- 18°. There is no significant change of the polarization properties of this phase bin with energy.

Deviations with respect to the optical polarization are prominent for Q/I in the left wings of both P1 and P2. U/I on the other hand is in very good agreement.

A simple PA swing over P1 does not seems capable by itself of explaining the presence of a highly polarized core in P1 with low polarization wings unless the PA swings much faster in X-rays than in the optical range. Intrinsic depolarization is most required.

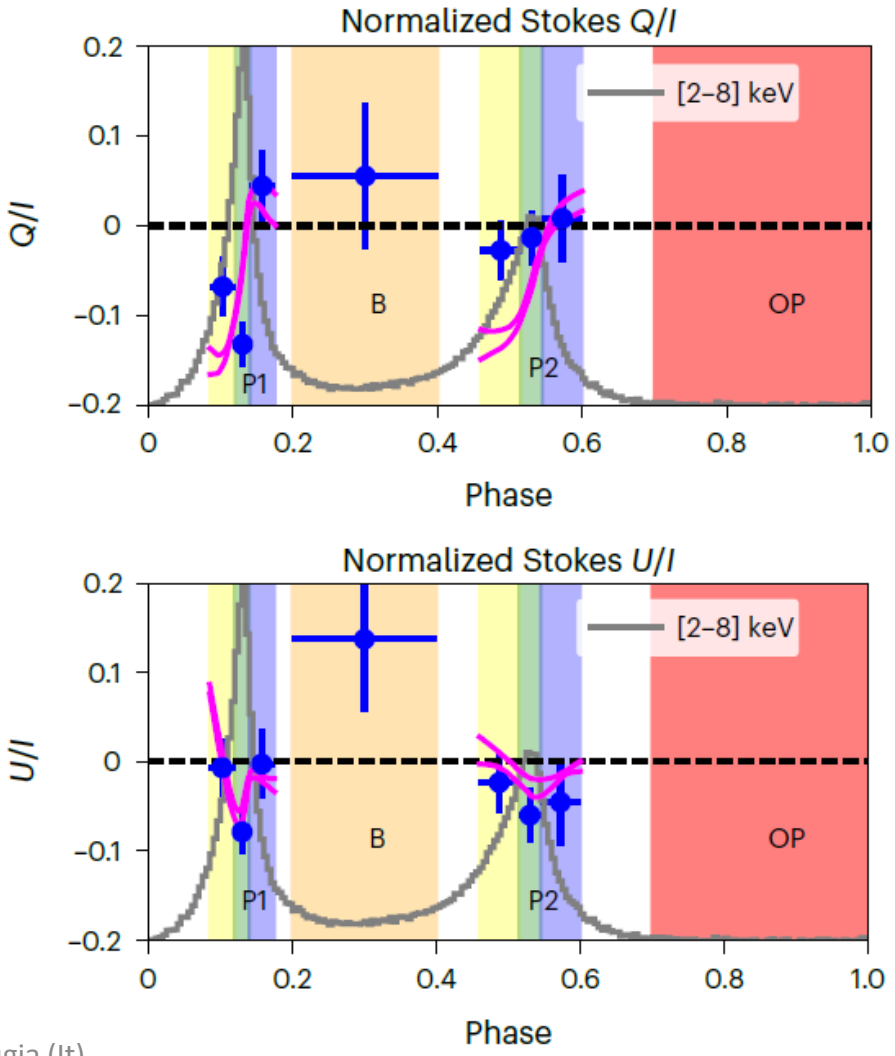

The Vela PWN

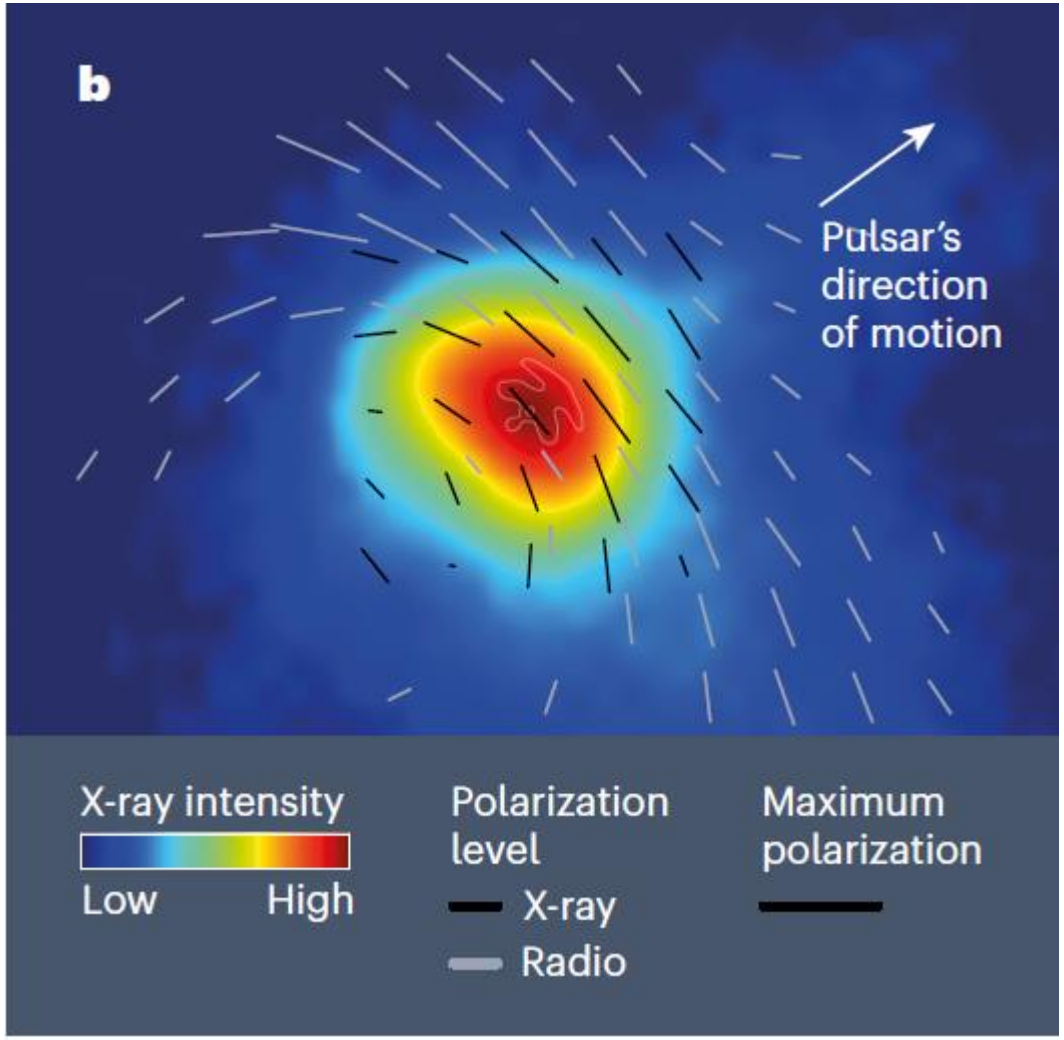

Average polarization of 45%, larger than 60% is some, small regions → close to the Synchrotron limit!

High polarization suggests B less turbulent than expected.

Polarization consistent with radio, but X-rays sample regions closer to the site of acceleration.

(Xie et al. 2022)

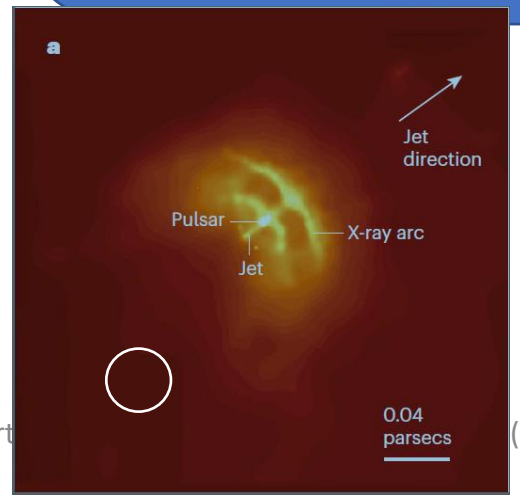

SuperNova Remnants

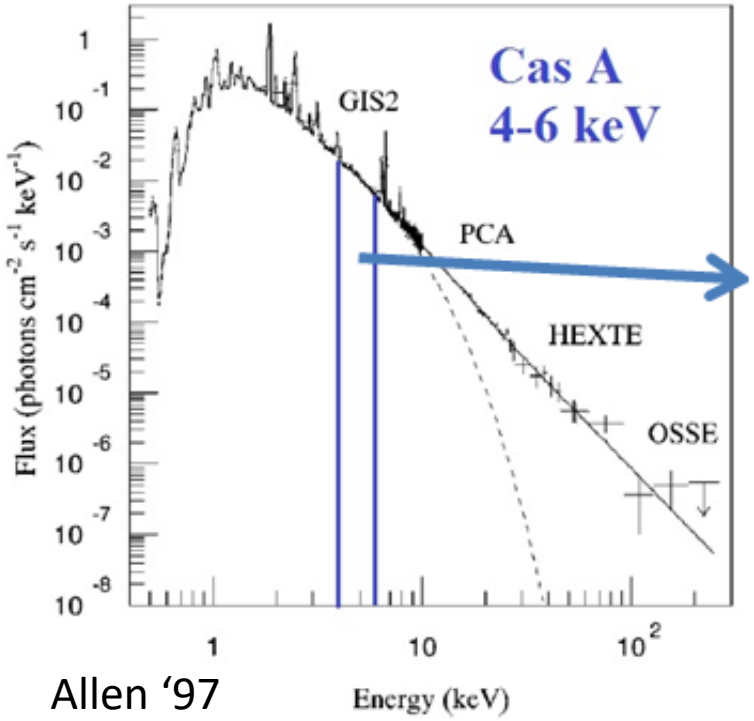

Allen '97

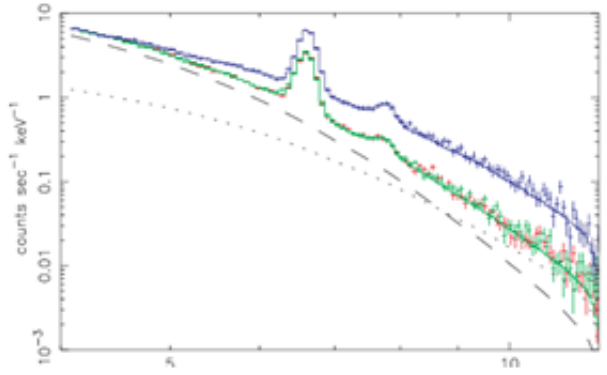

Bleeker 2001

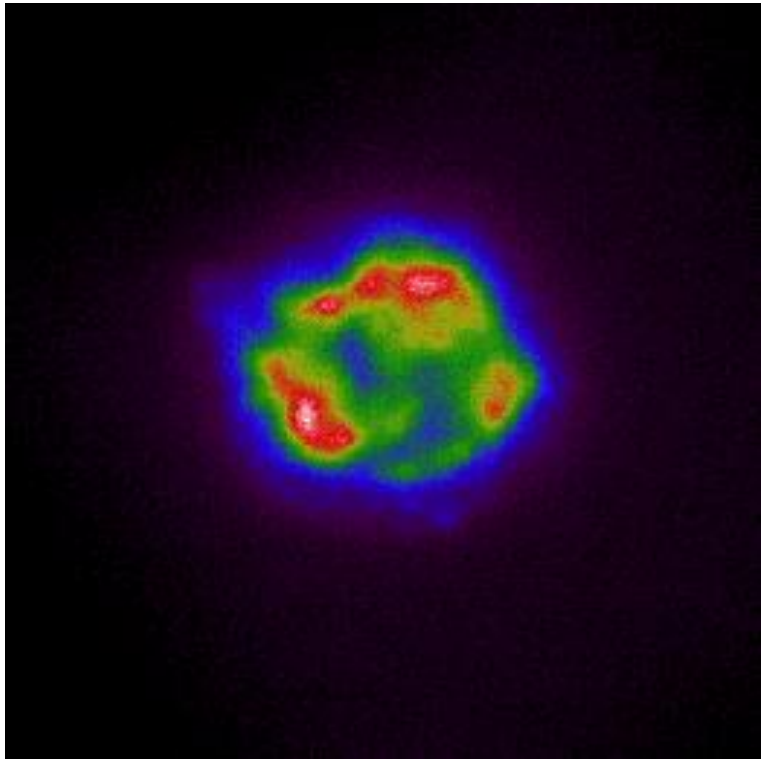

Rotating each photon with respect to the center and selecting the energy range between the calcium line and the Iron line we demonstrated that, as in radio, the polarization angle is perpendicular to the radius of the SNR as in radio band *(Vink et al. 2022)*

Spoiler

We measured X-ray polarization also from SN 1006 with magnetic field parallel to the shock normal. Polarization for non thermal emission is increasingly high for Cas A, Tycho and SN 1006.

Magnetars

- **Anomalous X-ray Pulsars and Soft-gamma ray repeaters**
  - $P \approx 2 - 12$ s $\dot{P} \approx 10^{-14} - 10^{-10}$ s s^{-1}
  - $B_{sd} \approx 10^{14} - 10^{15}$ G
  - $L_{X,\mathrm{persist}} \approx 10^{35} - 10^{36}$ erg s^{-1} (typically $> \dot{E}_{\mathrm{rot}} = 10^{33}$ -10^{34}
  - Bursting activity (short bursts – intermediate/giant flares)
  - Enhanced activity in transient sources (outbursts)
  - Two components (thermal and PL) spectra

  - **Powered by their own magnetic energy**

A twisted magnetic field is coupled to flowing charged particles which upscatters (power law) the radiation emitted from the neutron star surface (Thermal)

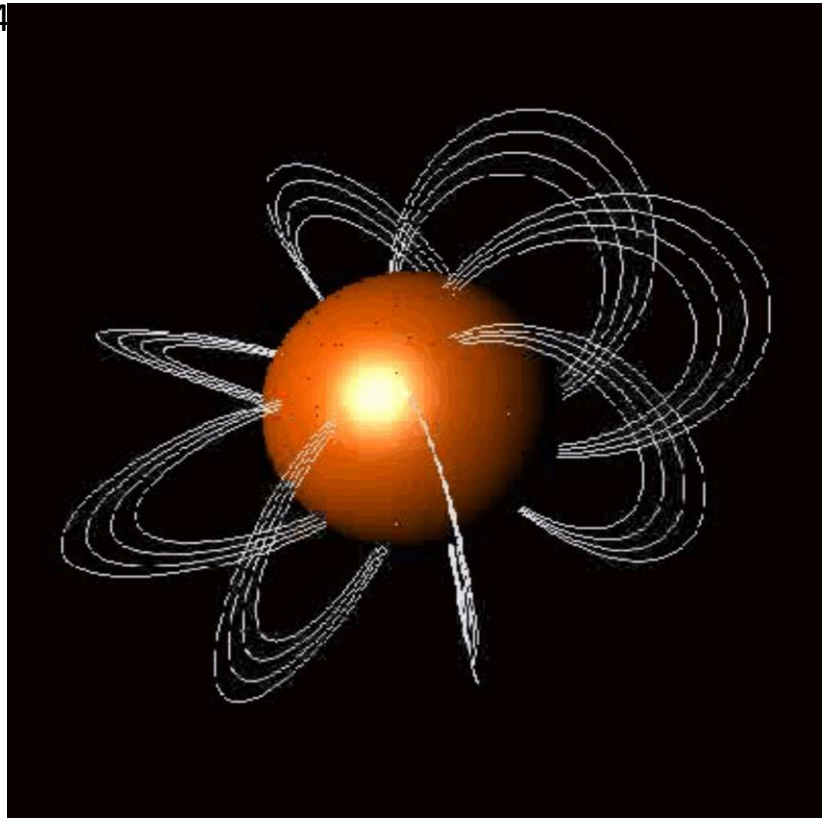

Magnetars: 4U 0142+61

Strong dependence on energy, suggesting a switch of the dominant mode from low to high energies *(Taverna et al. 2022).*

Polarization degree drops to ~ 0 at around $4-5$ keV

Polarization angle swings by 90°

Averaged PD = (13.5+/-0.8)%

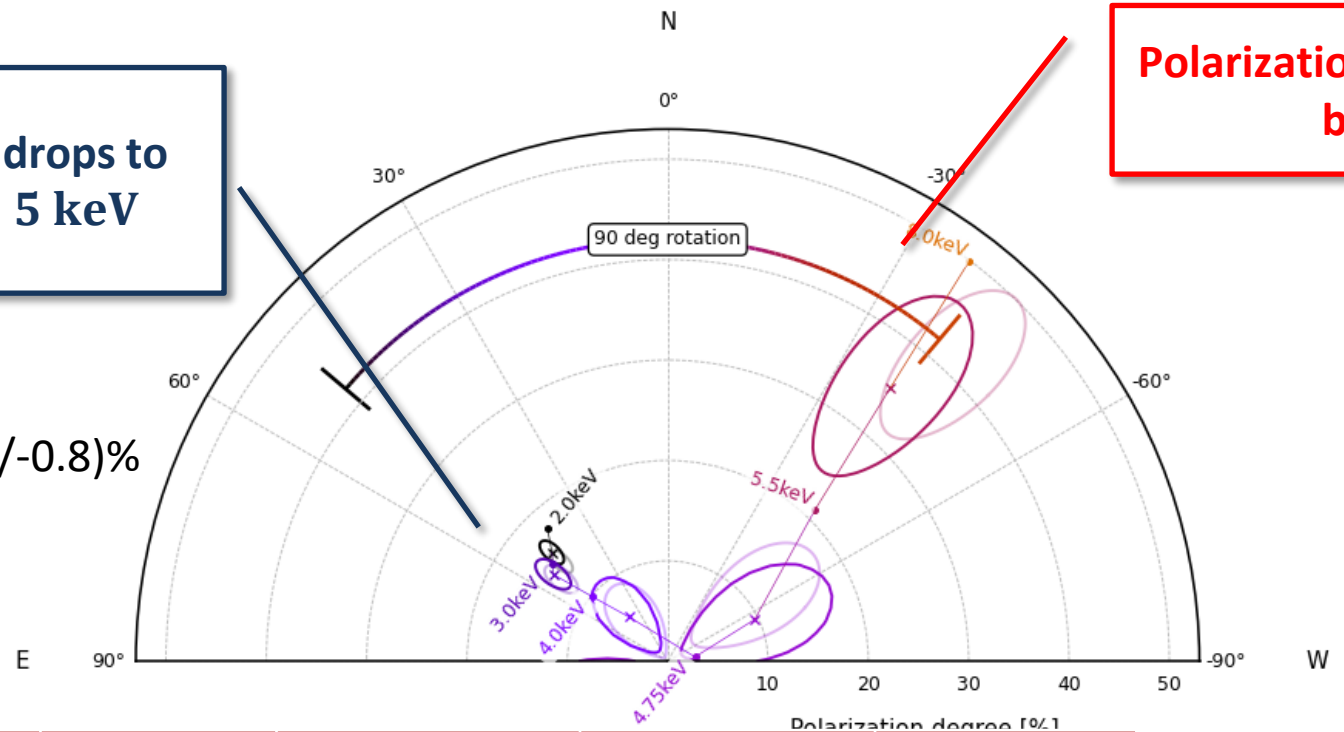

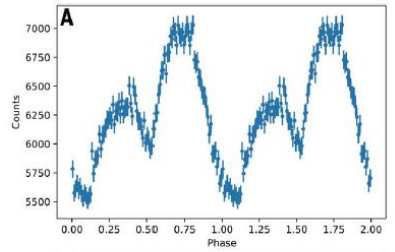

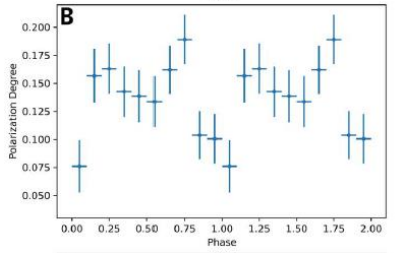

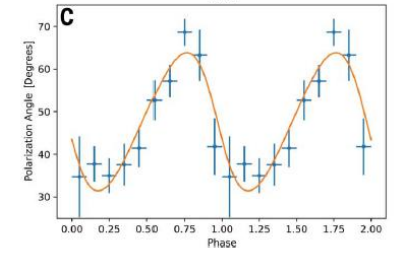

	2-3 keV	3-4 keV	4-4.75 keV	4.75-5.5 keV	5.5-8 keV
PD (%)	16^{+2}_{-2}	14^{+2}_{-2}	6^{+5}_{-5}	10^{+8}_{-8}	35^{+11}_{-11}
PA (deg)	47^{+3}_{-3}	53^{+4}_{-4}	41^{+26}_{-26}	64^{+29}_{-64}	39^{+9}_{-9}

Magnetars: 4U 0142+61

- Two spectral components differently polarized
- Polarization angle swing by 90°
- Modest low-energy polarization
- Phase-dependent behavior of Flux, PD and PA

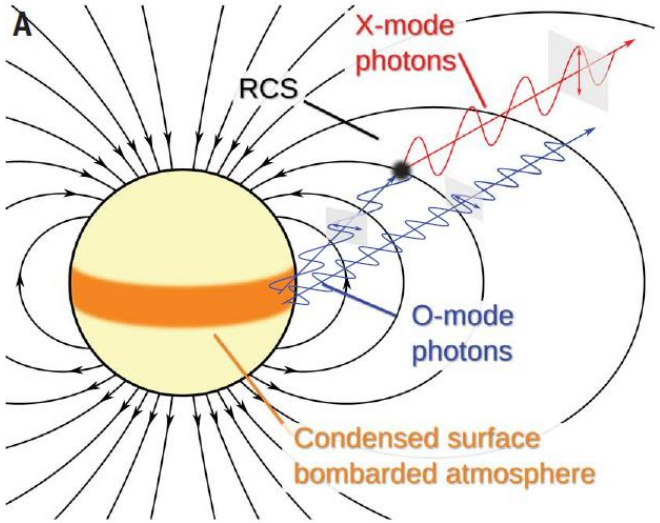

Most likely interpretation

Thermal + Resonant Compton Scattering
Ordinary (Extraordinary) mode dominating at low (high) energies
Resonant Compton scattering produce X-mode polarization at high energies
Condensed surface is invoked for producing low energy O-mode
The atmosphere is condensed due to the high magnetic field: The atoms attain a cyclindrical structure and the elengated atoms form molecular chains by covalent bonding along the field directon.

Consistent with Vacuum Birefringence expected in QED (but never verified experimentally)

Magnetars: J1RXS J170849.0-400910

A second magnetar (J1RXS J170849.0-400910) has then been observed.

Averaged PD =(35.1+/-1.6) %

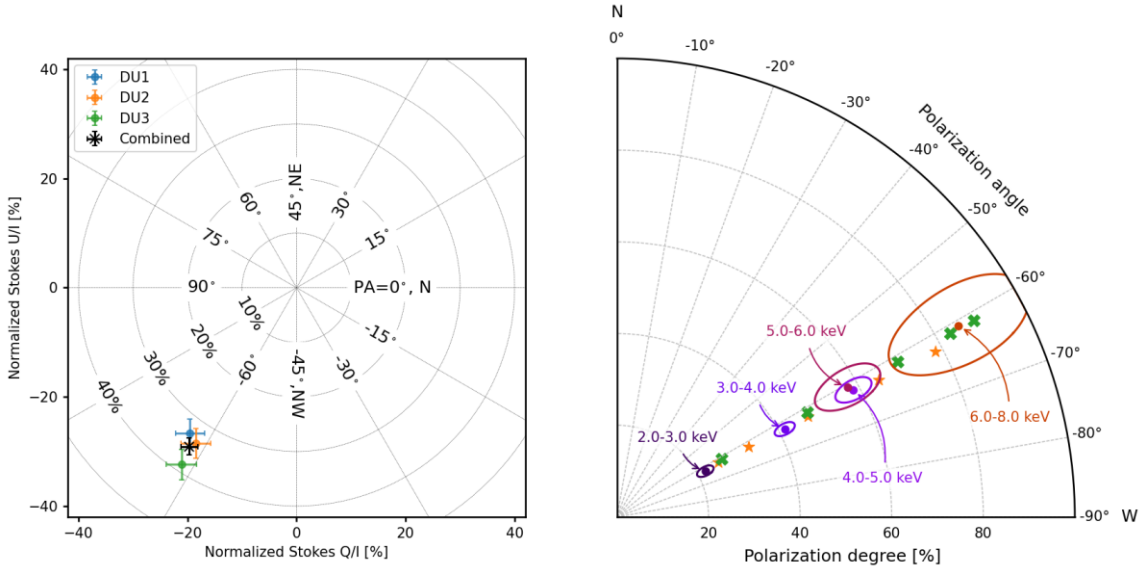

PD increases with energy (up to 80%!!), but the PA stays constant *(Zane et al. 2023).*
The model foresee the cohesistance of a warm condensed region and a hot atmospheric spot to explain (1) the low energy smaller polarization
(2) the higher high polarization

Due to the small size of the emitting regions, QED Vacuum Birefringence cannot be probed yet *(Zane et al. 2023).*

Accreting NS – X-ray Pulsars Her X-1

An X-ray pulsar is a binary system made of a magnetized neutron star (10^{12} G) accreting matter from a normal stellar companion. Gas is accreted from the stellar companion and is channeled by the neutron star's magnetic field on to the magnetic poles producing two or more localized X-ray hot spots.

Average PD = (8.6+/-0.5)%

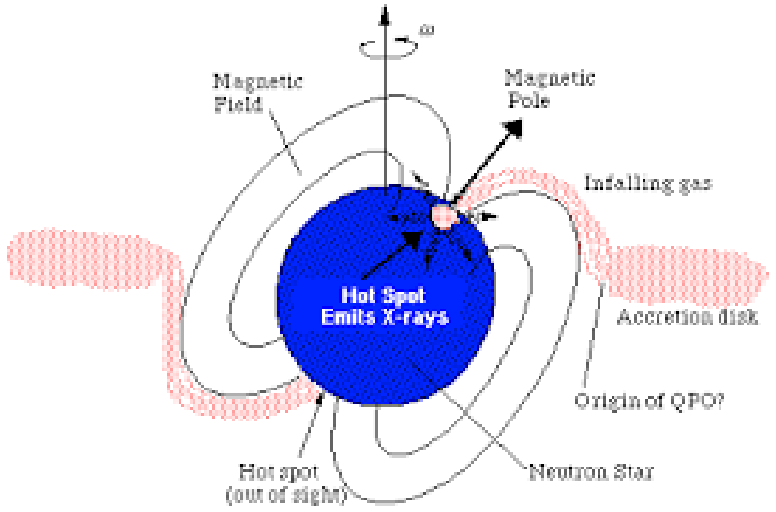

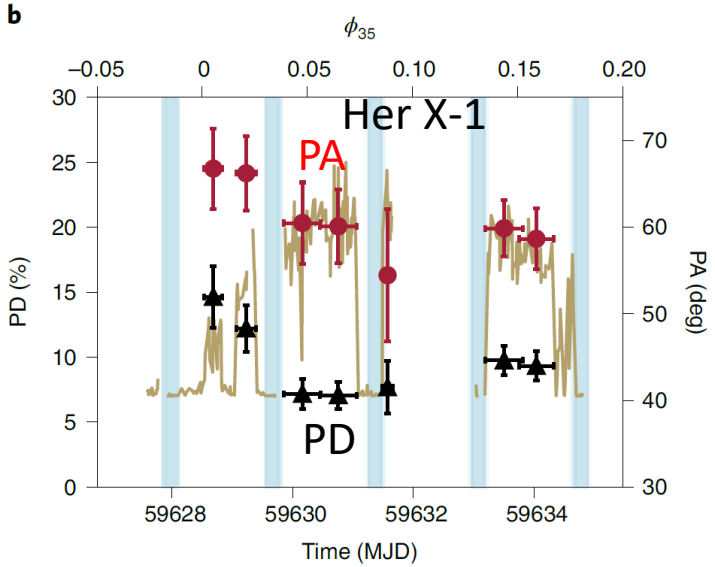

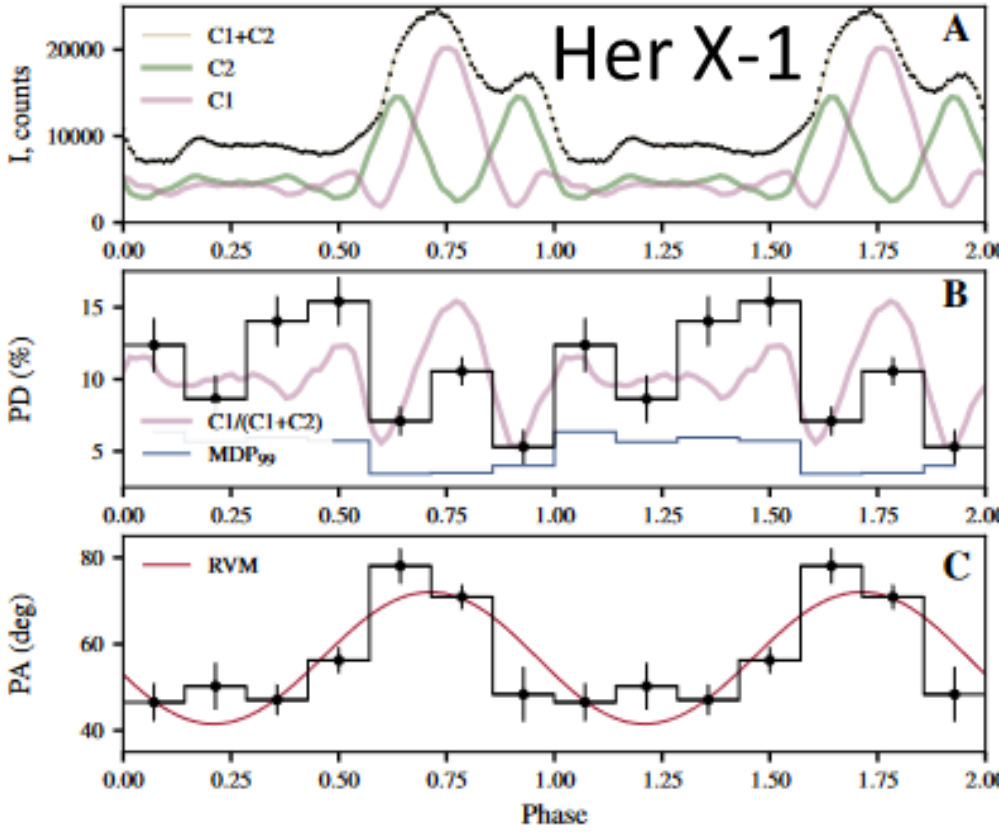

X-ray pulsars are predicted (Meszaros et al., 1988, Caiazzo and Heyl, 2021, to be very highly polarized, because of the two different opacities while the polarization is lower than expected, but detected with very high significance in a number of sources, e.g. Her X-1 (*Doroshenko et al. 2022*), Cen X-3 (*Tsygankov et al. 2022*), Vela X-1 (*Poutanen et al. 2023*), GRO J1008-57 (*Tsygankov et al. 2023*) + …

Doroshenko et al. 2022

Determination of geometrical parameters

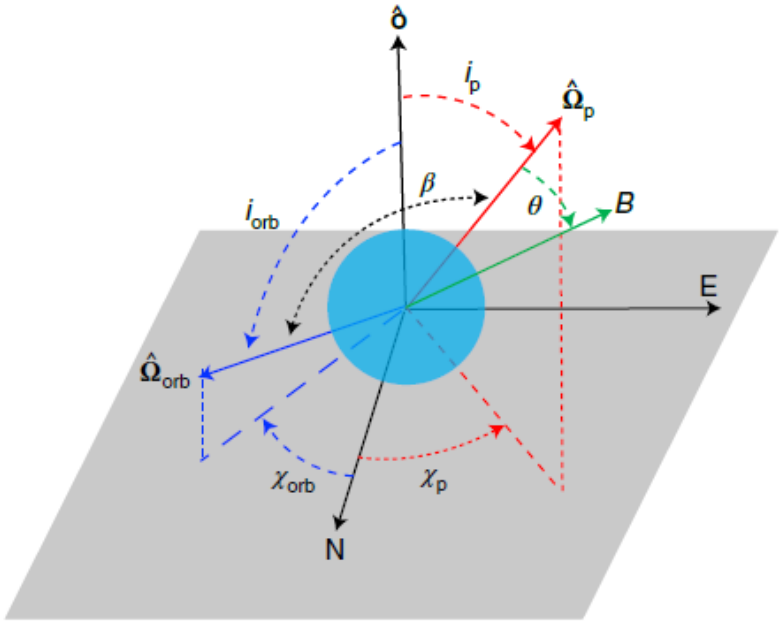

Fig. 4 | Geometry of the system from the observer's perspective. The grey plane is the plane of the sky, labelled with north and east axes, perpendicular to the line of sight towards the observer $\hat{\mathbf{o}}$. The angles between the line of sight and the vectors of the pulsar spin $\hat{\Omega}_p$ and the orbital angular momentum $\hat{\Omega}_{orb}$ are the inclinations i_{orb} and i_p. The corresponding position angles χ_p and χ_{orb} are the azimuthal angles of the spin vectors projected onto the sky, measured from north to east. The misalignment angle β is defined as the angle between $\hat{\Omega}_p$ and $\hat{\Omega}_{orb}$. The magnetic obliquity θ is the angle between magnetic dipole and the rotational axis.

Table 1 | Orbital and pulsar geometrical parameters of Her X-1

$\chi_{p,*}$	θ	i_p	$\chi_{orb,*}$	i_{orb}
deg	deg	deg	deg	deg
56.9±1.6	12.1±3.7	Eq. (2)	28.9±5.9	100.4±4.9

$$\tan(\mathrm{PA} - \chi_p) = \frac{-\sin\theta \sin(\phi - \phi_0)}{\sin i_p \cos\theta - \cos i_p \sin\theta \cos(\phi - \phi_0)}$$

As promised from the swing of the polarization angle is possible to derive geometrical properties: Projection of the spinning vector in the plane of the sky and the angle between the rotationa axix and the dipole axis.
These are usually free parameters in spectral fittings now they are directly measured by X-ray polarimetry

IXPE
Imaging
X-Ray
Polarimetry
Explorer

Cen X-3 disentangling the geometry

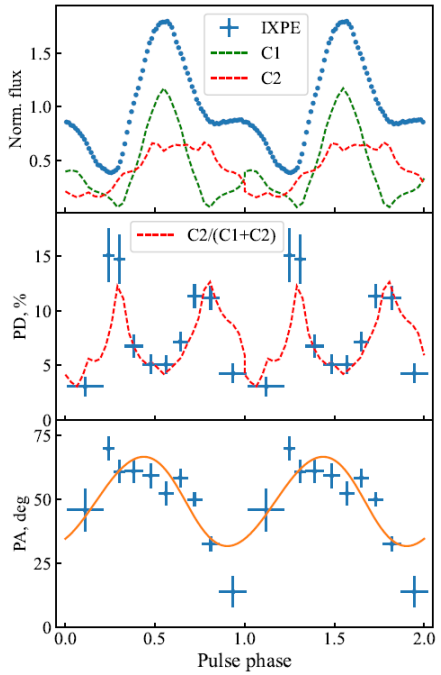

Rotating Vector Model	
Magnetic obliquity	Θ = 16.4(±1.3)°
Inclination	I_p = 70°.2
Position angle	X_p = (49.2 ± 1.1)°

4U 1626-67, GX 301-2 and X Persei have PD < MDP
Averaged PD = (5.6 +/-0.3)%
Anticorrelation between the flux and the polarization degree.
A full interpretation of the obtained result request an assessment of possible Scenario and accretion/emission mechanism

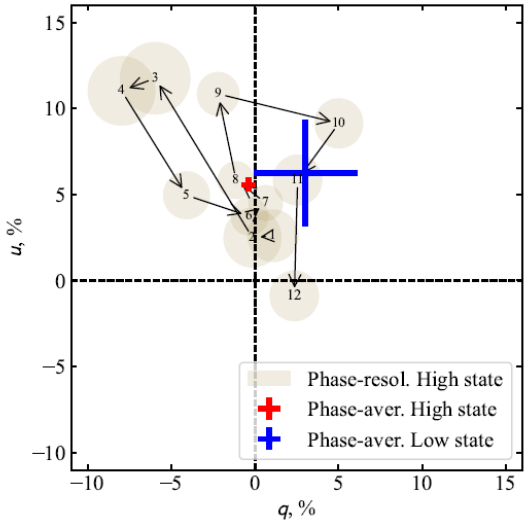

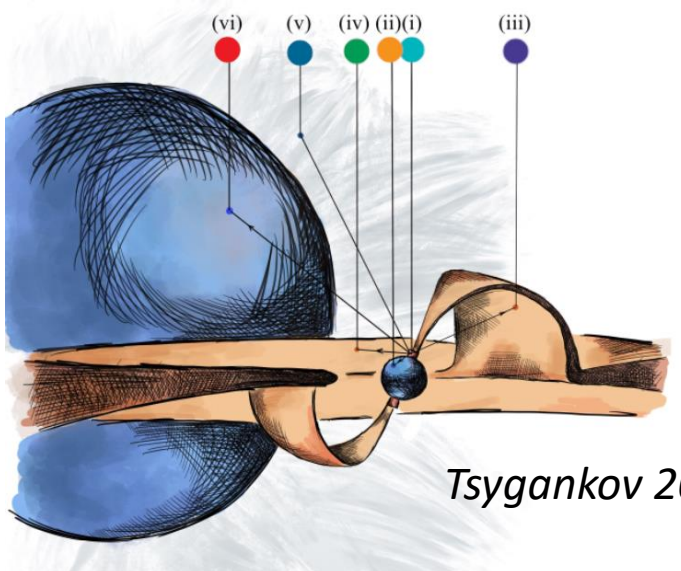

Tsygankov 2022

Intrinsic polarization from the hotspot
Reflection from the NS surface
Reflection from the accretion curtain
Reflection from the accretion disk
Scattering by the stellar wind
Reflection from the optical companion

IXPE
Imaging
X-Ray
Polarimetry
Explorer

(see in astro-ph: Doroshenko et al 2023)

LSV +44 (Be-XRB) was observed in supercritical and subcritical accretion rate
Phase-resolved polarization degree and angle are very different for the two states.

Accreting Stellar-mass BH

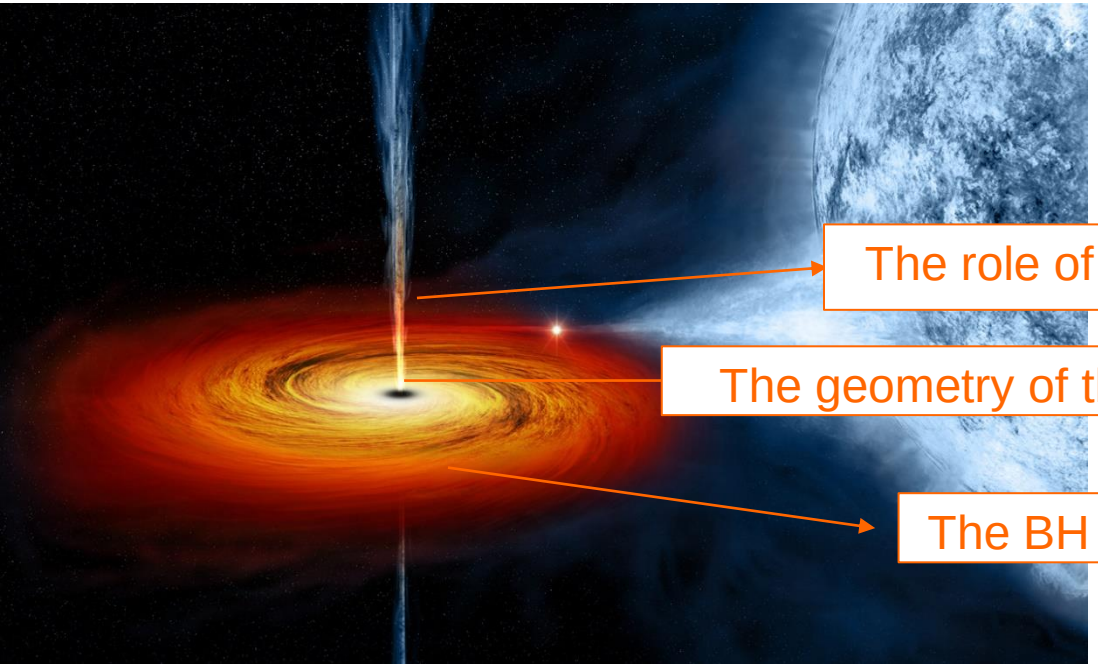

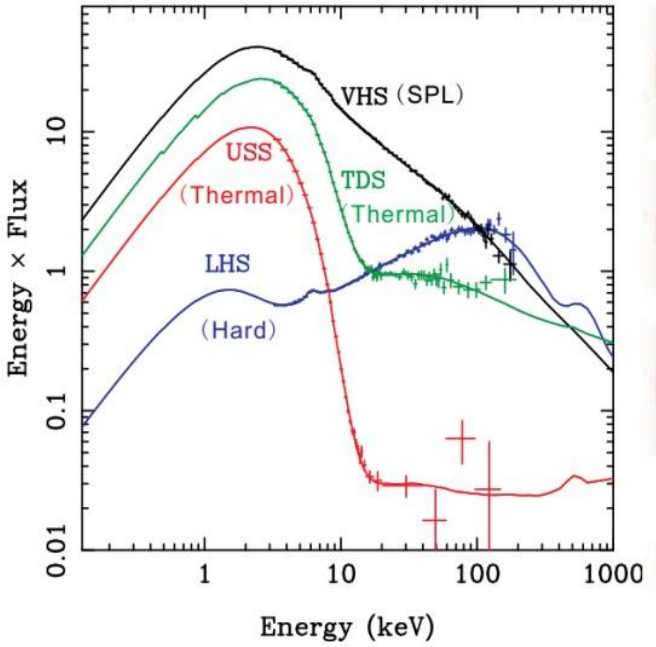

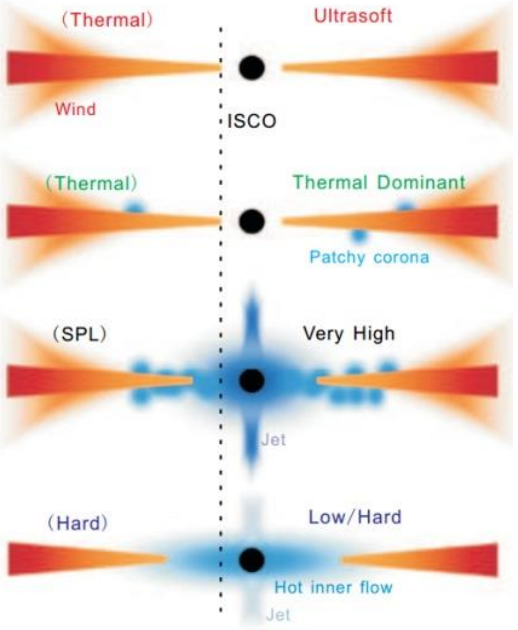

Polarimetry of Black Holes in soft state can probe General Relativistic effects with the measurement of the BH Spin because the inner disk touches the Innermost circular orbits and the polarization angle rotates with energy with a spin-dependent rotation amplitude.

Polarimetry of Black Holes in Hard State can probe the coronal geometry and the jet-Corona interplay.

Cyg X-1 Low-Hard state

Cyg X-1 observed for about 250 ks in hard state, in coordination with NICER and NuSTAR

Krawczinsky, H. et al., 2022

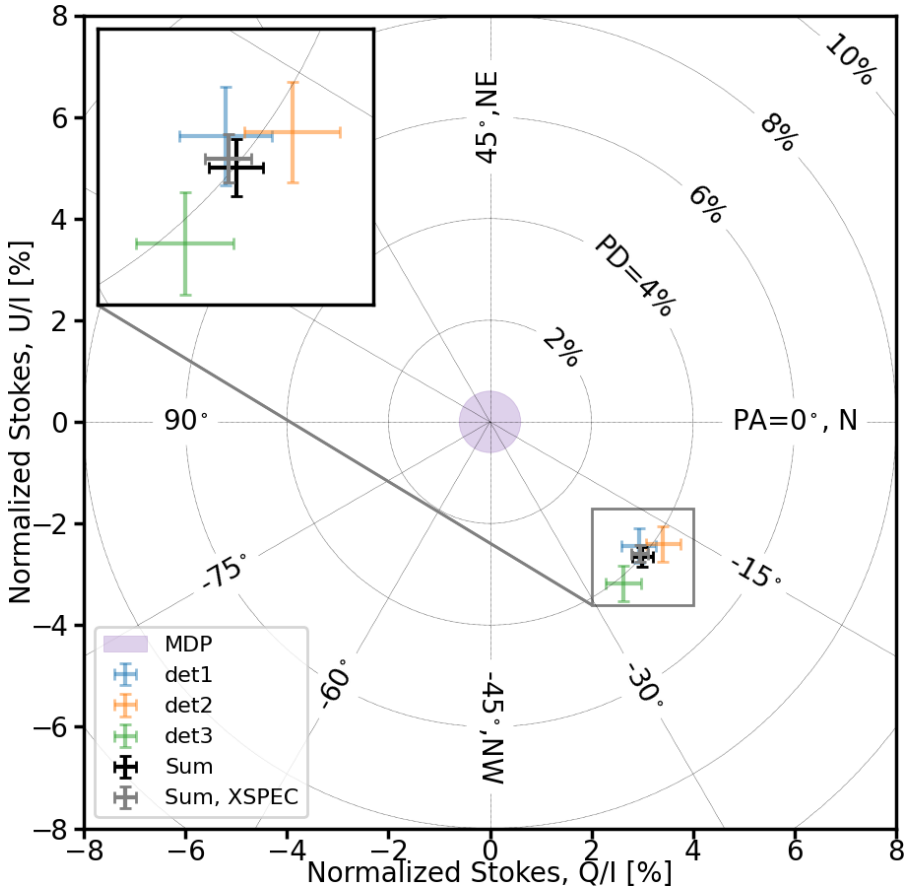

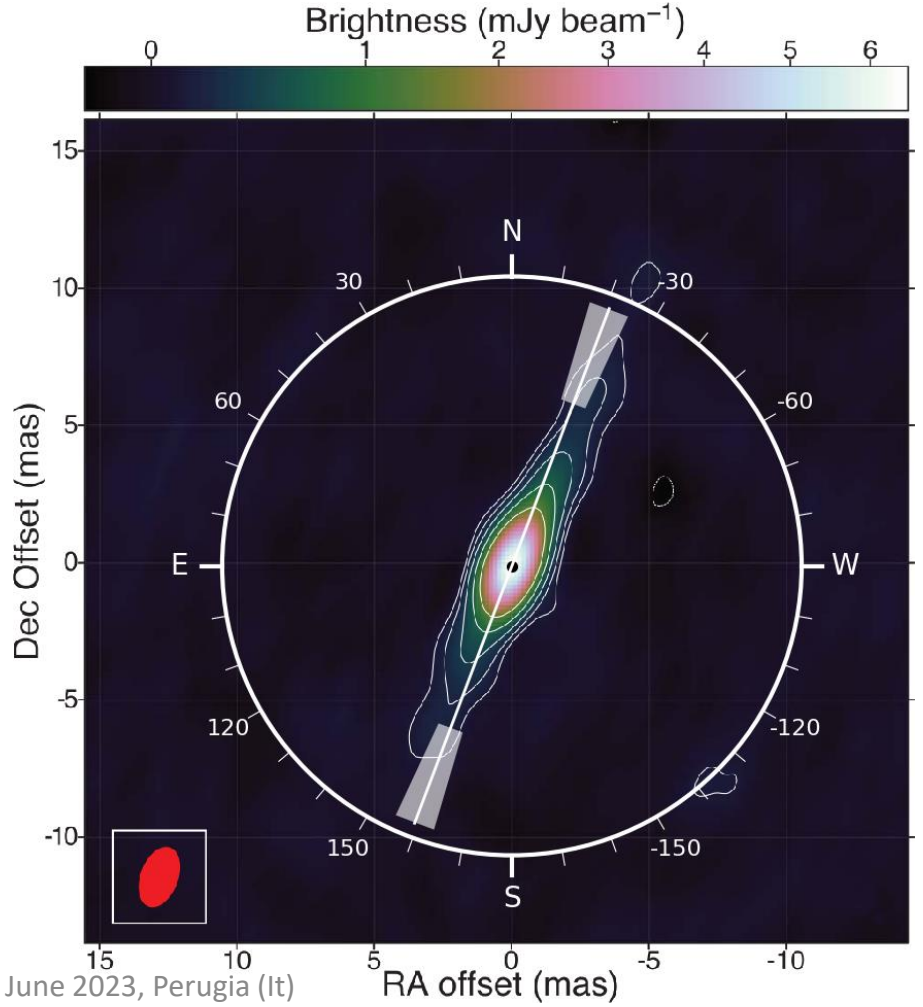

Cyg X-1 in hard state

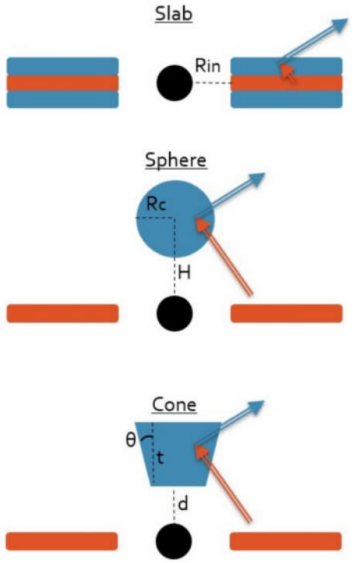

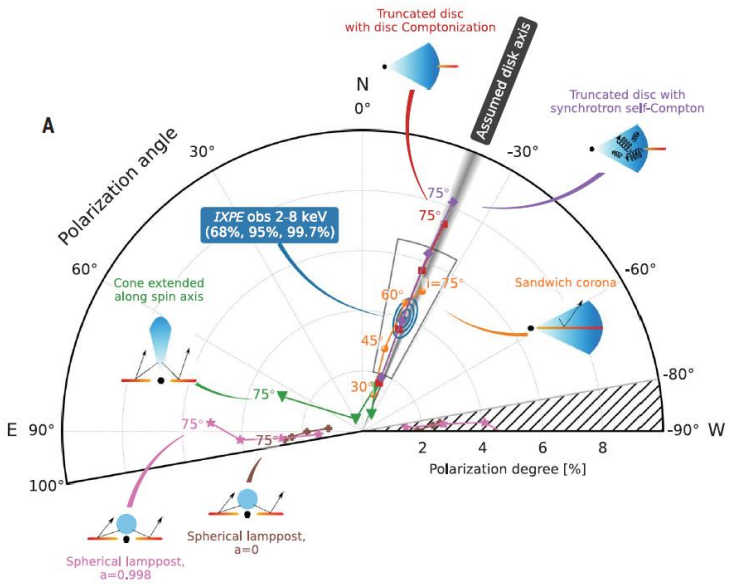

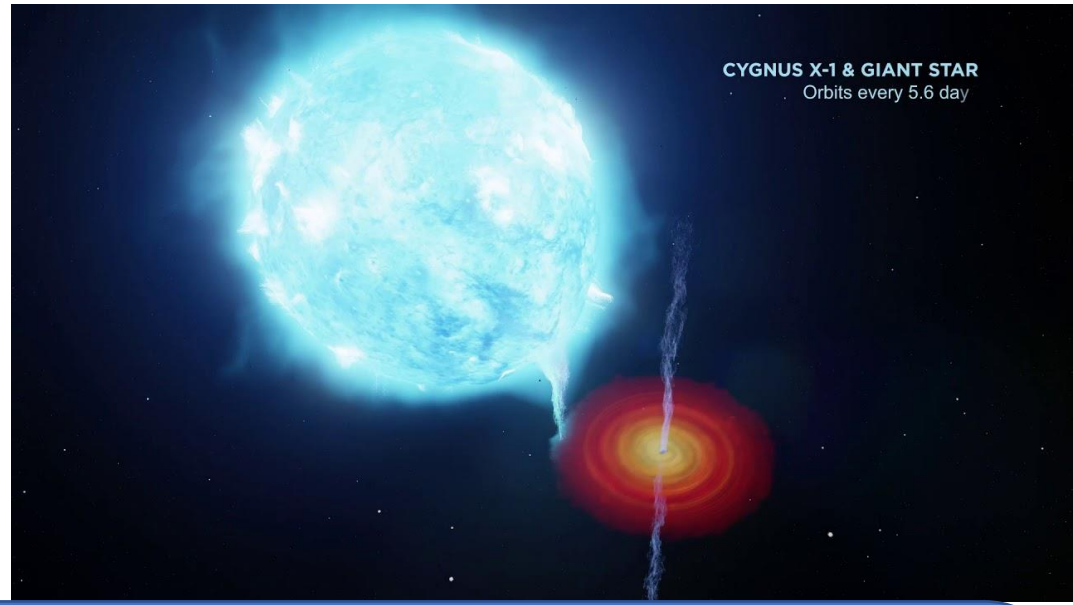

Polarization degree (2-8 keV): 4.0+/-0.2

Larger than expected given the ≈30° orbital inclination

Misalignement between the inner accretion flow and the orbital plane?

Flattish configuration of the emitting region

Polarization angle parallel to the radio jet

Observational evidence of link between disc and jet

Sandwich Corona geometry favored. Lamp-post/Cone excluded.

Polarimetry from Extragalactic Sources

Synchrotron-dominated

Blazars, multi-λ polarimetry probes **the structure** of the jet and of its **magnetic field**

Inverse Compton dominated

Blazars, multi-λ polarimetry observations can determine:

- **the composition of the jet**

(hadronic vs. leptonic, Zhang & Bottcher, 2013)

- **the origin of the seed photons**

Synchrotron-Self Compton (SSC) or External Compton (EC) (Celotti & Matt, 1994; Poutanen 1994)

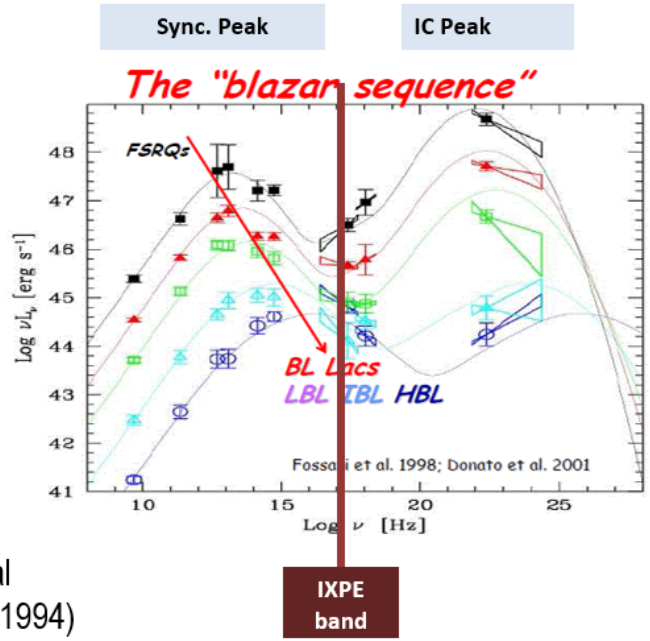

A blazar is an active galactic nucleus (AGN) with a relativistic jet directed closely towards the observer. Relativistic beaming from the jet makes blazars appear much brighter than they would be if the jet were pointed in a direction away from Earth.

Blazars

High Synchrotron peaked

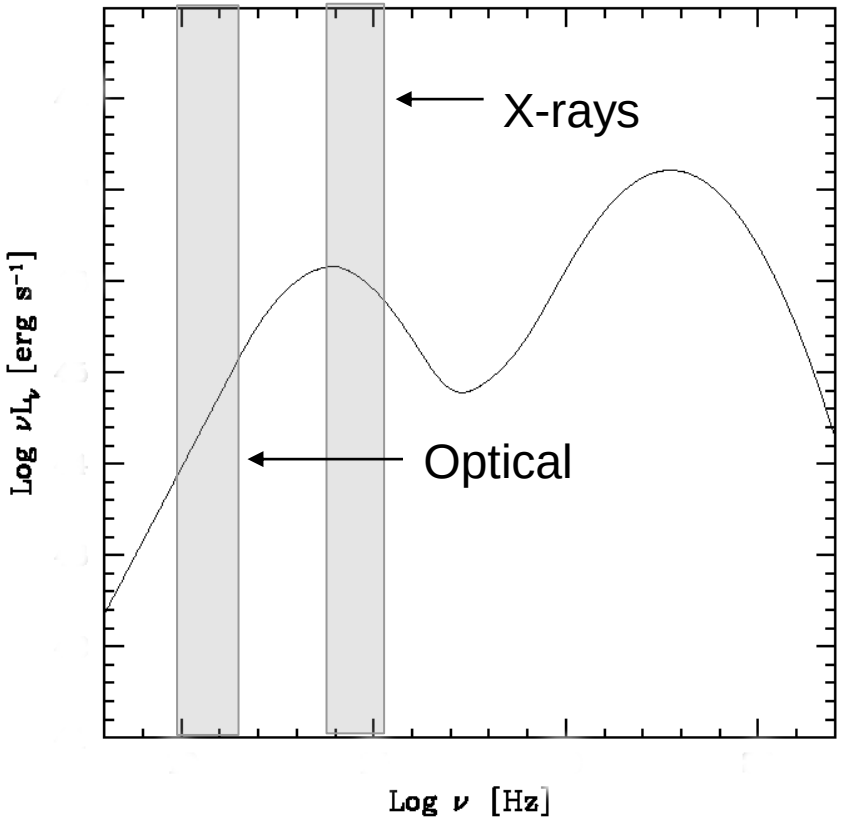

Blazars are promising sources for X-ray polarimetry. High Synchrotron Peak Blazars like Mrk 501 (*Liodakis et al. 2022*) and Mrk 421 (*Di Gesu et al. 2022*) are indeed significantly polarized. Multifrequency observations permit to discriminate among models.

IC peak sources are instead much less polarized (e.g. Cen A, *Ehlert et al. 2022,* BL Lac*, Middei et al. 2022*).

IXPE
Imaging
X-Ray
Polarimetry
Explorer

MRK 421

Multi-wavelength campaign from radio to X-ray was performed for Mrk 421

Mrk 421 was observed three times each time with 100 ks net observing time
This work refers to the first observation occurred in May 4th – May 6th 2022

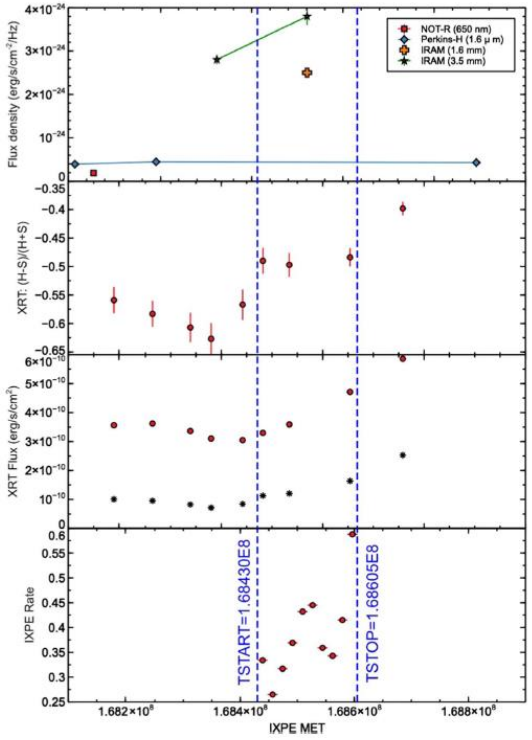

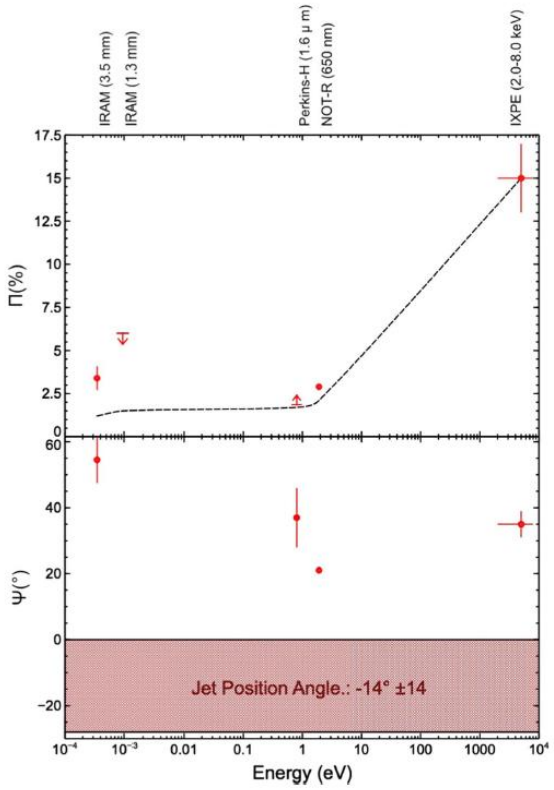

The polarization degree in X-rays is 7 times larger than in the optical and millimetric.

- The polarization is stable in degree (below +/- 4 %) and angle (below +/- 7°)

The particle emitting mm/IR/optical/X-rays are energy stratified as in Mrk 501.

The polarization vector is expected to be parallel to the radio jet but is not. A misalignment is possible between radio jet and jet regions where the X –rays are produced.

… but multiple observations of these sources show a significant variability in the polarization e.g. a rotation of 360° in 4.5 days (di Gesu et al., 2023, Nature Astronomy)

100 ks observing time

Di Gesu et al., 2022

RADIO QUIET AGN (POLARIMETRY DETERMINES THE GEOMETRY OF THE CORONA)

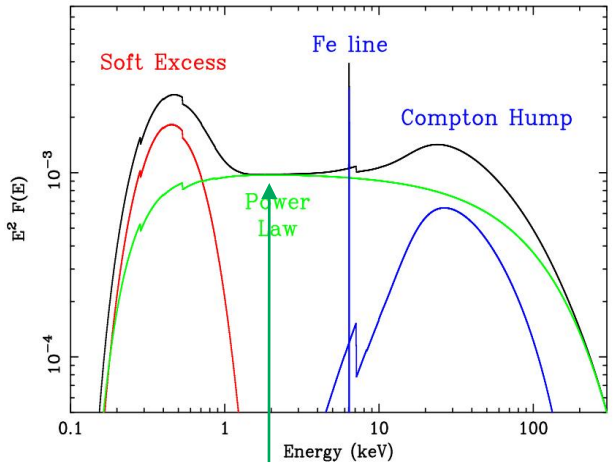

Hot Corona

About 6 days of net observation

- The primary X-ray emission in AGN is due to Comptonization of soft optical/UV photons from the disk.
- The Comptonization happens in a hot corona located possibly above the disk.
- While Spectroscopy is capable to determine the physical status of the corona, it is rather insensitive to its geometry

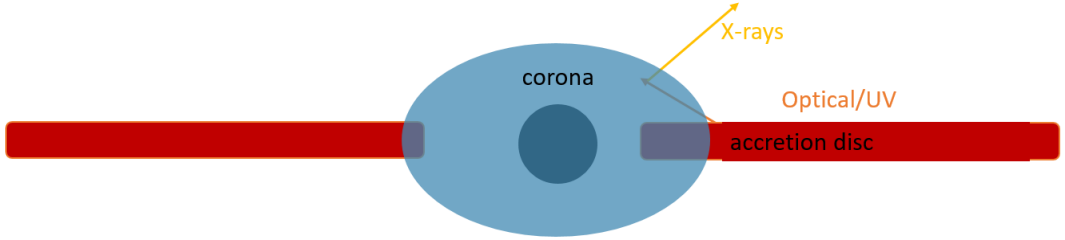

Magnetic instabilities in the disk ?

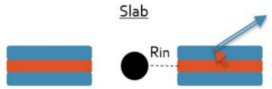

Magnetic reconnection

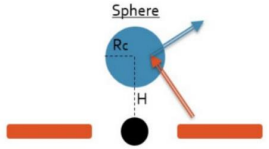

Base of jet ?

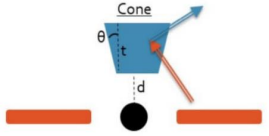

The geometry of the corona can be probed by means of X-ray polarimetry.

Radio Quiet AGN

Three unobscured RQ AGN have been observed:

MCG-5-23-16 – PD <3.2% (Marinucci et al. 2022, Tagliacozzo et al. 2023). Possibly aligned with the NLR axis. Slab (or wedge) preferred for the corona

Similar results for IC4329A (Ingram et al. 2023)

Positive detection in NGC 4151 (Gianolli et al. 2023). PD=4.9±1.1%, aligned with the radio jet. Again, slab or wedge corona preferred

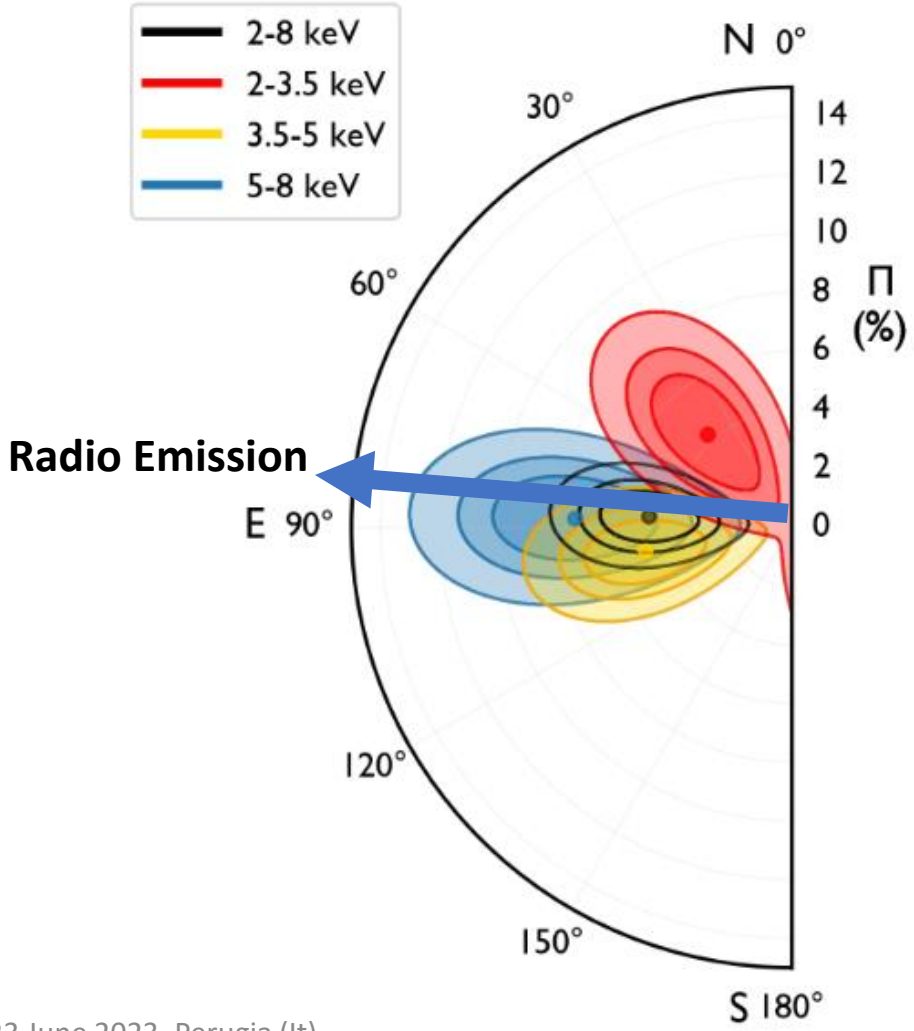

Compton-thick AGN

X-ray emission is dominated by reflection, so it should be highly polarized.

Polarization degree from the torus depends on the geometry of the system (inclination angle, torus opening angle)

The polarization vector is expected to be orthogonal to the torus axis.

The ionization cone/NLR may also scatter (and polarize) the primary emission.

Polarization vectors from ionization cone and torus are the same, if coaligned.

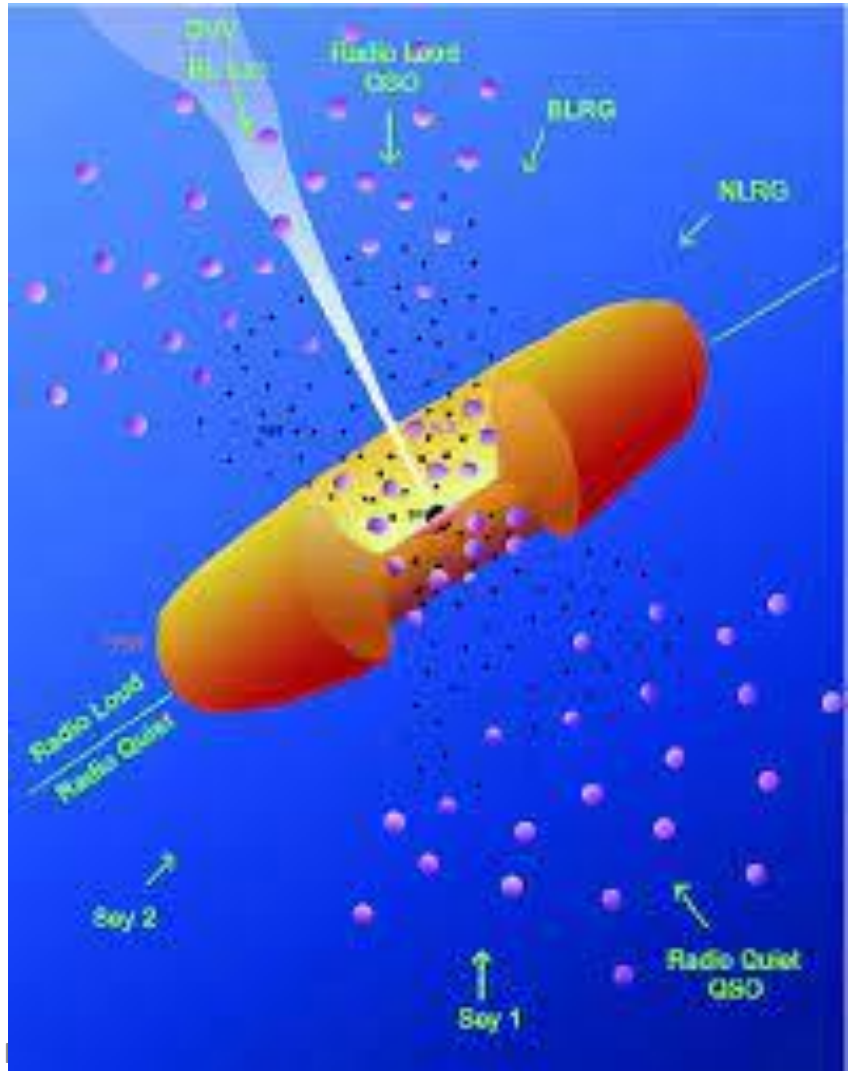

CIRCINUS GALAXY (URSINI ET AL., 2022)

- 70 % of local AGNs are obscured by gas and dust
- The obscuring medium is geometrically thick and axisymmetric (torus)
- If the column density NH > $1/\sigma_T$ = 1.5 x 10^{24} cm^{-2} they are called Compton thick

- The X-ray spectrum is dominated by reflection from both neutral (cold) and ionized (warm) matter surrounding the nucleus.

Circinus galaxy is a close AGN (D = 4.2 Mpc).
It shows prominent [O^{III}] ionization cone, starburst rings and a radio jet
On sybparsec scales shows an edge on, accretion disk (from H_2O maser emission at 1.3 cm). $F_{2\text{-}10\ keV}$ = 1.5x10^{-11} cgs

Simultaneous Chandra observation were used to monitor and model the spectrum of two ULXs within the extraction region of IXPE.

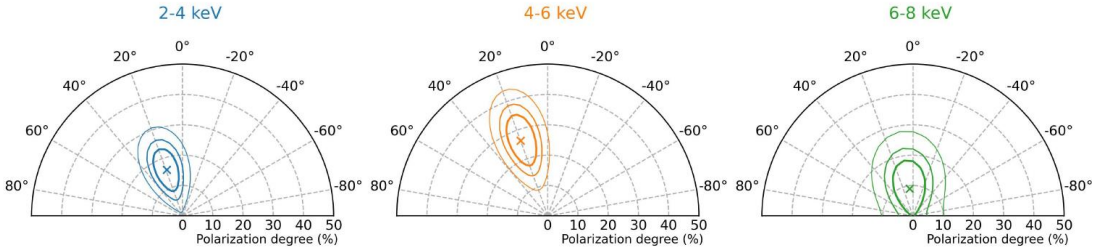

In 2-4 keV and 4-6 keV polarization is detected by more than 99 % CL. In 4-6

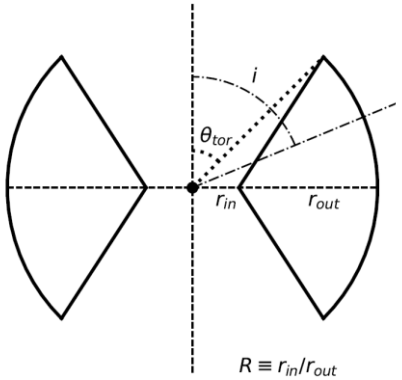

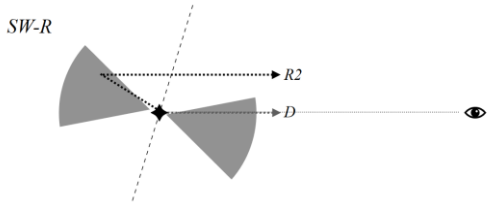

in reflection dominated AGNs the polarization of the reflected component is perpendicular to the torus axis.

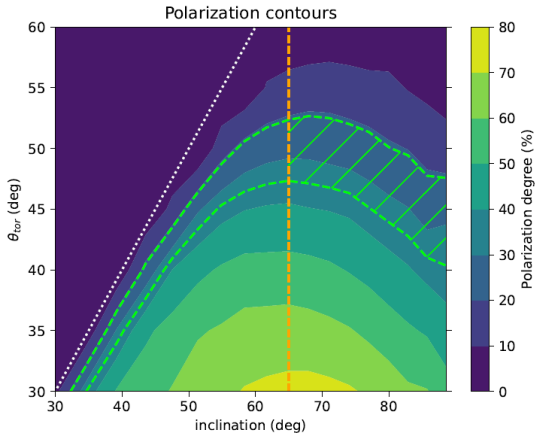

Cold reflection

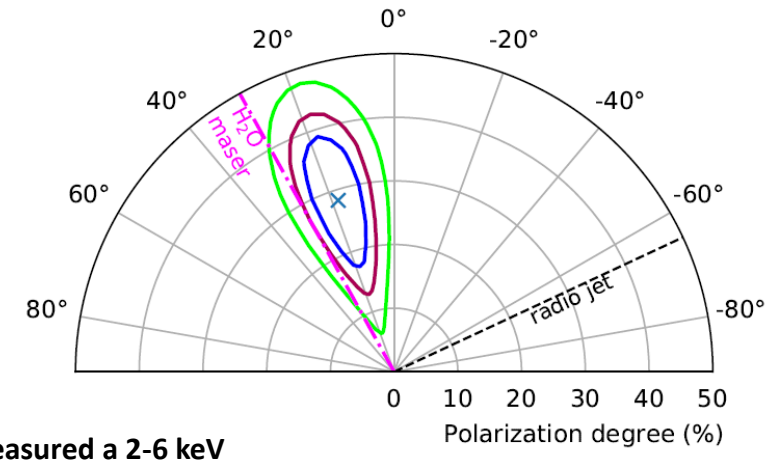

the cold reflector IXPE measured a 2-6 keV polarization of:
P = 28 %+/- 7% and Theta = 18° +/-5°

68 %, 90 % 99 %

Jet, ionization cone and thorus axis are aligned

General Observer Program

The IXPE baseline program ends on February 2024.

The next NASA senior review for mission is foreseen in 2025.

NASA on 6 June 2023 approved an extension of IXPE until September 2025.

GO program is at the present time foreseen from February 24 to September 2025

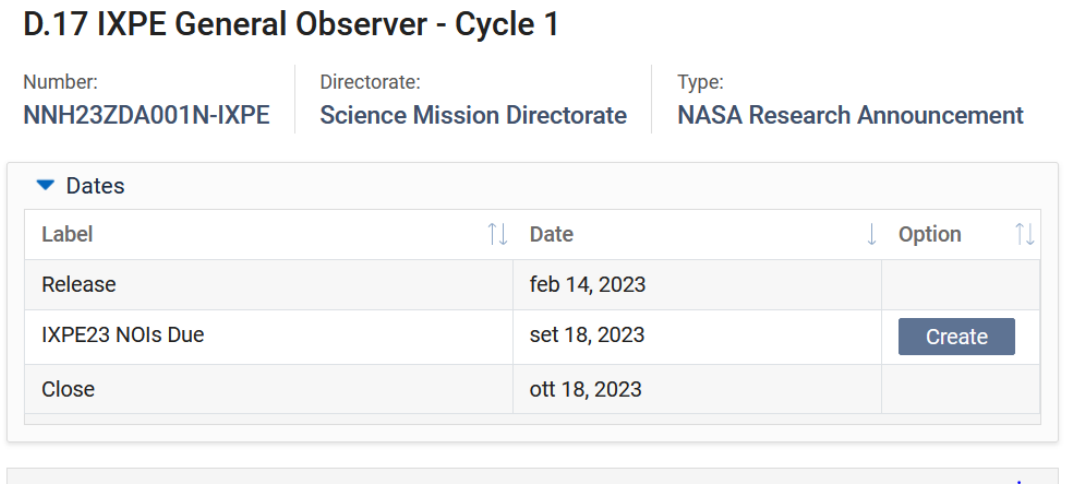

D.17 IXPE General Observer - Cycle 1

Number: NNH23ZDA001N-IXPE

Directorate: Science Mission Directorate

Type: NASA Research Announcement

Dates

Label	Date	Option
Release	feb 14, 2023	
IXPE23 NOIs Due	set 18, 2023	Create
Close	ott 18, 2023	

IXPE is working great. Consider to participate to the IXPE GO program!

IXPE
Imaging
X-Ray
Polarimetry
Explorer

A ROTATION OF THE POLARIZATION ANGLE IS DETECTED IN X-RAYS

- During X-ray rotation millimiter-wave, infrared and optical polarization angle didn't vary substantially.
- Rotation in optical light is few-few tens of degree/day
- PD_X was roughly constant and higher wrt Optical, Infrared and Radio
- At GeV was in a quiescent state

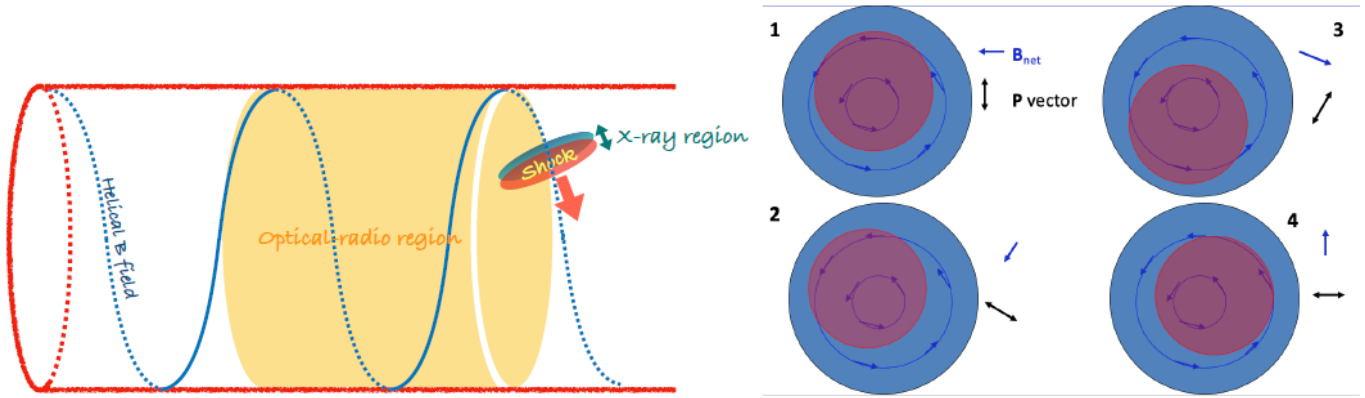

Fig. 2 Sketches of the scenario proposed to explain the X-ray polarization angle rotation in Mrk 421. Left: an off axis emission feature, e.g., a magnetosonic shock, propagates along helical magnetic field lines down the jet. Right: the appearance of the emission feature, magnetic field, and polarization vector at 4 azimuthal positions along its spiral path as viewed by a distant observer aligned with the jet. The red circle represents the emission feature, while the blue-shaded region is the ambient jet.

Di Gesu, Nature Astronomy in press

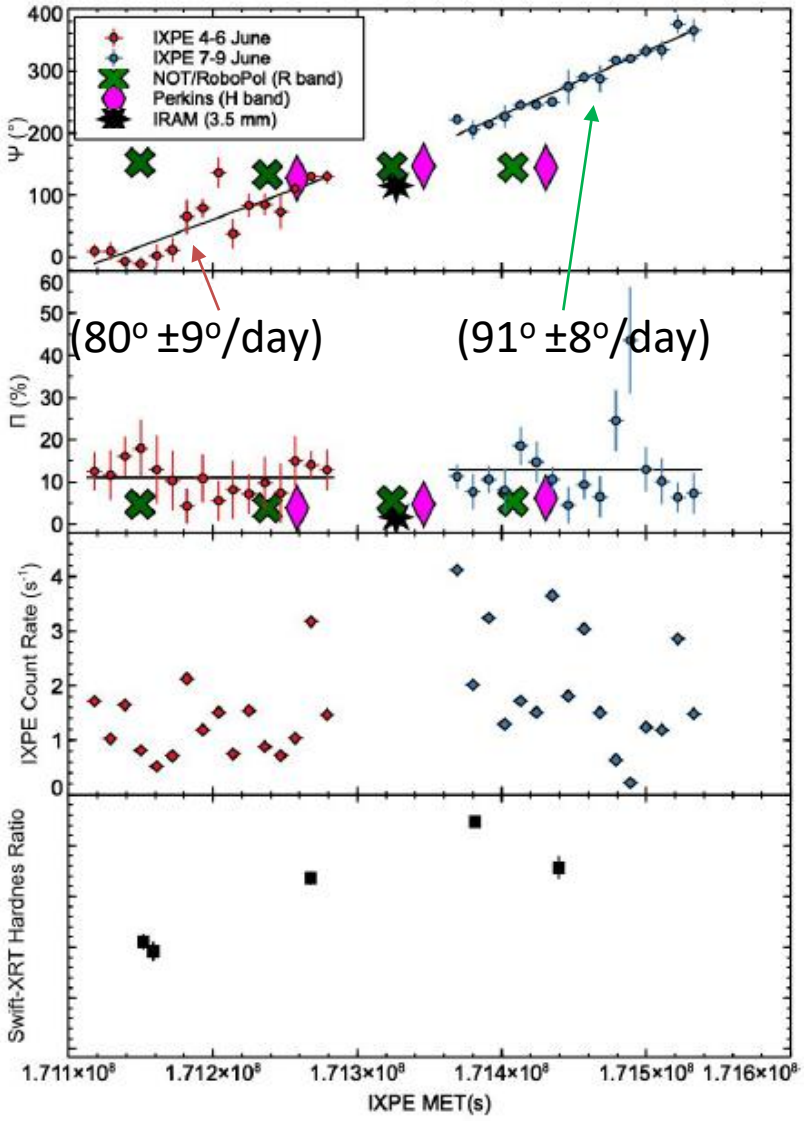

Was the galactic center active 200 years ago ?

- **Galactic Center molecular clouds (MC) are known X-ray sources**
  - Are MCs reflecting X-rays from Sgr A* ? (supermassive black hole in the GC)
    - X-radiation would be *highly polarized* perpendicular to plane of reflection and indicates the direction back to Sgr A*
    - Sgr A* X-ray luminosity was 10^6 larger ≈ 300 years ago

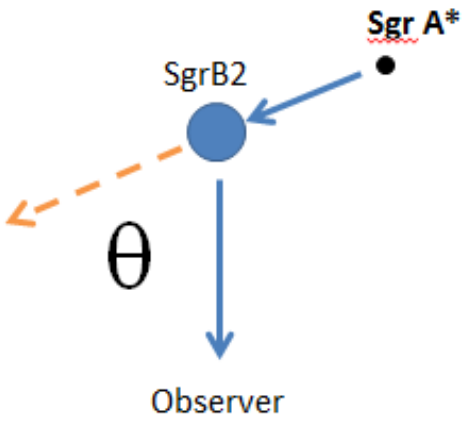

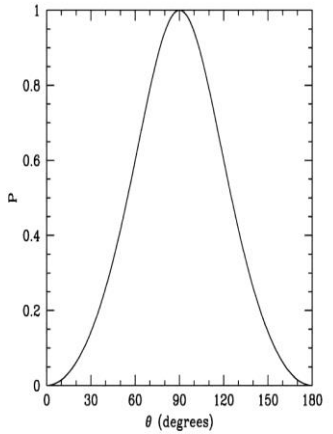

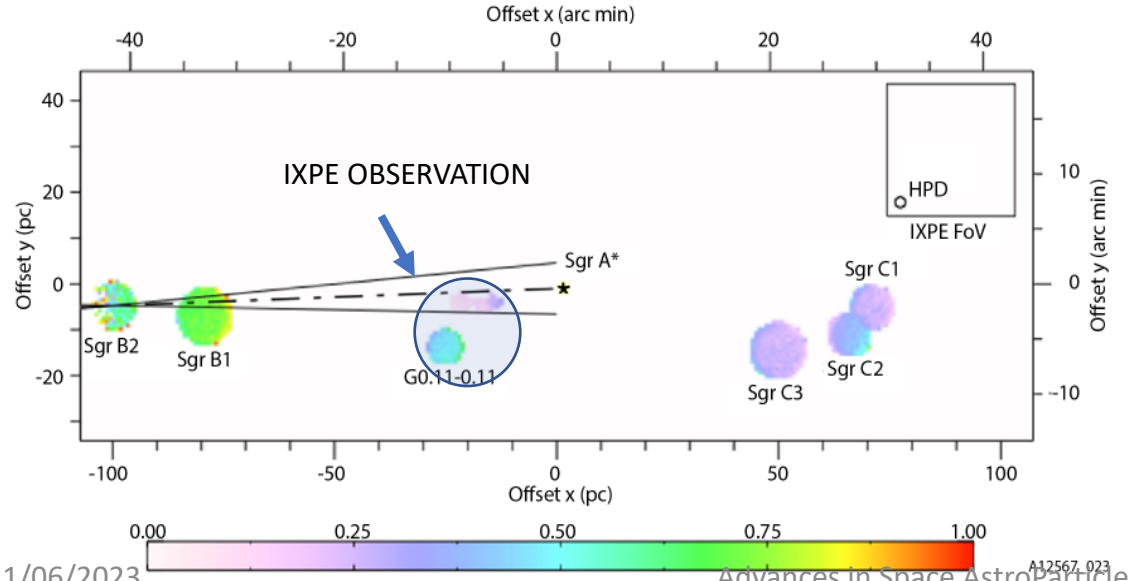

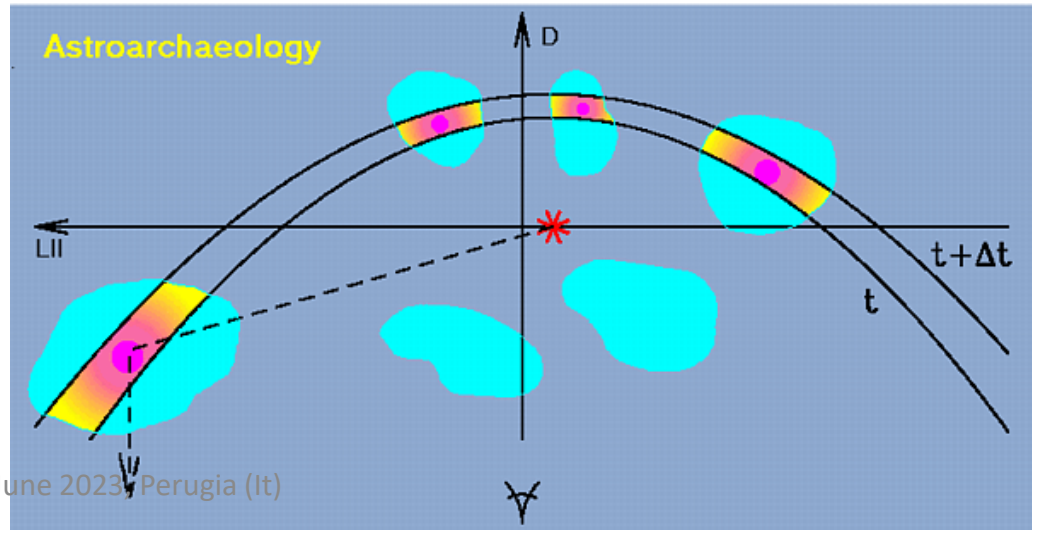

Was the galactic center active 200 years ago ?

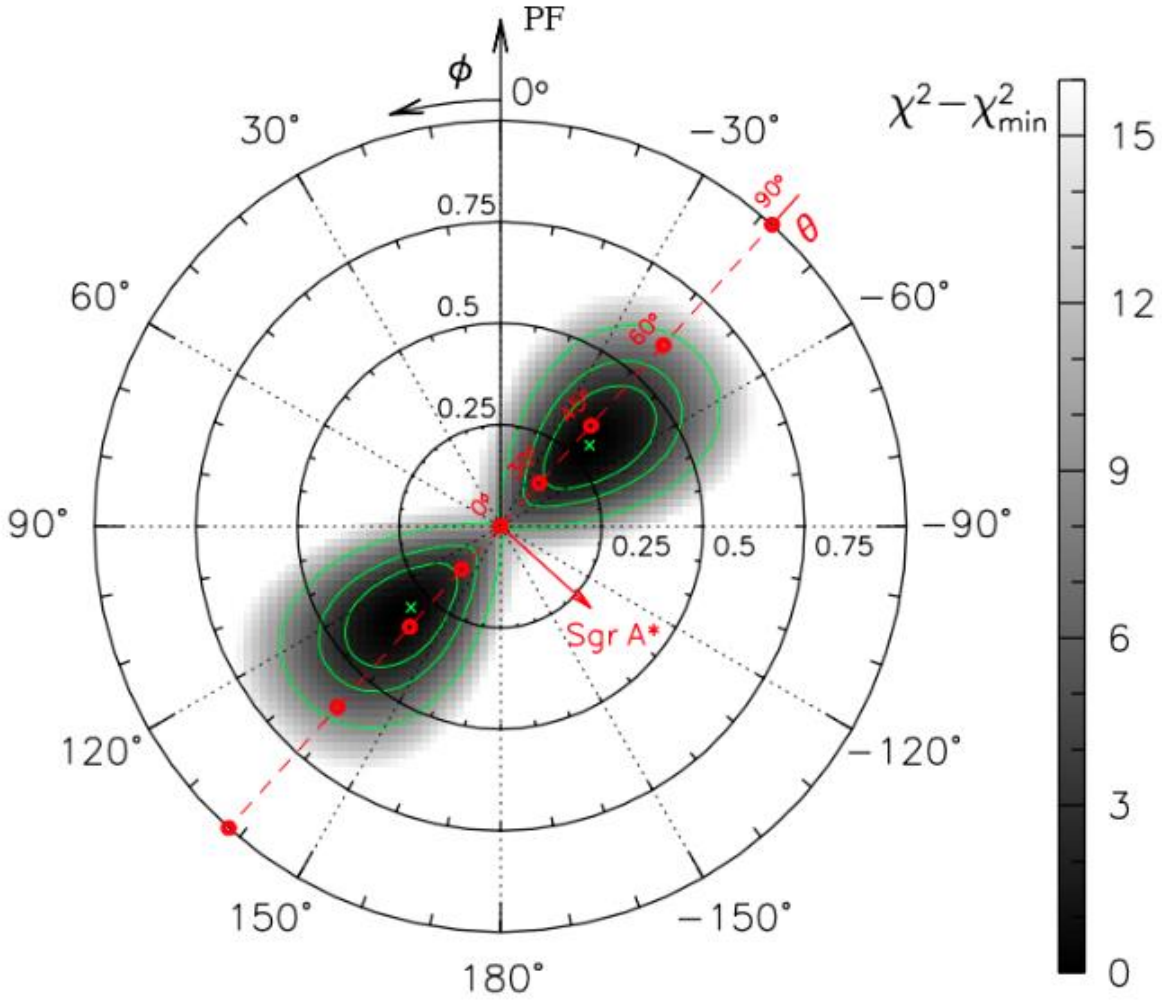

2.8σ result. Polarization angle consistent with Sgr A* as the origin of the illuminating radiation.

From the polarization degree, two solutions for the age of the burst: ~30 or ~200 years ago. Second solution much more probable a flare 30 years old should have been visible.

Marin et al., Nature in press (June 2021)

Recap of Cyg X-1 high energy polarimetry

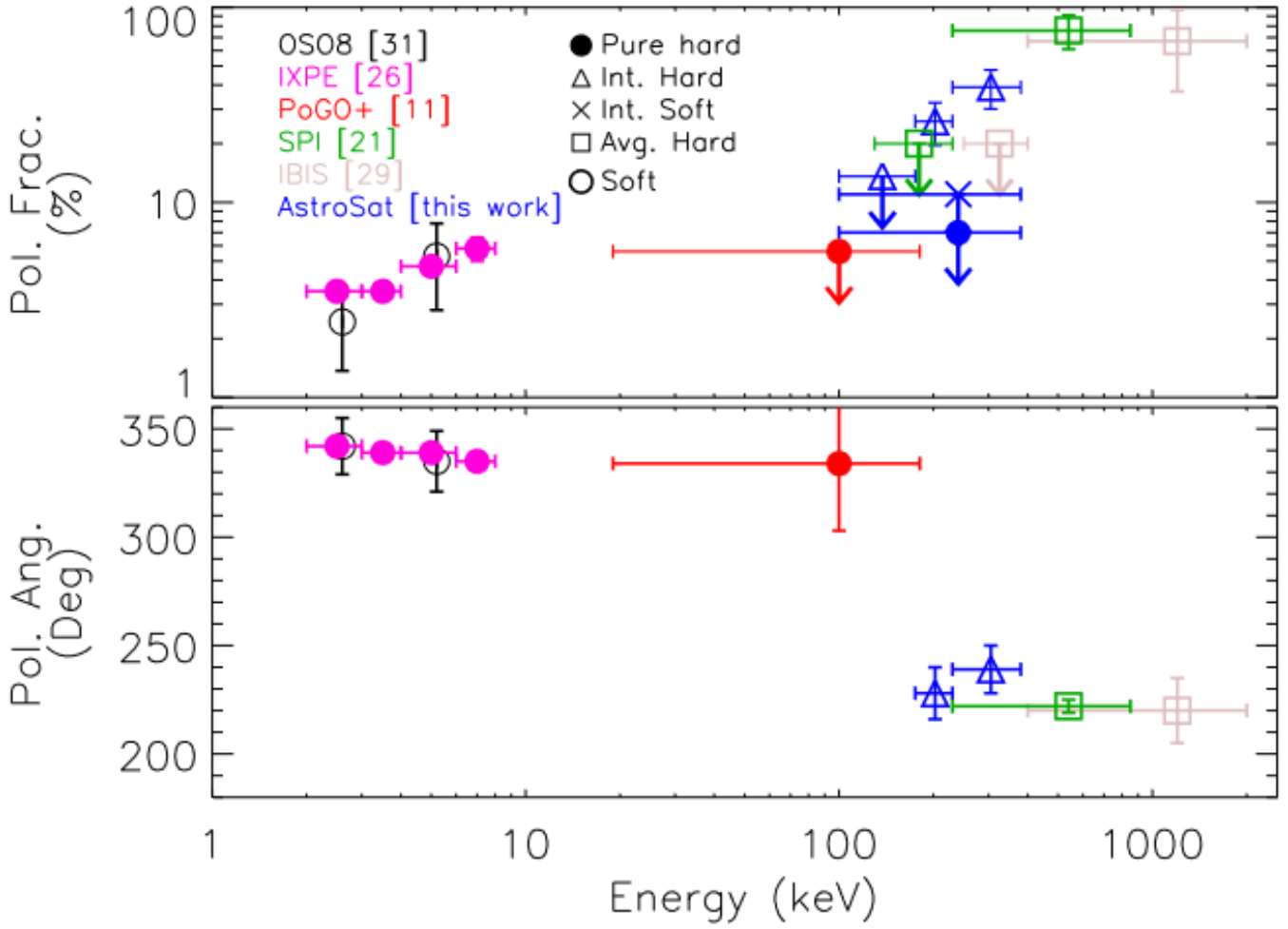

Chattopadhyay et al. 2023

BL Lac

In the LSP BL Lac X-ray emission is no longer dominated by electron Synchrotron. The source was pretty faint when observed by IXPE, and only an u.l. of 12.6% (99% c.l.) to the polarization degree could be obtained (*Middei et al. 2022*).

Hadronic models disfavoured in this source!

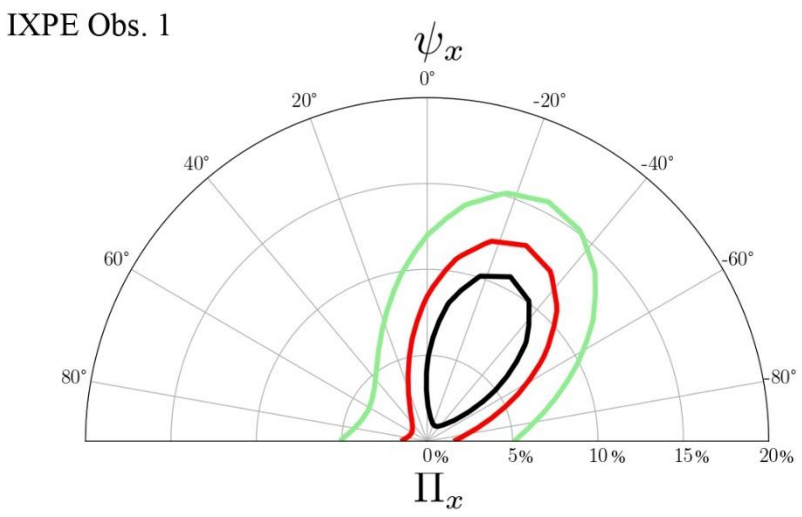

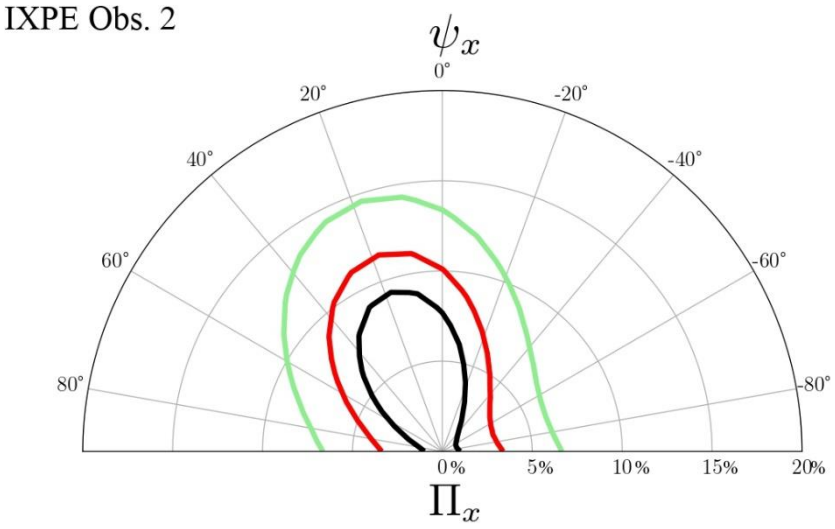

But polarization detected later on during an outburst (*Peirson et al 2023*) → Synchrotron emission likely extending to the IXPE band

Magnetars

Two modes, with very different opacities

Ordinary mode: E field parallel to the k-B plane

Extraordinary mode: E field perpendicular to the k-B plane

The X-mode from deeper, hotter layers

The radiation emerging from an atmosphere very likely is mostly extraordinary mode because the opacity is smaller

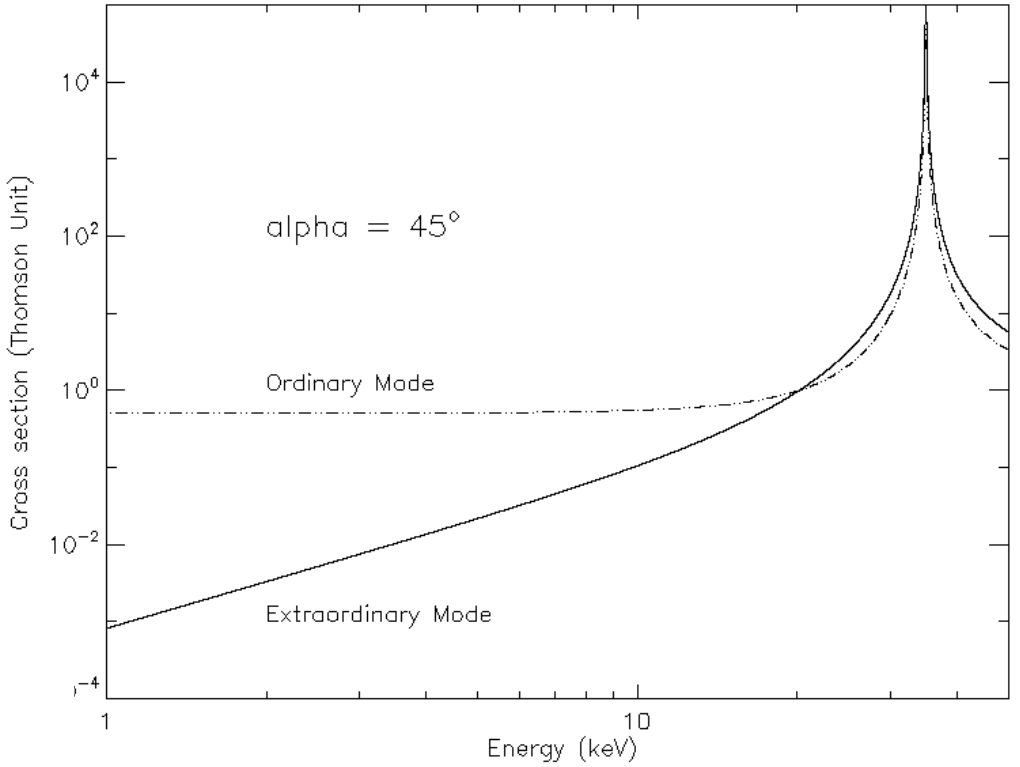

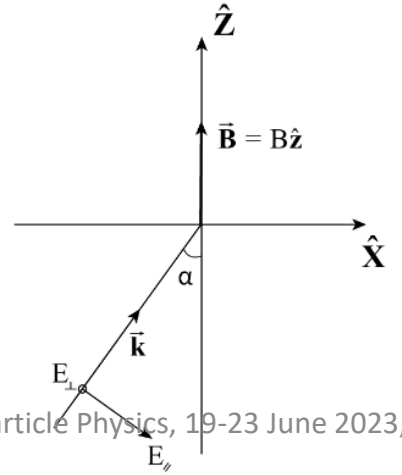

IXPE
Imaging
X-Ray
Polarimetry
Explorer

Marshall Space Flight Center

agenzia spaziale italiana

II YEAR OBSERVING TARGETS

TWG	Name	Obs. Tim (ks)
1-PWN & Pulsar	Crab G21.5 SNR 54-29 PSR B0540-69	300 1000 1000 90
2-SNR	RX J1713.7-3946 RCW 86 Tycho SN1006 NE Kes 75	1000 1000 230 300 1000
3-Acc BH	Cyg X-3 LMC X-1 SS-433 lobe Cyg X-1 (HS state) 4U 1957+115 LMC X-3 4 ToS	600 600 900 100 500 500 5400
4-Acc. NS	GRO J1008-57 4U 1820-303 Her X-1 Sco X-1 4U1626-67 Cir X-1 GX 5-1 LSV+44 17 Cir X-1 4U 1624-49 Sco X-1 LMC X-4	400 100 800 100 300 300 100 400 300 600 50 140
5-Magnetars	SGR 1806-20 1E1841-045 or 1RXS J1708 1E 2259+586 TOO Outburst	1000 1000 1000 500
6-AGN/GC	NCG 4151 MCG-5-23-16 SGR A* Nebulae	700 700 1000
7-Blazar	MRK 421 Mrk 501 1ES1959+65 PG1553+113 3C454.3 PKS 2155-304 TOOs + Flare Flare	750 300 200 250 700 1600

7.2Ms TOO

IXPE
Imaging
X-Ray
Polarimetry
Explorer

(see in astro-ph: Doroshenko et al 2023)

LSV +44 (Be-XRB) was observed in supercritical and subcritical accretion rate
Phase-resolved polarization degree and angle are very different for the two states.

Was the galactic center active 200 years ago ?

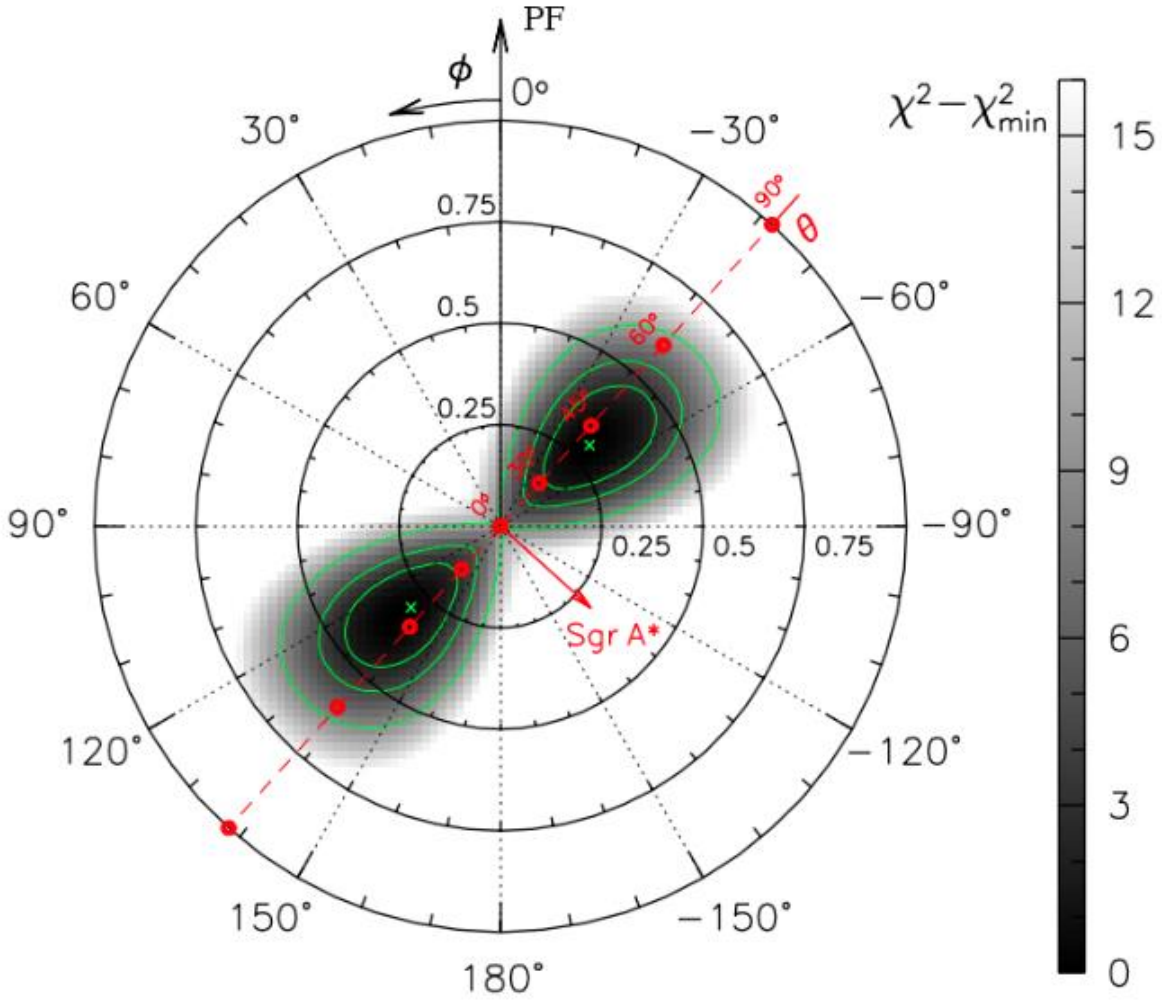

2.8σ result. Polarization angle consistent with Sgr A* as the origin of the illuminating radiation.

From the polarization degree, two solutions for the age of the burst: ~30 or ~200 years ago. Second solution much more probable a flare 30 years old should have been visible.

Marin et al., Nature in press (June 2021)

General Observer Program

The IXPE baseline program ends on February 2024.

The next NASA senior review for mission is foreseen in 2025.

NASA on 6 June 2023 approved an extension of IXPE until September 2025.

GO program is at the present time foreseen from February 24 to September 2025

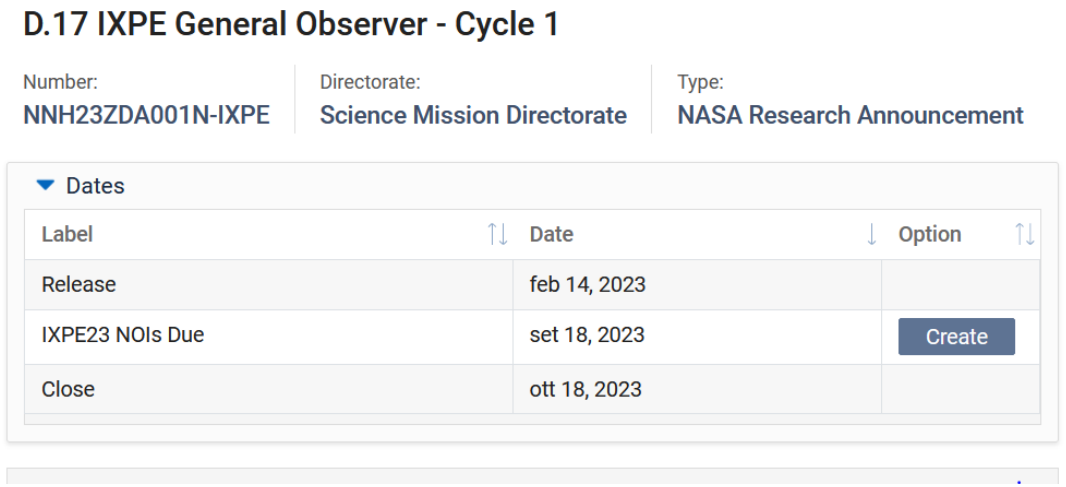

D.17 IXPE General Observer - Cycle 1

Number: NNH23ZDA001N-IXPE

Directorate: Science Mission Directorate

Type: NASA Research Announcement

Dates

Label	Date	Option
Release	feb 14, 2023	
IXPE23 NOIs Due	set 18, 2023	Create
Close	ott 18, 2023	

IXPE is working great. Consider to participate to the IXPE GO program!

Weakly Magnetized Accreting NS

Comparison with theoretical predictions shows that the X-ray emitting region of GS 1826-238 either has a spherical symmetry or the system is less inclined than believed

For the other sources, and in particular for Cyg X-2 where the polarization is parallel to the radio jet, emission in the spreading layer (plus contribution from reflection) is the most likely explanation

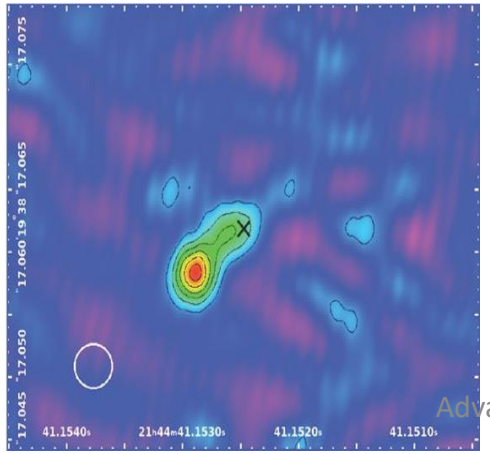

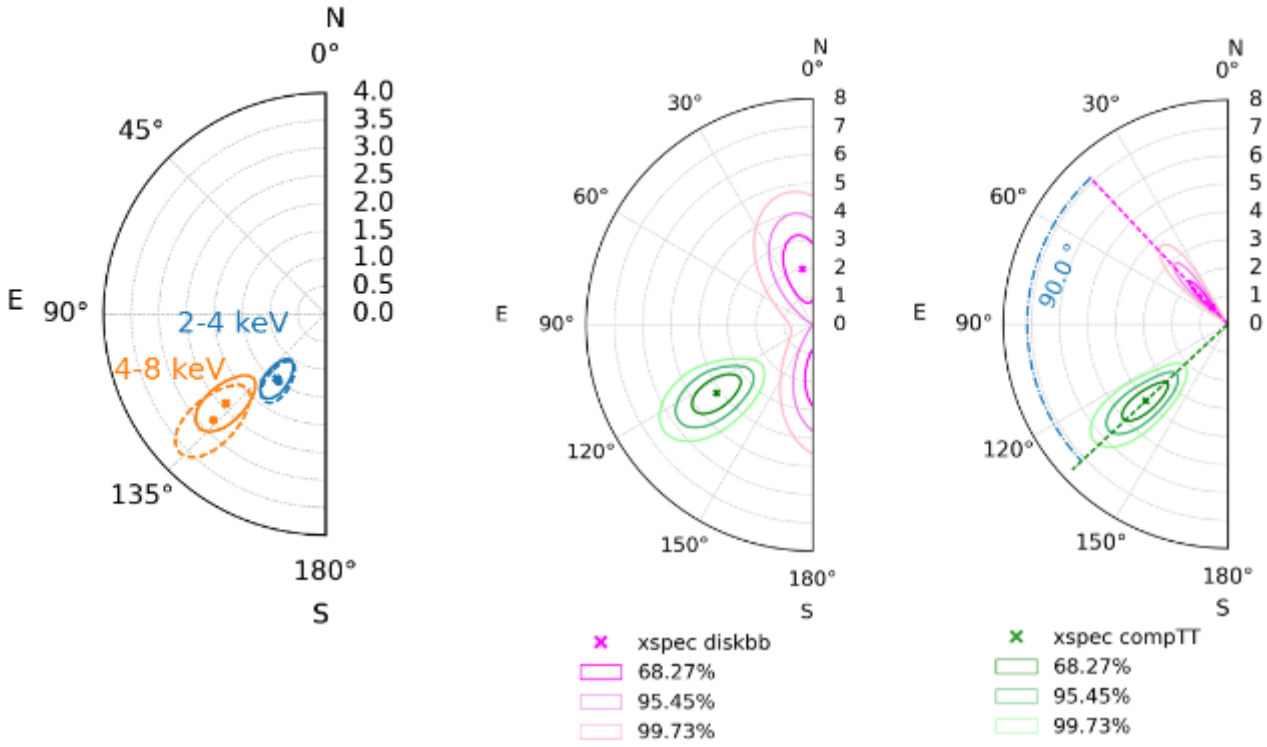

Farinelli et al. 2023

Weakly Magnetized Accreting NS

Not pulsating accreting NS were expected to be much less polarized (e.g. *Gnarini et al. 2022)*. IXPE is confirming this prediction, with a tight upper limit for GS 1826-238 (*Capitanio et al. 2023*) but a positive detection for Cyg X-2 *(Farinelli et al. 2023*), GX9+9 (*Ursini et al. 2023*), and XTEJ1701-462 (*Cocchi et al. 2023)*

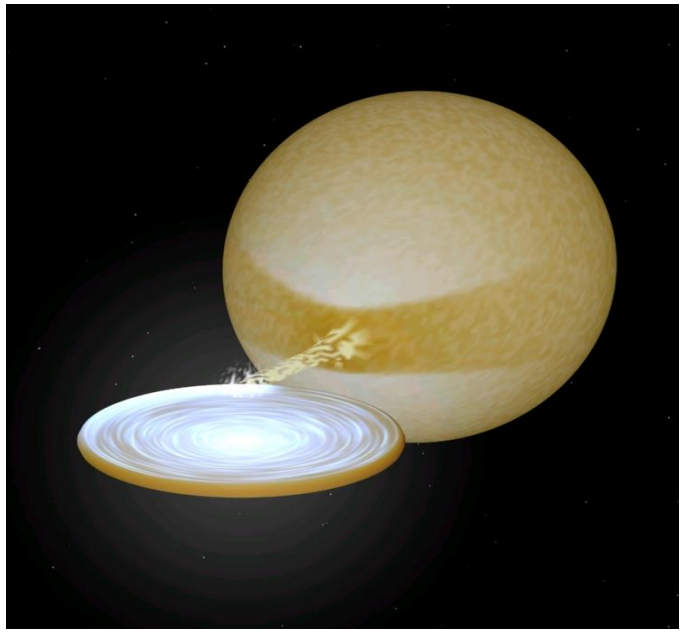

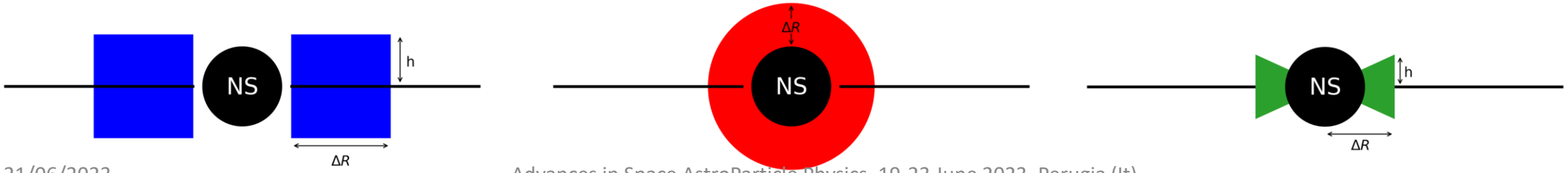

Radio Quiet AGN

X-ray spectroscopy can constrain the physical parameters of the corona.

However, it is almost insensitive to its shape and location.

Polarimetry, on the contrary, is very sensitive to the geometry of the corona, and can measure deviations from a spherical symmetry.

The coronal geometry is related to its physical origin.

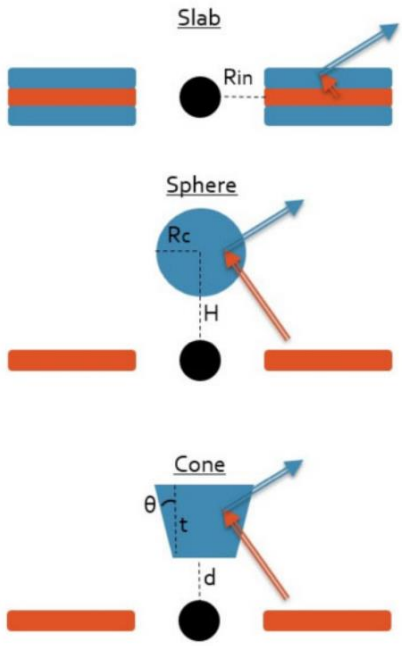

Three unobscured RQ AGN have been observed:

MCG-5-23-16 – PD <3.2% (Marinucci et al. 2022, Tagliacozzo et al. 2023). Possibly aligned with the NLR axis. Slab (or wedge) preferred

Similar results for IC4329A (Ingram et al. 2023)
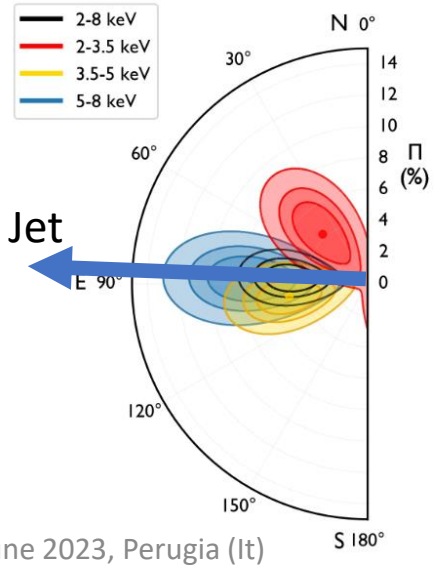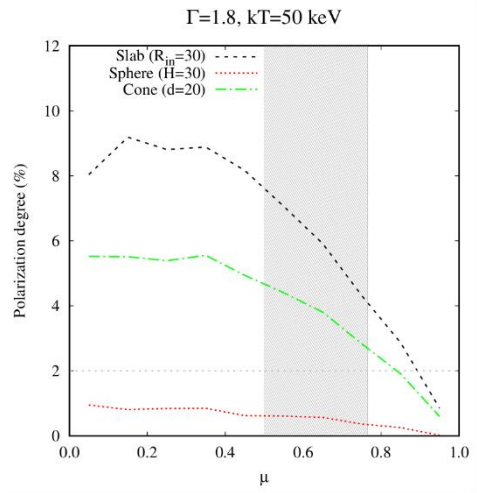
Positive detection in NGC 4151 (Gianolli et al. 2023). PD=4.9±1.1%, aligned with the radio jet. Again, slab or wedge preferred